Assessment of the Heart Rate Variability in Parkinson's Disease

Master's Degree Thesis in Biomedical Engineering

Supervisors:
Prof. Danilo Demarchi
Prof. Paolo Bonato

Candidate:
Giulia Clotilde Vana

POLITECNICO DI TORINO
Dipartimento di Ingegneria Industriale e Aerospaziale

Torino, December 2019

Abstract

Parkinson's disease (PD) is a chronic neurodegenerative disorder, second in frequency only to Alzheimer's disease. Although the well-acknowledged motor symptoms of PD have dominated clinical discourse, people with a PD diagnosis typically disclose several debilitating non-motor symptoms, even at the early stages of the disorder. Furthermore, typical antiparkinsonian medications such as levodopa are shown to have an effect on these non-motor symptoms, inducing fluctuations throughout the day. The non-motor signs include autonomic symptoms that are related to neuronal damages in the autonomic nervous system. Cardiovascular dysautonomia, for example, is caused by the loss of sympathetic and parasympathetic innervation throughout the heart and has been reported to precede the motor stage of PD and to progress in parallel with the disease.

The accurate recognition and monitoring of PD's non-motor symptoms remains a distinct challenge from a motor symptom assessment. Current approaches are mainly based on questionnaires and self-reports, which inherently lack objectivity. The heart rate variability signal (HRV) has proved to be a feasible and non-invasive instrument to assess cardiac autonomic dysregulation. The spectral analysis of the HRV allows for a deeper understanding of the complementary sympathetic and parasympathetic influences on the sinoatrial (SA) node, thus revealing the cardiac autonomic outflow. Particularly, the high-frequency (HF) component (0.15-0.4 Hz) of the power spectrum has been reported as a hallmark of vagal activity.

This thesis is part of the larger BlueSky Project and aims to assess the heart rate response in advanced Parkinson's patients under levodopa. For this purpose, data had been collected and analyzed in the Spaulding Rehabilitation Hospital Motion Analysis Laboratory (Boston, MA) from twenty-six affected subjects. Split over two visits, subjects were first monitored in a supervised setting over a full medication cycle, starting from the "Off" -levodopa state, to the "On" condition, and then turning back "Off". During the second visit, participants were tracked in a simulated home environment. Electrocardiogram (ECG) recordings were segmented to isolate periods of relaxation and then processed with a QRS complexes-detection algorithm applied to the wavelet transform to extract the ECG peaks. The resulting R waves have been carefully inspected and corrected to remove occasional ectopic or erroneous beats. The R events have been modeled as a history-dependent inverse Gaussian distribution by a point-process method able to reflect the stochastic nature of the heartbeat occurrences and the influences of the autonomic divisions on the SA node. The HF content has been obtained from the point-process algo-

rithm spectral analysis and interpreted as a marker of parasympathetic activation. The HF-HRV of the PD subjects were first compared with the HF-HRV of healthy controls, then longitudinally monitored over the medication cycle to investigate the effects of levodopa.

Parkinson's patients displayed a lower HF-HRV when compared to healthy controls, denoting suppressed parasympathetic activation consistent with previous literature. Furthermore, HRV parameters monitored during the medication cycle differed before and after the medication intake. The mean RR intervals and HF-HRV exhibited significant decreases ($p = 0.0108$ and $p = 0.0003$, respectively) in subjects shifting from "Off" to "On", suggesting an additional depressor effect on the vagal modulation of the heart due to the levodopa.

Acknowledgments

First, I would like to thank Danilo Demarchi for addressing me to work on this thesis and Paolo Bonato for allowing me to spend 8 months in his laboratory, the Spaulding Rehabilitation Hospital's Motion Analysis Lab in Boston. This experience has been a privilege and has encouraged me to grow up in both personal and professional prospects.

I would also like to thank all the members of the Motion Analysis Lab for being such a good colleagues and true friends. These months with all of you have been great. Particularly, I would like to say thank to Greta, Andrea, and Matteo for being always there as a second family. A very special thank goes to Stefano Sapienza, who guided me with his precious support from the beginning to the end.

I cannot forget to thank all my lifelong friends and Filippo for encouraging me from far away during these months and for embracing me as soon as I returned home.

I will always be immensely grateful to my parents and grandparents for the moral and economic support that they always accord to me. Without them I wouldn't be here today. Finally, I would like to thank my brother Andrea, who has always been my first exemplar.

Prima di tutto vorrei ringraziare Danilo Demarchi per avermi indirizzata a lavorare a questa tesi e Paolo Bonato per avermi permesso di trascorrere otto mesi nel suo laboratorio, il Motion Analysis Lab dello Spaulding Rehabilitation Hospital a Boston. Questa esperienza è stato un privilegio e mi ha incoraggiata a crescere sia da un punto di vista personale che professionale.

Vorrei anche ringraziare tutti i membri del Motion Analysis Lab per essere stati degli ottimi colleghi e veri amici. Questi mesi insieme a voi sono stati fantastici. In particolare, vorrei ringraziare Greta, Andrea e Matteo per esser sempre stati presenti come una seconda famiglia. Un ringraziamento molto speciale va a Stefano Sapienza, che mi ha guidata con il suo prezioso supporto dall'inizio fino alla fine.

Non posso dimenticare di ringraziare i miei amici storici e Filippo per avermi incoraggiata da lontano durante questi mesi e per avermi riabbracciata non appena sono

ritornata a casa.

Sarò per sempre immensamente grata ai miei genitori e ai miei nonni per il supporto morale ed economico che non mi hanno mai fatto mancare. Senza di loro oggi non sarei qui. Infine, vorrei ringraziare mio fratello Andrea, che è da sempre il mio primo punto di riferimento.

Contents

List of Figures

List of Tables

List of Acronyms

αS Alpha-synuclein

ANS Autonomic nervous system

AR Autoregressive

AV Atrioventricular

BMI Body mass index

CSS Controlled speech sample

CVLM Caudal ventrolateral medulla

CWT Continue wavelet transform

DMV Dorsal motor nucleus of vagus nerve

DWT Discrete wavelet transform

ECG Electrocardiogram

FFT Fast Fourier Transform

fMRI Functional magnetic resonance imaging

HDIG History-dependent inverse Gaussian

HF High-frequency

HR Heart rate

HRV Heart rate variability

H&Y Hoehn & Yahr

IG Inverse Gaussian

IML Intermediolateral nucleus

KS Kolmogorov-Smirnov

LF Low-frequency

MDS Movement Disorder Society

MoCA Montreal cognitive assessment

MODWT Maximal overlap discrete wavelet transform

NA Nucleus ambiguous

OH Orthostatic hypotension

PD Parkinson's disease

PNS Parasympathetic nervous system

PSD Power spectral density

SA Sinoatrial

SADLs Scripted activities od daily living

SDNN Standard deviation of the RR intervals

SNS Sympathetic nervous system

RVLM Rostral ventrolateral medulla

ULF Ultra low-frequency

UPDRS Unified Parkinson's disease rating scale

VLF Very low-frequency

Chapter 1

Aim of the research

Parkinson's disease (PD) is a severe neurological disorder that profoundly impairs the quality of life of people that suffer from it. Although greater attention has been focused on the motor aspect of the disorder, it is now well established that several non-motor symptoms can occur at the onset of the pathology, frequently preceding the motor stage. These non-motor signs are typically linked to a dysfunction in the autonomic nervous system and manifest in multiple ways, including an impaired cardiovascular response. Moreover, typical medications used to improve the motor performances, such as levodopa, showed to further impact on the non-motor symptoms occurrence.

As the autonomic nervous system (ANS) provides substantial innervation to the heart through its two branches, the sympathetic (SNS) and parasympathetic nervous systems (PNS), the activity of the sinoatrial (SA) node is intensely modulated by the complementary activation of them. Thus, the assessment of the cardiac response can provide a definite comprehension of autonomic integrity. Particularly, the heart rate variability (HRV) signal has proved to represent a valid and effective tool to non-invasively investigate the cardiovascular dysautonomia over the progression of the disorder.
The HRV is computed from the electrocardiogram (ECG) recordings and reflects the intervals in time between consecutive R waves. Among the parameters that can be extracted from the HRV signal, the spectral analysis has previously shown a great understanding of the mechanisms behind the activation of the two divisions of the autonomic nervous system. Particularly, the power content in the high-frequency band of the spectrum has proved to reflect the parasympathetic contribution on the modulation of the heart and has been employed as a reliable marker of vagal outflow.

This thesis is part of the larger BlueSky Project and is addressed to study and assess the HRV signal in patients with a diagnosis of Parkinson's disease under levodopa-carbidopa treatment. The BlueSky Project has been released in 2016 by the pharmaceutical company Pfizer and has been designed to collect data from Parkinson's patients using mobile and wearable devices. The principal purpose was to continuously track motor and non-motor manifestations of the disorder and develop algorithms to provide real-time objective estimates for the severity of the symptoms.

The protocol encompassed four distinct cases of studies and gathered data from both healthy volunteers and Parkinson's subjects. Data collections have been carried in different environments and under diverse contexts, particularly:

1. Controlled environments with the administration of supervised and scored tasks;

2. Passive monitoring in simulated home settings.

Study 1 collected data from healthy volunteers in a controlled laboratory environment (Pfizer, Cambridge, MA & IBM Watson Research Center, Yorktown Heights, NY). Study 2 enrolled people diagnosed with Parkinson's disease and collected data at two distinct time points, i.e. before and after the administration of the medication (Tufts Medical Center, Boston MA). Study 3 focused on long-term treated Parkinson's subjects experiencing motor fluctuations and recorded data under a full medication cycle during two separate visits, first in a controlled laboratory and then in a simulated apartment (Spaulding Rehabilitation Hospital, Charlestown MA). Study 4 focused on the passive monitoring of Parkinson's subjects at home or in community settings. Particularly, this thesis is based on Study 3 of BlueSky Project and all the analysis have been performed on the ECG recorded in the Motion Analysis Lab and the simulated apartment in the Spaulding Rehabilitation Hospital.

The first part of this thesis aims to compare the cardiovascular response in subjects with a diagnosis of Parkinson's disease and healthy controls. A consistent portion of the previous literature reports a dissimilar heart response between these two populations, suggesting that the autonomic outflow is impaired in Parkinson's patients. Particularly, the high-frequency component of the power spectrum of the HRV has been presented as diminished in the affected patients, indicating a depression of vagal activation.
This current work is initially directed to investigate whether the high-frequency content is lower in Parkinson's patients compared with healthy people, to further corroborate what has been reported previously.

Although most of the past work focused on differences across populations, the heart changes in response to the intake of the common medications used to mitigate the motor symptoms are still poorly investigated. The second part of this thesis aims to track the cardiac response in Parkinson's patients during a full medication cycle to assess whether the autonomic modulation of the heart is varied after a dose of levodopa-carbidopa. Newly, the high-frequency content of the HRV signal is employed as a primary marker of vagal activity to reflect the potential side effects of the treatment on the parasympathetic activation and control of the heart rate.

Chapter 2

Introduction

This chapter provides a brief introduction to contextualize the principal themes covered over the entire thesis and support the understanding of the reader.
The first part aims to delineate the role of the autonomic nervous system in the control of the heart rate activity. First, an anatomic and physiologic explanation of the autonomic innervation of the heart is provided and particular emphasis is addressed to define the contribution of the sympathetic and parasympathetic nervous systems. Second, the primary non-motor symptoms in Parkinson's disease and the physiologic reasons behind their occurrence are presented. Particularly, the involvement of the autonomic neuronal pathways and the incidence of a cardiovascular dysautonomia are described. Moreover, the mechanisms behind the action of the main therapy employed for the motor improvement are discussed.
The second part aims to present the principal metrics of the HRV signal. First, the main features of the ECG waveform are briefly described. Then, the methods of assessment and quantification of the HRV are presented and particular attention is posed on the introduction of a novel point-process framework. Finally, a physiologic explanation of the principal spectral components of the HRV is provided.

2.1 Autonomic control of the heart

The autonomic nervous system is the functional part of the nervous system. It encompasses two distinct divisions, which together modulate the bodily functions through a homeostatic mechanism. The two divisions of the ANS are the sympathetic system and the parasympathetic systems. The ANS plays a key role in the control of the cardiac electrophysiology, altering not only the heart rate and the strength contraction, but also the cellular properties of individual cardiomyocytes [1].
The heart is innervated by both the two branches of the ANS and cardiac activity is regulated by the complementary effects of them. Particularly, the sympathetic system is the exponent of the fight-or-flight response and is dominant in certain conditions such as physical exercise or posture changes. Its activation is finalized in increasing the heart rate and the vessel resistance to maintain the blood pressure. Parasympathetic activity is significant at rest and evokes the opposite response, decreasing the heart rate and contractility. Disorders of the ANS typically lead to an altered cardiovascular response and this can be observed in several neurological disorders, including Parkinson's disease.

This section provides a brief explanation of the autonomic control of the heart, focusing on the anatomy and physiology of the cardiac ANS. Figure 2.1 pictures a scheme of the autonomic innervation of the heart, highlighting the principal pathways that project the sympathetic and parasympathetic fibers through the cardiac muscle.

2.1.1 Parasympathetic modulation

The vagus nerve (tenth cranial nerve) is the principal nerve of the parasympathetic system and originates in the medulla oblongata, the lowest part of the brain stem [1], [2]. The primary contribution of heart innervation comes from the nucleus ambiguous (NA) of the vagus nerve, but part of it is also supplied by the dorsal motor nucleus (DMV), which mainly provides innervation to the gastrointestinal tract [3]. Pre-ganglionic parasympathetic fibers are projected to the heart within the vagus nerve and richly innervate the sinus and atrioventricular nodes [1]. A vagal stimulation has a different effect on atria and ventricles myocytes. In the atria, it shortens the refractory period and promotes early afterdepolarization [1]. In the ventricles, it prolongs the action potential duration and the effective refractory period [1]. The overall result is a decrease in the heart rate. As a cranial nerve, the vagus nerve control on the heartbeat dynamics has a very short latency. Thus, its effect is almost instantaneous and is detectable on a beat-to-beat basis [4].

2.1.2 Sympathetic modulation

The pre-ganglionic sympathetic neurons originate from the cervical and thoracic regions of the spinal cord and reach the cervicothoracic sympathetic ganglia, including

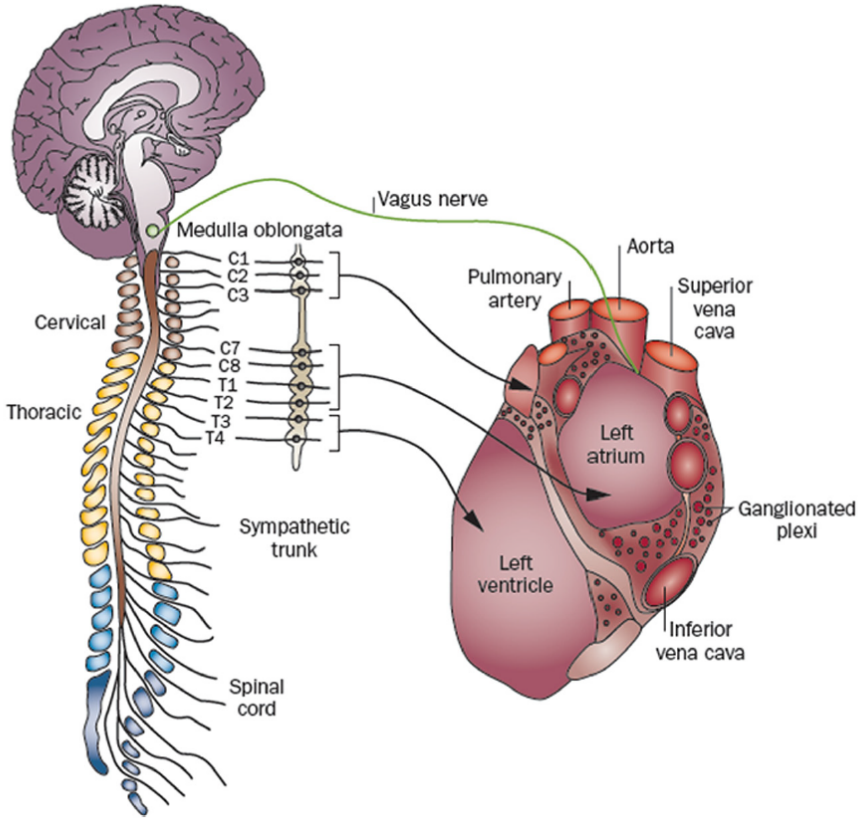

Figure 2.1: Sympathetic innervation originates from the cervical and thoracic regions of the spinal cord and reaches the cervicothoracic sympathetic ganglia. Parasympathetic innervation originates in the medulla oblungata and migrates within the vagus nerve [1].

stellate ganglia. From the cervicothoracic sympathetic chain, post-ganglionic sympathetic fibers extend to the heart. Particularly, post-ganglionic fibers leaving from the left stellate ganglion innervate the atrium-ventricular node, left atrium, and posterior aspect of the left ventricle, whereas post-ganglionic fibers leaving from the right ganglion mainly supply the sinus node, the right atrium, and the anterior left ventricle [2]. A sympathetic stimulation has comparable repercussions on both atrial and ventricular myocytes and typically causes a shortening in the action potential duration, leading to an increased heart rate [1]. Whereas vagal activity is typically fast, sympathetic cardiac effects are considerably slower, with a delay that can approach the tens of seconds [4].

2.2 Parkinson's Disease

Parkinson's disease is a progressive multisystem neurological disorder, second in frequency only to Alzheimer's disease. It primarily affects the elderly, with a high

incidence in the population over 60, but can occur even in younger people. No specific genetic or environmental risk factors have been identified, although previous studies report that it is slightly more likely to affect the men then the women [5].
The disease is always symptomatic and typically manifests as in both motor and non-motor signs, impairing severely the quality of life of people who suffer from it. The first description of the disorder dates to 1817, when the physician James Parkinson, after observing postural and movement abnormalities in six patients, reported them in his work "An Essay on the Shaking Palsy". Particularly, he identified it as a movement disorder and described the "shaking palsy" as an "involuntary tremulous motion, with lessened muscular power, in parts not in action and even when supported" [6]. Since then, many researches attempted on the study of the mechanisms underlying the insurgence and progression of the disease, focusing primarily on the motor manifestations.
The main evidence is the presence of protein intracellular inclusions, named Lewy bodies and Lewy neuritis. These inclusions spread through the central and peripheral nervous system, affecting the neuronal pathways and leading to a neuronal loss. The diagnosis is almost always made after the appearance of the motor signs, which originate due to a loss of dopaminergic neurons within the substantia nigra compacta. Principal motor symptoms include bradykinesia, slowness, freezing of gait, resting tremor, decreased dexterity, and rigidity.
Although these motor manifestations dominated the clinical scenario for several years, it is now well established that those who suffer from PD present also several non-motor symptoms. These non-motor features include gastrointestinal dysfunctions, urinary dysregulations, olfactory alterations, thermoregulatory anomalies, and cardiovascular abnormalities [7], and can precede the onset of motor signs by several years, offering an opportunity for an early diagnosis.
Currently, there is no cure for PD. The main treatment consists in the levodopa, a precursor of dopamine which aims in restoring the motor functions. Although the role of the dopamine replacement therapy on the motor signs is well known, its repercussion on the non-motor symptoms is still unclear.

2.2.1 Physiopathology

PD belongs to the family of the alpha-synucleinopathies, a group of neurodegenerative disorders resulting from the pathological alpha-synuclein (αS) aggregation in the nervous system. The αS is a presynaptic neuronal protein, normally expressed in the nervous system in its unfolded and cytosol-soluble form. It becomes pathogenic once its encoding gene mutates, causing the misfolding of it in a β-sheet structure [8]. The reasons and conditions that lead to the mutation of the encoding gene remain unclear. The misfolded αS is insoluble and tends to aggregate with other misfolded αSs within the cell bodies, forming cytoplasmatic inclusions named Lewy bodies and Lewy neuritis. These abnormal protein aggregates spread through the nervous system, involving central and peripheral neurons [9]. Different locations of αS aggregates through the nervous system lead to distinct clinical manifestations of the disease.

The typical motor signs of Parkinson's disease are due to the presence of Lewy bodies and Lewy neuritis in the basal nuclei of the cerebrum, at the level of the substantia nigra compacta. The basal nuclei are subcortical structures responsible for the control of the posture and the voluntary movements. Two distinct circuits can be observed in the basal nuclei, each extending to different output structures. The direct pathway stimulates the disinhibition of the thalamus and, as result, the excitation of the cortex, whereas the indirect pathway reinforces the normal inhibition of the thalamus. The substantia nigra compacta stays at the turn between the two circuits: it releases the neurotransmitter dopamine, which can either activate the direct pathway or inhibit the indirect pathway. When the substantia nigra is active, the direct pathway is stimulated and a movement is promoted; else, when the substantia nigra is silent, the indirect pathway chiefs and a movement is inhibited [10]. The presence of Lewy bodies and Lewy neuritis within the substantia nigra determines the loss of dopaminergic neurons, undermining the modulatory mechanisms of the two pathways and leading to an impaired control of posture and voluntary movements.
Although the motor symptoms are the basis for a proper diagnosis, several studies report that Lewy bodies are also located in other regions of the nervous system. Particularly, they spread according to a specific pattern, involving first other structures and then, only in a second time, the substantia nigra. According to Braak's theory, the diffusion of the Lewy bodies follows six distinct neuropathological stages, starting from the enteric nervous system and rostrally spreading to the other central structures [11]. The first two stages involve the DMV, where the first protein inclusions can be observed, whereas the involvement of substantia nigra only occurs starting from stage 3 (Figure 2.3). This suggests that the motor manifestations of the disease are preceded by other signs. Braak's theory, although still controversial [9], has gained considerable attention since seems to explain the pre-motor phase of the disorder [8].
The non-motor signs are generally referred to a dysfunction of the ANS. The ANS has distinct components, each functionally and neurochemically different from the others. The British physiologist J.N. Langley, who coined the term "autonomic nervous system", hypothesize the presence of three parts: the enteric nervous system, the sympathetic nervous system, and the parasympathetic nervous system. The enteric nervous system innervates the gastrointestinal tract and contributes to regulate the gastrointestinal functionality. The sympathetic nervous system is associated with the "fight-or-flight" response and plays a key role in the regulation of the heart rate and the blood pressure during different activities, such as exercise and postural changes. Particularly, the stimulation of the sympathetic nervous system increases the heart rate and the myocardial contractility. The parasympathetic nervous system is dominant at rest and cooperates with the sympathetic nervous system to regulate the cardiovascular response.
The principal nerve of the parasympathetic nervous system is the vagus nerve, which contributes with two sources of innervation. The first consists of the DMV, which innervates the gastrointestinal tract and the splanchnic organs, modulating the gastrointestinal functions. The second is the NA, which supplies preganglionic parasym-

pathetic neurons innervating the heart [3]. A stimulation of the parasympathetic nervous system decreases the heart rate and myocardial contractility. Lewy bodies are not confined into the central nervous system but have been also identified into the peripheral nervous system, particularly in superior sympathetic ganglia and in the vagus nerve [8], [11]. Denervation of distinct constituents of the autonomic nervous system leads to different clinical manifestations. Sympathetic denervation primarily affects the cardiovascular control, determining an impaired heart rate modulation and blood pressure maintaining. Parasympathetic denervation and enteric denervation are difficult to be distinguished, since both systems innervate the gastrointestinal tract, and manifest as constipation, altered esophageal peristalsis, and abdominal discomfort.

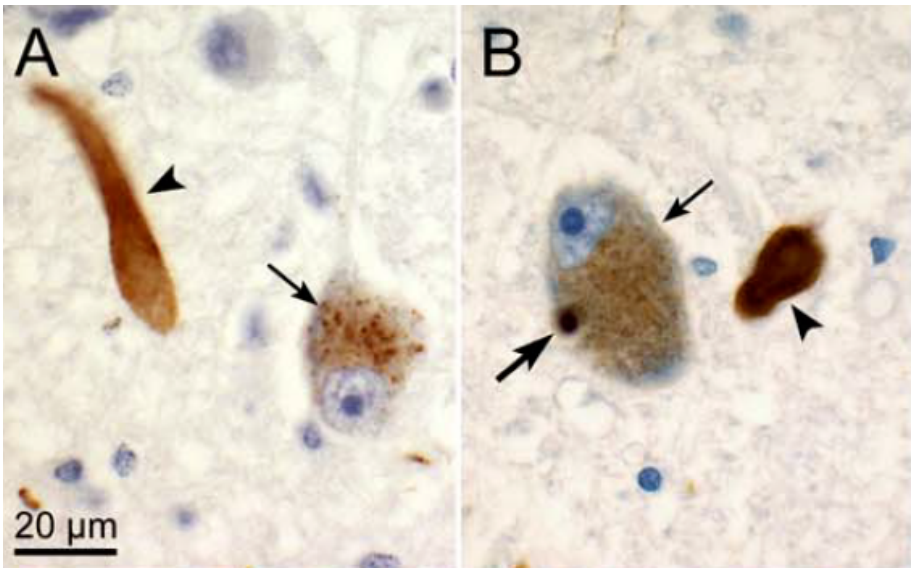

Figure 2.2: Inclusion of pathology structures within the cholinergic neurons of the DMV. The arrowheads indicate the presence of Lewy neuritis, whereas mature Lewy bodies in the nerve cells are pointed by the larger arrows and the αS aggregates by the smaller arrows [12].

2.2.2 Cardiovascular dysautonomia

Among the various non-motor manifestations, people with a diagnosis of PD typically present an impaired cardiovascular response with a weighty impact on daily living and goodness of life [14], [15] . There are neuroimaging, neurochemical, and neuropharmacological evidences of substantial sympathetic denervation in the heart since the early stages of the disease [3], [16]–[20]. Particularly, in 2009, Goldstein et al. showed that this loss of innervation can precede the well-recognized motor symptoms of the disease by several years [17] and, in 2012, they demonstrated a worsening of the cardiac denervation in parallel with the progression of the disease [21]. Figure 2.4 shows a decreased myocardial uptake of a sympathoneural radiotracer, highlighting the progressive loss of cardiac sympathetic innervation over the

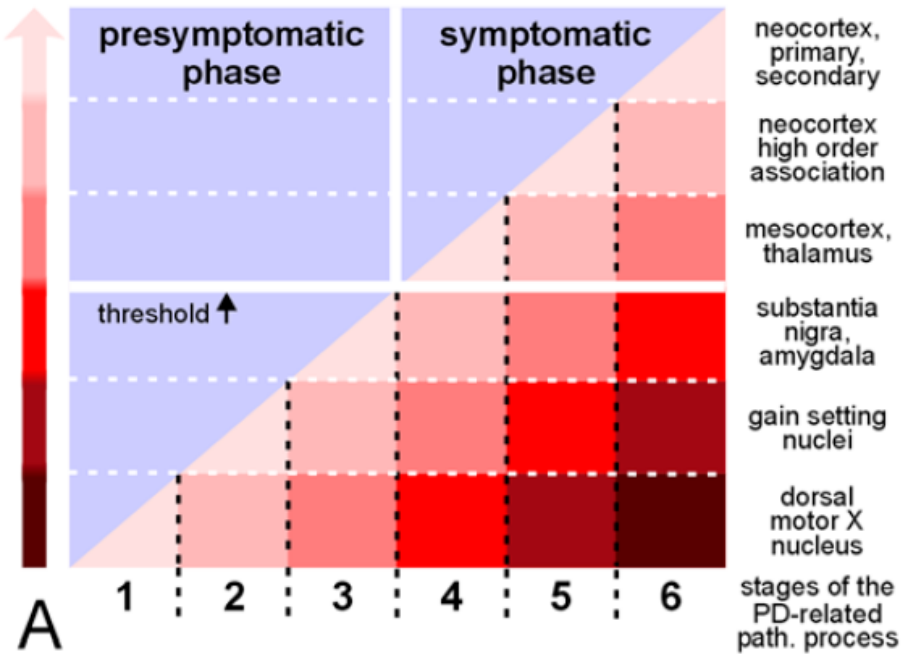

Figure 2.3: Theory of brain involvement hypothesized by Braak et al. [13]. DMV is the first structure affected by the presence of Lewy bodies, whereas the involvement of the substantia nigra compacta only occurs from the third stage [12].

advancement of the pathology. All these findings seem to be in line with Braak's theory and emphasize the existence of a pre-motor phase.
In addition to the sympathetic denervation, myocardial norepinephrine levels are drastically lower in patients with Parkinson's disease, mainly due to the loss of sympathetic neurons and to a lower intake of norepinephrine from the remaining nerves. Norepinephrine is the neurotransmitter of the sympathetic nervous system and primarily regulates the blood pressure during postural changes. After standing up from a supine position, plasma norepinephrine levels typically double in healthy subjects, causing the vasoconstriction adequate to maintain the blood pressure. This regulatory mechanism is impaired in patients with PD, who are not able to sustain the blood pressure. This leads to an orthostatic hypotension (OH), which is the main feature of cardiovascular response impairment in PD [14]. The OH is generally defined as the repeated decrease of at least 20 mmHg in systolic blood pressure or 10 mmHg in diastolic blood pressure after three minutes of standing up [3]. Several previous studies report that an OH occurs in about 20 to 50% of Parkinson's patients [9], [22], and that it can be both symptomatic and asymptomatic. Symptoms of the OH vary among patients and include weakness, fatigue, blurred vision, lightheadedness, and loss of consciousness [3], [20]. Although previous studies demonstrated that patients with OH have a more severe cardiac sympathetic denervation and lower norepinephrine levels, this loss of innervation occurs in patients without OH as well and does not determine the baroreflex failure itself [3].

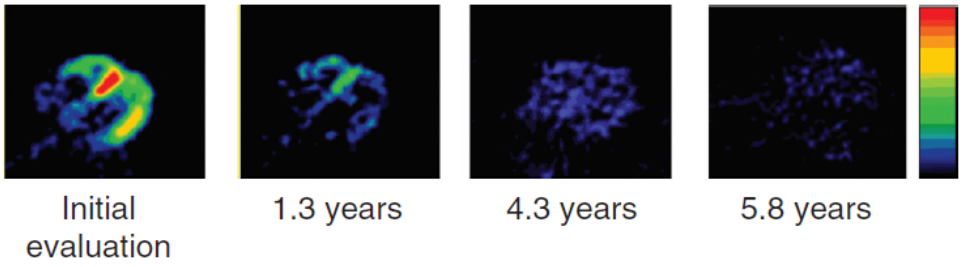

Figure 2.4: Evolution of cardiac sympathetic denervation in a Parkinson's patient emphasized by the decreased myocardial concentration of sympathoneural radiotracer [3].

2.2.3 Other autonomic dysfunctions

Gastrointestinal dysregulation is common among Parkinson's patients, and it is due to a vagal or enteric denervation. Autopsy findings showed the presence of Lewy bodies along the whole gastrointestinal tract, from the esophagus to the colon [22]. Symptoms of gastrointestinal dysfunction include a slower motility, constipation, extended esophageal spasm, and diminished peristalsis [22]. Urinary symptoms are also typically observed in Parkinson's patients, and manifest primarily as urgency and frequency, nocturia, and, in some cases, urinary retention. Thermoregulatory abnormalities include abnormal sweating and facial flushing. Sexual dysfunctions manifest as erectile dysfunction and ejaculation problems in men and vaginal dryness in women.

2.2.4 Levodopa therapy

The dopaminergic replacement therapy is the current most effective treatment for the motor symptoms of Parkinson's disease. Particularly, the levodopa is the gold standard medication. It is an amino acid precursor of dopamine, and it is administered since it is able cross the blood-brain barrier, whereas the pure dopamine cannot. Once that levodopa reaches the brain, it is rapidly decarboxylated to dopamine, stimulating the dopaminergic receptors and restoring the dopamine lack in the brain. Levodopa is generally administered with carbidopa, a dopamine decarboxylase inhibitor. It inhibits the conversion of the prodrug into dopamine peripherally and does not pass through the blood-brain barrier, thus allowing the decarboxylation into the brain. This consents to diminish the levodopa dose administered, since more dopamine can be provided to the dopaminergic receptors. The therapeutic window of the antiparkinsonian drug tends to become narrower over time, requiring higher doses. This limits the beneficial effects of the levodopa, since high doses are associated with enteric side effects. Moreover, long-term treated patients show fluctuations in the symptoms, developing other clinical manifestations, such as dyskinesia.
Although the effects of levodopa on the motor signs of the disorder are well estab-

lished, its repercussion on the autonomic nervous system is still unclear [23]. Results among different researches are controversial: some report that it acts on the sympathovagal balance whereas other failed in showing such effect. Several studies report a vasodepression and a reduction in the cardiac output after the administration of the levodopa [24]. Such depressor effect may appear paradoxical, as levodopa is a precursor for adrenaline and noradrenaline, the neurotransmitters designed to the activation of the sympathetic nervous system and the vasoconstriction necessary to maintain the blood pressure [25]. However, peripherally, dopamine acts on the receptor sites on the vascular smooth cells, competing with the noradrenaline, and its constrictor effect is much less than that of the sympathetic neurotransmitter [23], [24]. Although being deeply investigated, a clear and defined short-term and long-term effect of the levodopa on the sympatho-vagal balance has not been explained yet.

2.2.5 Fluctuations

The long-term administration of levodopa triggers dynamic changes of the disorder symptoms over the day. These variations are named fluctuations and refer both to the motor and non-motor manifestations. The clinical spectrum of the motor fluctuations has been amply inspected during the past few years.
Patients under dopaminergic replacement therapies are know to manifest, after a while, complications of motor symptoms and dyskinesia. Motor fluctuations manifest as "wearing-off", which consists in the reappearance of the typical motor signs near the end of the therapeutic window, unpredictable "Off" periods without any obvious connection with the levodopa intake, and failures in the "On" response.
Dyskinesia refers to involuntary altered movements or postures, including chorea and dystonia, and can affect either the arms, the legs, or the entire body. It is determined by the variations in the dopamine synaptic levels and usually occurs during the "On" state.
The non-motor features of the disease can fluctuate as well under the long-term levodopa treatment [7]. Although the relationship between motor and non-motor manifestations is still unknown, it is well established that patients with motor fluctuations also suffer of non-motor fluctuations [26]. The spectrum of the non-motor fluctuations encompasses three distinct categories: neuropsychiatric, sensory, and autonomic fluctuations. Neuropsychiatric disturbances include depression, anxiety, apathy, mood impairment, fatigue, slowness of thinking, mental hyperactivity, confusion, aggressive behaviour, and cloudiness. Sensory symptoms include visual disorder, neuralgic pain, and diffuse discomfort. Autonomic fluctuations include constipation, abdominal bloating and pain, facial flushing, bladder dysfunction, drooling, abnormal sweating, and sexual disorders [7].
The time occurrence of these motor fluctuations in relation to the levodopa cycle is still unclear. Among neuropsychiatric manifestations, signs such as depression or anxiety are more likely to be observed during the "Off" phase and might be attributed to a reduced dopaminergic stimulation [7]. However, the connection between an impaired mood and the "Off" motor state might also suggest that the

neuropsychiatric fluctuations are barely a reaction to the motor condition. Since an association between motor and autonomic oscillations is less obvious, the fluctuating nature of autonomic symptoms is more likely to reflect the treatment effect rather than a response to the motor behavior.
The expression of the autonomic fluctuations in relation with the "Off" and "On" phases is unclear and previous studies reported controversial information. In 2002, Witjas et al. showed an association between some autonomic symptoms, such as constipation and urinary urgency, with an "Off" state and failed in showing this connection with other symptoms such as sweating and abdominal disturbances [27]. In 2017, Ossig et al. reported that sweating was more frequent in the "Off" state, whereas urinary urgency or sialorrhea did not vary from the "Off" to the "On" state [28]. In 2015, Fauser et al. showed that the association between autonomic oscillations and motor states was not constant, suggesting an intra-individual variability of autonomic fluctuations [29].

2.3 Heart Rate Variability

2.3.1 Clinical applicability

The heart rate variability has proved to be an effective and non-invasive assessing tool in several applications and in disparate disorders featured by an impaired cardiovascular response, such as PD and congestive heart failure. Particularly, the status of the cardiac autonomic regulation in both healthy and not healthy people has been deeply investigated by evaluating and interpreting the heart rate (HR) and the heart rate variability pattern.
As the SA node activity is modulated by both the influences of sympathetic and parasympathetic systems, which provide substantial innervation to it, cardiac rhythms and inter-beats intervals are deeply affected by the interplay of these two branches [30]. Thus, the quantification of the amount of variability over the cardiac cycles can be employed as a dynamic measure of cardiovascular response, providing a picture of sympathetic and parasympathetic activation in response at unexpected and transitory stimuli and illustrating the autonomic nervous system functioning at the heart level [4].
Over the past research, it has been assessed both by itself or coupled with other techniques, such as the functional magnetic resonance imaging (fMRI) [4], [31], to reflect the neural functions and the connection between cardiac denervation and cardiovascular response.

2.3.2 ECG waveform

The electrocardiogram (ECG) is a simple time-voltage graph that consists of very specific waveforms, segments, and intervals representing the cycle of depolarization and repolarization processes into the heart.
The ECG signal features the electrical currents that originate within the SA node

and spread through the cardiac muscle. The electrical pulses resulting from the synchronous activity of the pacemaker cells in the SA node first proceed toward the atria, then toward the ventriculi through a system named Purkinje fibers. The electrical activation is called depolarization.
When the cardiac cells are stimulated, the heart depolarizes, generating a difference in the electric voltage on the cells' surface [32]. This difference induces the formation of an electrical current that is captured and pictured on the ECG signal by the P waves and the QRS complexes. The repolarization occurs when the cells potential returns at the resting condition, and the repolarization of the ventriculi is portrayed by the final T wave.
The ECG waveform comprises a set of distinct waves, each marking a specific physiologic event. The first component that can be observed is the P wave, which features the atria depolarization. As the atrial musculature is not substantial as the ventricular, the voltage change characteristic of the P wave is quite small if compared with the following waves [30].
The main constituent of the ECG waveform is the QRS complex, which follows the P wave. The QRS is the largest part in terms of amplitude and features the ventricular depolarisation. Although this is not always observed, it typically encompasses three distinct deflection, Q wave, R wave, and S wave respectively. If the first deflection of the complex is negative, this consists in the Q wave. The R wave is the positive deflection of large amplitude that is commonly observed in the ECG graph. Finally, the S wave is the last negative deflection that occurs after the R wave [32].
The ventricular repolarization is represented by the T wave, which follows the S wave of the QRS complex, whereas the atrial repolarization is typically not seen in the ECG, since its amplitude is too low and hidden by the ventricular depolarization.
The ECG segments consist in the distances between separate waveforms. There are three main segments: the PR segment, which marks the beginning of the atrial repolarization, the ST segment, which represents the ventricular repolarization, and the TP segment, which coincides with the resting condition and is commonly interpreted as the baseline status [32].
The intervals are fractions of the ECG which include one or multiple waveforms. The PR interval begins with the P wave and ends at the beginning of the QRS complex. The QRS interval measures the duration of the QRS complex. The QT interval encompasses both the QRS complex and the T wave, since it starts at the beginning of the QRS and ends at the end of the T wave [32]. Finally, the RR measures the distance between distinct QRS complexes and is fundamental to compute the heart rate.
Figure 2.5 represents the principal features appreciable on a ECG recording.

2.3.3 RR tachogram

The heart rate variability signal is measured as the distance between consecutive R waves in the QRS complexes and reflects the variation over time of the RR interval in the ECG recording. The graphical representation of the HRV resides in the RR

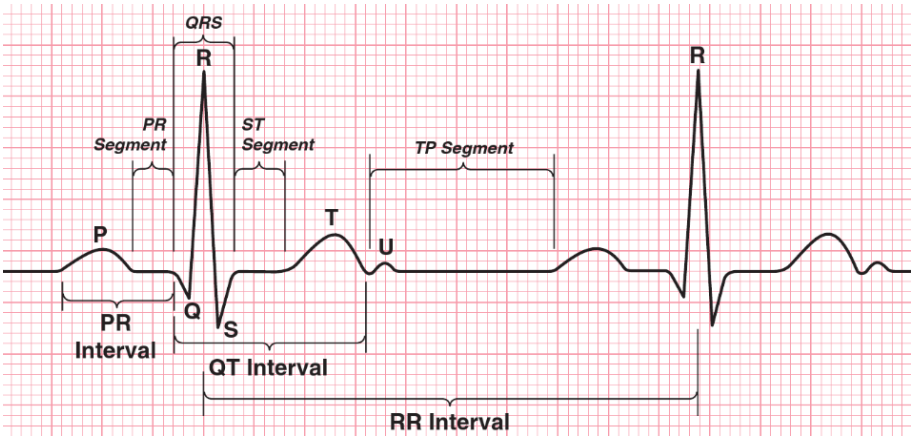

Figure 2.5: Principal components of the ECG waveform grouped in waves, intervals, and segments [32].

tachogram (Figure 2.6), which displays the RR intervals in function of time. The HRV is uniquely related to the HR and primarily reflects its physiologic rises and drops. A baseline HR is not constant but varies continuously in an intra-person and inter-person basis, even in similar conditions, in a manner that depends on the subject's cardiovascular fitness [30].

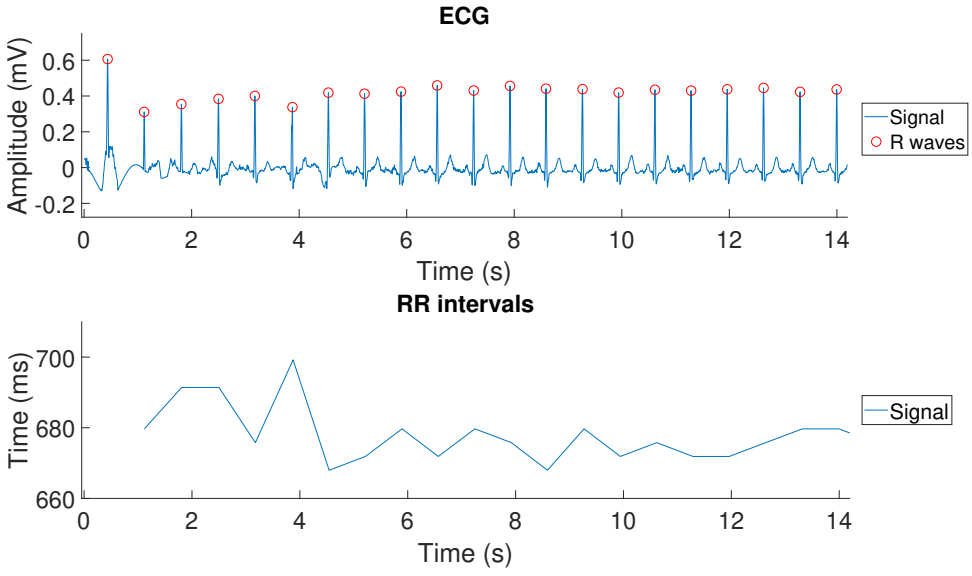

Figure 2.6: The first plot displays the ECG signal with the R waves marked with the red dots, whereas the second shows the relative RR intervals computed as differences between consecutive R waves.

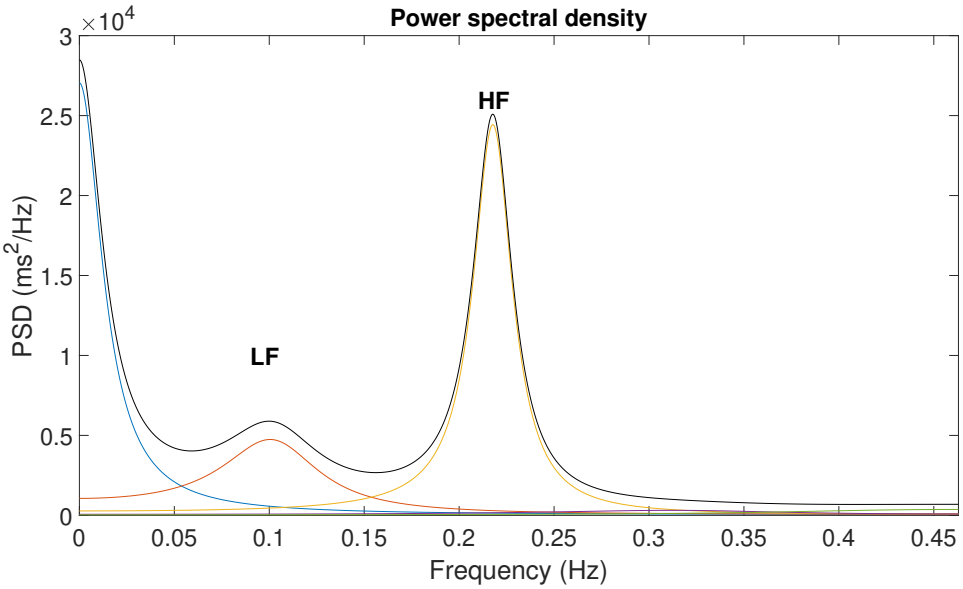

Figure 2.7: The principal frequency ranges investigated in the HRV spectral analysis consist in the LF band (first peak around 0.1 Hz) and the HF band (second peak around 0.225 Hz).

2.3.4 Quantification techniques

HRV signals can be assessed through several methods and techniques. Among them, conventional time and frequency domain analysis are markedly implemented as considered the highest validated and interpretable ones.
Time-domain analysis is the most obvious way to quantify the amount of variability over consecutive cardiac cycles [33] and consists in statistical measures of the HR and RR intervals. The principal time domain indices include the mean HR, the mean RR distance, the standard deviation of the RR distances, and the square root of the mean squared differences of successive intervals.
Although the time analysis is a simple way to extract the amount of variability from the RR series, it does not provide a clear separation for the sympathetic and parasympathetic influences. The spectral analysis aims in supplying such a distinction by highlighting how the power diffuses as a function of frequency [34]. The power spectral density (PSD) (Figure 2.7) is commonly computed through non parametric, such as the Fast Fourier Transform (FFT), and parametric autoregressive (AR) methods. The FFT is a simple and computationally easy to implement, whereas the AR model provides a smoother spectrum and a more accurate measurement of the power distribution among distinct components.
However, both techniques require a stationary signal. As the HRV is typically non-stationary, these estimates do not identify potential autonomic transitions during the time interval object of analysis and only provides averages that might obscure the dynamics of the autonomic modulation [34]. It might suggest the use of shorter observation periods, but shortest recordings limit the frequency components that can be distinguished. Several requirements should be followed to reliably perform a

spectral estimation. First, the ECG recording should be long enough to discriminate the frequency bands of interest. Second, the sampling rate should be sufficiently high that the Nyquist frequency of the spectrum is higher than the frequency range of interest. Third, the detection of the QRS complexes requires to be performed with an accurate algorithm able to correctly locate the R waves in time. Finally, the proper identification and removal of erroneous or missing data, ectopic beats and arrhythmic events known to affect the PSD estimation is fundamental.
The principal frequency ranges appreciable from short-term recordings (about 2-5 minutes) are the following: the very low-frequency (VLF) band (0.0033-0.04 Hz), the low-frequency (LF) band (0.04-0.15 Hz), and the high-frequency (HF) band (0.15-0.4 Hz). An additional frequency band, the ultra low-frequency (ULF) band (0.0001-0.0033 Hz), can be detected in long-terms recordings of 24 hours, although is commonly not assessed. The VLF band might be affected by baseline or trend removal algorithms [34] and might require long-term recordings of at least 1 hour to be interpreted in a reliable way. Thus, the VLF range is commonly excluded from the spectral evaluation of recordings shorter than 5 minutes.

2.3.5 Point-Process method

Typically, traditional methods implemented to characterize the heart rate variability are not able to highlight the physiological meaning of this marker, underestimating important features of it. First, such approaches tend to consider it as a continuous-valued signal rather than recognizing it as a train of discrete episodes, ignoring the stochastic nature of the heartbeats. Second, conventional methods do not provide instantaneous measures of heart rate variability but only averaged estimates over time [35].
To characterize properly the HRV, it is fundamental to understand the physiology behind them. Each R wave of the QRS complex marks the synchronous depolarization of the heart's pacemaker cells in the SA node [36]. After each depolarization, the cellular membrane potential drops to the resting potential, featuring the start of a new interval that persists until the next depolarization.
According to this concept, R waves can be delineated as isolate events unrelated to the previous or next ones, since they are determined by the pacemakers' cell depolarization. Under this assumption, the rise of the membrane potential can be modelled as a Gaussian random walk with drift, whereas the RR series follow an inverse Gaussian (IG) [35]. However, this hypothesis is not completely accurate since it does not consider the effects of the sympathetic and parasympathetic nervous system on the SA node. As these two subdivisions provide consistent innervation to the heart, they also considerably affect the cardiac dynamics. Although their activation is fast, their effects on the cardiovascular outflow can last for several seconds, influencing the next ventricular depolarizations.
Thus, a proper illustration has to consider the stochastic nature of the heartbeats intervals together with the action of the two autonomic branches. To fulfill this requirement, a dependence from the history of the past beats has to be introduced. In 2005, Barbieri et al. [35] developed a novel model for human intervals dynamics.

Particularly, the R events are framed with a history-dependent inverse Gaussian (HDIG) that predicts the next occurrence as a function of the previous heartbeats and is able to provide exact probabilistic characterizations of heart rate variability with any selected time resolution [35], [36]. This point-process framework provides instantaneous estimates of HRV in both the time-domain and frequency-domain and does not require to interpolate consecutive R events.

2.3.6 Spectral meanings of the HRV

The spectral analysis of the heart rate variability signal has been considered the major basis for the autonomic regulation understanding. The physiological interpretation of the HRV frequency ranges has been highly debated over the previous works, especially for the LF band.
Whereas a physiological process underlying the VLF band has failed to be shown, the LF and HF bands are well established to reflect the two autonomic branches of the ANS. Their effects can be investigated by observing the power spectrum behavior: in conditions of physical exercise, the power content typically shifts to the low frequencies, determining a high peak in the LF band, whereas a high peak in the HF band is more likely to be appreciated during rest, when the parasympathetic activity is dominant. Since the vagal influences on the heartbeat dynamics are almost instantaneous [4], the HF is mainly mediated by the vagal outflow. For this reason, the HF band has been implemented as a marker of parasympathetic activation in numerous previous studies [31], [37]–[41]. Moreover, the HF band is also called the "respiratory-band", since it reflects the respiratory-induced heart modulations regulated by the vagal drive.
Although the interpretation of the HF band is consistent among the previous studies, the physiological meaning of the LF band is less clear and more controversial [4]. Some have suggested that the mechanisms behind the LF component are mediated by the sympathetic activity, whereas others have disputed this assumption and theorized a combination of sympathetic and parasympathetic influences [42]. Whereas the slower activation of the sympathetic system does not allow it to influence the high frequency components of the spectrum, the vagal activity can feature both the low and the high frequencies.
Thus, since it is not possible to discriminate between the inputs of the two subdivisions from the LF band, focusing the attention on the evaluation of the HF band of the HRV signal has proved to be an efficacious and reliable approach to study the vagal contribution in the autonomic regulation [43] and many investigators based their analysis on this feature.

2.3.7 Circadian rhythms

It is now well established that the HRV signals can be influenced by several factors, such as gender and age [44]. Among them, the time of the day is also known to play a key role in modulating the homeostatic mechanisms.
Diverse studies have previously demonstrated that heart rate and heart rate vari-

ability are not constant during the 24 hours but fluctuate over the different phases of the day, especially between daytime and night [40], [41], [45]–[47]. In particular, they report an increased vagal tone during the night and the early hours of the morning. This pronounced parasympathetic effect is detectable by observing the HF component of the power spectrum, which has been found considerably higher throughout the sleep time and the first hours after the awakeness.
This phenomenon is known as circadian variations and is governed by a biological "clock" located in the suprachiasmatic nuclei of the anterior hypothalamus [47]. In 2005, Bilan et al. [46] investigated the circadian rhythms of the spectral indices of the heart rate variability signal in healthy subjects, to evaluate the diurnal fluctuations. Particularly, they compared the LF, HF and LF/HF indices between three phases of the day: during the morning (from 6 am to 10 am), the day (from 3 pm to 8 pm), and the night (from midnight to 6 am). They reported clear diurnal variations of the HF and LF/HF values, with higher values of HF during the night and the morning. According to this work, the HF content decreased by about 18% from the morning to the afternoon in the healthy subjects, indicating a decreased vagal activation.
As inclusions of αS have been observed in the anterior hypothalamus, the normal circadian pattern might be altered in subjects with a diagnosis of PD [48]. However, previous researches showed that in affected patients the HF content is lower as well during the daytime, proving that the rhythms observed in healthy people are at least in part preserved over the progression of the disorder.

Chapter 3

State of the art

This chapter provides a brief summary of the previous work accomplished to evaluate the HRV signal in PD subjects. The methods employed to assess and quantify the cardiac response and the results achieved on the investigated populations are here presented. The attention has been addressed to discuss the main findings in connection with the spectral analysis of the HRV, as it has been reported as a reliable indicator of autonomic control of the heart activity. A particular emphasis has been posed on the high-frequency component of the power spectrum, since it has been shown to reflect the parasympathetic contribution. Particularly, the following chapter aims to highlight whether this specific marker has been found significantly different between healthy and affected people and between PD groups characterized by a diverse stage of the disorder to investigate the potential vagal dysfunction. Finally, the investigation of the role of the levodopa on the parasympathetic system is also presented.

The analysis of the heart rate response has been deeply employed as a feasible instrument to assess the cardiovascular dysautonomia in Parkinson's patients. Particularly, the spectral analysis of the HRV signal has been commonly implemented to evaluate the separate contributions of the sympathetic and parasympathetic nervous system on the SA node activity. Most of the past research aimed at investigating the differences between affected people and healthy controls, questioning whether the autonomic outflow is impaired in Parkinson's subjects. A consistent fraction of the previous works reports a deterioration of the parasympathetic nervous system, mainly demarcated from a decreased high-frequency component of the power spectrum in Parkinsonian subjects.

In 2000, Kallio et al. [37] measured the HRV at rest in 50 untreated patients with a diagnosis of PD and 55 healthy subjects to assess the cardiovascular response as a marker of autonomic nervous system failure. The spectral analysis performed on the HRV signal evidenced a decrease in all the components (LF, HF and LF/HF) in PD patients when compared with the healthy controls. Particularly, the HF content showed a statistically significant difference between the two populations ($p = 0.0043$), indicating that the parasympathetic system failure reaches statistical significance in patients with an early diagnosis of PD, even in an untreated condition.

In 2001, Haapaniemi et al. [38] recorded the ambulatory ECG for 24 hours in 54 untreated patients with a diagnosis of PD and 47 age matched healthy controls to investigate the cardiovascular dysautonomia and whether the dysfunction is correlated with the progression of the disease. They reported that both the standard deviation of the RR intervals (SDNN) and the spectral components were significantly lower in the patients than in the controls ($p = 0.024$ and $p = 0.004$, respectively). This result suggested a pathologic involvement of the autonomic nervous system manifested as suppressed variability and lower activation of the parasympathetic nervous system even at the early stages of the disease. The disease duration did not correlate with the HRV measures, leaving open the debate about a potential connection between the progression of the pathology and the cardiovascular impairment.

In 2002, Kallio et al. [39] aimed in investigating different methods to assess the HRV, focusing in the frequency-domain and non-linear analyses. They showed that the spectral components of the HRV were the most efficacious parameters to separate untreated patients with a diagnosis of Parkinson's disease and healthy subjects into two populations, pointing out the key role of the spectral analysis in the assessment of the HRV. Particularly, they reported that all the power components are decreased in PD patients, with a statistically significant difference for the HF ($p = 0.010$). Their findings were consistent with their previous study, evidencing one more time a depression in the parasympathetic activity [37].

In 2002, Pursiainen et al. [40] investigated the circadian fluctuation of the heart variability in 44 untreated patients with a diagnosis of PD and 43 age- and sex-matched control subjects. Particularly, they recorded the ECG signal for 24 hours and compared the cardiovascular response of the two groups during the 24 hours, at night (from midnight to 6 am) and during the day (from 9 am to 9 pm). They reported that both the spectral components of the HRV, the LF and HF, were lower in the PD patients, and that the differences were statistically significant during the

night (24-hour HF: $p < 0.05$; day-time HF: $p > 0.05$; night-time HF: $p < 0.05$). This finding suggests that the suppression of the vagal function might be more pronounced during the night, when the parasympathetic tone normally predominates on the sympathetic one.

Although most of the past literature is focused on the comparison between healthy and Parkinsonian subjects, diverse groups hypothesized that there might be an influence of the disease stage on the autonomic functions. In 2003, Devos et al. [41] assessed the HRV time- and frequency-domain measures and the motor handicap in three groups of patients of different stages and severity of Parkinson's disease, aiming to investigate whether the disease duration and progression might affect the autonomic impairment. Group I included untreated patients with less than 2 years of progression of the disease, Group II levodopa-treated patients not experiencing motor fluctuations, and Group III levodopa-treated patients experiencing motor fluctuations induced by the parkinsonian medication. The spectral analysis of the HRV showed a statistically significant decrease in the HF band during the night in Group III compared to the other groups ($p = 0.005$), whereas there was no significant difference in the day HF power. The HF content decreased in all the groups shifting from the sleep time to the day, suggesting that the circadian pattern is preserved in all the investigated classes of Parkinsonian patients. Subjects in Group III did not significantly differ from the subjects in the other groups in terms of disease duration, suggesting that the distance in the HF might be more likely due to a different disease severity rather than duration. Moreover, the night HF showed a negative correlation with the motor scores of the "Off" state and the subscores for the axial and limb bradykinesia. According to the authors, this result reinforced the potential connection between the disease severity and the neuronal loss to the sympathetic and parasympathetic system structures.

In 2008, Pospisil et al. [49] assessed the spectral parameters of the HRV in two subsets of subjects featured with a different degree of motor impairment evaluated according to the Hoehn & Yahr score. Particularly, they were divided in mild-stage and advanced-stage patients. The primary aim of the research was to investigate whether the phase of the disease is correlated with the severity of the autonomic impairment. According to the authors, statistically significant differences were observed in the LF, HF and total power contents between the two groups, whereas the LF/HF ratio did not show significant variations. Particularly, all these spectral parameters were found to be low in patients with a more severe motor deficiency. The decrease in the HF suggests a relation between the progression of the disease and the parasympathetic suppression likewise observed by other studies in patients with PD.

In 2014, Brisinda et al. [11] evaluated the cardiovascular regulation in subjects with a clinical diagnosis of PD or multiple system atrophy assessing the time-domain and frequency-domain indices computed from the HRV. They reported statistically significant lower values for all the parameters in both groups compared to the healthy controls. Particularly, the authors claimed a connection between disease duration, motor disability and HRV anomalies, whereas they did not report differences between patients under the effects of the medication and patients in pharmacological

washout.

In 2015, Ruonala et al. [25] focused on investigating the effects of levodopa on the autonomic nervous system by assessing the HRV during the morning at different time points. Particularly, they evaluated eleven patients with a diagnosis of Parkinson's disease under levodopa treatment in three distinct moments: first, at baseline, in a practically-defined "Off" condition, which means that subjects were "Off-medication" from at least 10 hours, then 30 minutes and 60 minutes after a high dosage of levodopa. An effective "On" state, induced by the beneficial effects of the medication, after 30 and 60 minutes was confirmed by evaluating the motor scores assigned by a clinician. The spectral analysis of the HRV showed a significant decrease of about 50% in the median of the HF component 30 and 60 minutes after the medication intake, denoting that levodopa might have an effect on the autonomic modulation of the heart. Particularly, this result suggests a further suppressing action on parasympathetic activation by the anti-parkinsonian medication. Both the LF content and the LF/HF ratio did not show significant changes between the three times of assessment.

All the above mentioned studies assessed the HRV with traditional approaches, which typically characterize the RR intervals as connected values in time by interpolating them or their reciprocal [36]. This genre of analysis does not allow to reflect the real nature of the R events, which are more likely discrete occurrences rather than continuous signals and need to be treated as separate points in time.

In 2005, Barbieri et al. [35] developed a novel approach for the HRV analysis based on a point-process method. This algorithm models the heartbeats as a history-dependent inverse Gaussian probability distribution, thus reflecting both the stochastic nature of the R events and the influence of sympathetic and parasympathetic systems on the SA node activity. They implemented this approach to obtain probabilistic definitions of HR and HRV, updating continuously the time-varying parameters of the distribution to gather instantaneous estimates with any time resolution desired [36]. This novel framework was tested by comparing simulated data and real data in both healthy subjects and patients with congestive heart failure [36], [50] and proved to be a reliable tool to model and analyze the R events.

In 2013, Barbieri and his team [51] started focusing on PD and assessed the HRV signal in healthy controls and in affected patients by applying the point-process algorithm on the RR series. Particularly, they extracted conventional parameters of the HRV together with the Lyapunov spectrum as nonlinear measure of heartbeats dynamics. They reported significant differences between healthy and affected patients only in the Lyapunov exponents, whereas common time-domain and spectral indices did not show significant variations between groups. Particularly, both the first and second Lyapunov exponents proved to be higher in Parkinson's patients, suggesting a less stable interval dynamics in the affected subjects.

In 2014, the same group [52] aimed in evaluating the HRV features extracted from the point-process method to investigate the potential connection between autonomic dysfunction and cognitive impairment in Parkinson's disease. Particularly, they compared eight cognitively preserved and eight mild-impaired patients. In addition to the conventional measures of HRV, they computed the approximated and sample

entropy as nonlinear parameters. They reported significant differences only in the sample entropy computed from the point-process, which proved to be higher in the cognitively preserved subjects ($p = 0.049$), whereas no other indices showed significant discrepancies between the two groups. This finding suggests that a cognitive damage might be related with an increased cardiovascular instability due to autonomic anomalies and that this relation can not be detected with traditional indices. In 2016, Valenza et al. [53] implemented the point-process algorithm to compare the HRV parameters between healthy controls and patients affected by PD. Particularly, they assessed the differences between groups and within Parkinson's patients to investigate whether the disorder is related with an impaired autonomic regulation of the cardiac rhythms and the potential correlation between autonomic impairment and disease progression. Interestingly, they reported a significant correlations between HRV estimates and neuropsychological evaluations, leaving open the hypothesis of the existence of a link between autonomic dysfunction and cognitive impairment.

Latterly, the research has started moving the point of interest through the joint investigation of the HRV parameters and the neuronal affection via neuroimaging techniques. In 2009, Hænsch et al. [54] assessed the autonomic disturbances in 58 treated patients with a diagnosis of PD evaluating the connection between the cardiac sympathetic denervation analysed via neuroimaging techniques, the OH and the HRV. The authors aimed at understanding the potential concurrence of loss of sympathetic innervation, baroreflex failure and impaired autonomic regulation. All the PD patients showed a severe decrease in I23I-metaiodobenzylguanidine, a tracer for sympathetic neuron integrity and function, confirming a severe cardiac sympathetic denervation. This reduced uptake did not significantly differ between patients with or without OH, suggesting that the two aspects are unrelated to each other. All the spectral components of the HRV were lower in PD patients with OH when compared with PD patients without OH, indicating a relationship between the occurrence of the OH and the autonomic dysregulation. However, the authors did not report the correlation between sympathetic denervation and measures of HRV, whereas it could be interesting evaluating the relationship between the loss of sympathetic nerves and the cardiac response.

In 2019, Tessa et al. [31] investigated the connection between the HRV parameters and the cerebral activation of the brain regions involved in the autonomic control, comparing healthy subjects and newly-diagnosed Parkinson's patients. Particularly, they conducted a joint analysis between the fMRI time-series and the HF content of the HRV power spectrum, to assess whether the central circuitry that controls the parasympathetic activation is affected at the onset of the disorder. They reported a weaker anti-correlation between fMRI time-series and HF-HRV in newly-diagnosed subjects compared to healthy controls, suggesting that an altered parasympathetic control of the heart develops at the initial phases of the pathology and is likely due to a loss of innervation.

Chapter 4

Materials and methods

The following chapter aims to present the participants enrolled in the study and the methods employed to analyze the HRV signals.
The first section focuses on the data collection, discussing the attended steps and the protocols designed for both the laboratory and the simulated apartment visits. As preliminary procedures, the positioning of the wearable sensors and the other technologies implemented are described. Moreover, the distinct stages that have been covered during the entire data collections and the explanation behind their subdivision are discussed.
The second section presents the demographic characteristics of the participants enrolled in the study and the results of the neurological tests performed to evaluate the stage of the disorder and the cognitive status. The inclusion and exclusion criteria are also reported.
The third section explains the criteria employed to select and isolate time intervals of interest, distinguishing between the measures obtained from the data collection in the laboratory and simulated apartment.
The fourth section provides a substantial presentation of the guidelines and methods conformed to analyze the HRV data. Particularly, it starts describing the ECG pre-processing, with regard to the techniques employed to clean the raw data and identify the QRS complexes. After, it describes the step attended to detect and correct potential erroneous R waves due to a miscalculation in the previous stage or to physiologic reason. For this particular purpose, an algorithm able to recognize and revise ectopic and arrhythmic events is presented.
The fifth section presents the point-process algorithm implemented to model the R waves computed in the previous steps. Particularly, it focuses on the description of the mathematical explanations behind this framework and the benefits that its implementation offers.
Finally, the last section shows the indices extracted to perform the analysis, distinguishing between time-domain and frequency-domain parameters.

4.1 Data Collection

4.1.1 Laboratory

Preliminary procedures

This thesis is part of the larger BlueSky Project and all the analysis have been accomplished on data collected from Study 3 of it.
The Institutional Review Board at Spaulding Rehabilitation Hospital approved this study (#2016P002422). The data collection was structured in two separate visits.
Visit 1 was performed in the Spaulding Rehabilitation Motion Analysis Laboratory (Figure 4.2a). First, every subject signed the consent form. Then, patient demographics, medical and medication history were meticulously documented. The stage of the disease was investigated with the Hoehn & Yahr (H&Y) scale and the global cognitive status was assessed with the Montreal Cognitive Assessment scale (MoCA).
Wearable sensors were positioned on the subject body. The Opal sensors were placed on the left and right feet, left and right wrists, sternum and lower back to record the acceleration, the angular velocity, and the orientation data. The Biostamp RC sensors were positioned on the manubrium, right anterior thigh, left anterior thigh, left and right forearms (over the flexor muscles), left and right forearms (over the extensors muscles), and left and right shanks to record the acceleration, the angular velocity, the surface electromyographic data, and the electrocardiogram. The Shimmer sensors (Figure 4.1b) were positioned on the chest and clavicula to record the electrocardiogram and the galvanic skin response, respectively. Particularly, the ECG has been recorded by placing three electrodes in V1, V3 and V5 shown in Figure 4.1a. Other technologies implemented in the study included a pressure mat, 9 server-based cameras, 2 Microsoft Kinetics, and High-quality microphone setup with Audacity.

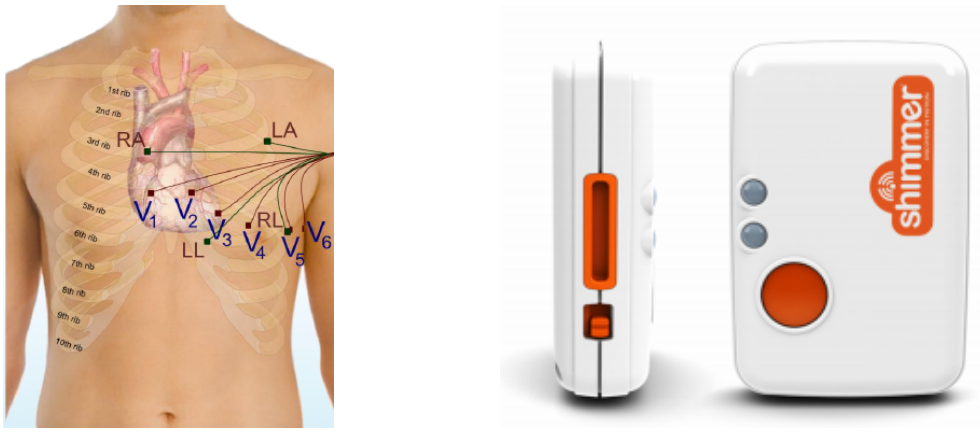

(a) (b)

Figure 4.1: Shimmer setup.

Sessions setup

Visit 1 lasted approximately the duration of one cycle of the levodopa-carbidopa administration and encompassed five distinct sessions (Figure 4.2b), each linked to a different stage of the cycle. When in use, other medications were not discontinued. Subjects took their normal medication dose in the morning and started the visit in an "Off" condition, approximately two hours prior to their scheduled second normal medication dose. Although several studies adhere to the practically defined "Off" condition, which requires a last intake dating back to the day before, here it was avoided to reproduce a real-life condition. An effective "Off" status was self-reported by the subjects, who were continuously asked to confirm their perceived condition. This first phase corresponds to session 1.
The medication intake marked the end of session 1 and the beginning of session 2, during which subjects experienced the transition to the "On" phase as an ameliorate in the motor symptoms. The duration of session 2 was not regular but compatible with the rapidness of the transitioning.
Session 3 referred to an "On" condition and started when the subjects were able to confirm a beneficial response to the levodopa due to the improved motor performances.
Session 4 opened in concurrence with the vanishing of the medication effects and was recognized as the transitioning to the "Off" phase. Session 4 lasted until subjects claimed to feel "Off" again, condition that formalized the beginning of session 5.
Whereas session 1, 3, and 5 have been fulfilled by the totality of the subjects, session 2 and 4 lack in part of them who experienced a very fast transitioning to a status to the other.
During every session, the subjects were asked to perform specific tasks, and every task was continuously timed and assessed by the clinician in multiple ways. A first battery included the administration of the Unified Parkinson's disease scale promoted by the Movement Disorder Society (MDS-UPDRS III), controlled speech sample (CSS) and scripted activities of daily living (SADLs), and was performed during sessions 1, 3 and 5. A second battery included the administration of the MDS-UPDRS III and the speech assessment and was performed during session 2 and session 4. Moreover, during each session subjects were asked to answer specific questions, indicating their status ("On"/ Transitioning to "On"/ "On" with dyskinesia/ Transitioning to "Off"/ "Off"), an explanation of the status and the current level of fatigue, difficulty to move and difficult to concentrate in a scale between 0 and 10 (where 0 identifies no fatigue and 10 high level of fatigue). In addition, every 30 minutes the subjects experienced 3 minutes of rest, during which they were asked to assume a comfortable seated position and to be silent, and 30 seconds of Alternative Hand Movements for both left and right hand.
Clinical scores for tremor, dyskinesia, and bradykinesia were assigned by the clinician during each task of the activities of daily living and during the three minutes of rest. The tremor was assessed in terms of amplitude in a scale between 0 to 4, where 0 defines the absence of the symptom, 1 a tremor with an amplitude inferior than 1 cm, 2 a tremor with an amplitude between 1 and 3 cm, 3 an amplitude between

3 and 10 cm and 4 a tremor with an amplitude greater than 10 cm. The dyskinesia was assessed in terms of type (dystonic, choreic, or both) and amplitude (0-4, with the same criteria adopted for tremor). The bradykinesia was assessed with a score ranging from 0 to 4, according to the MDS-UPDRS III.

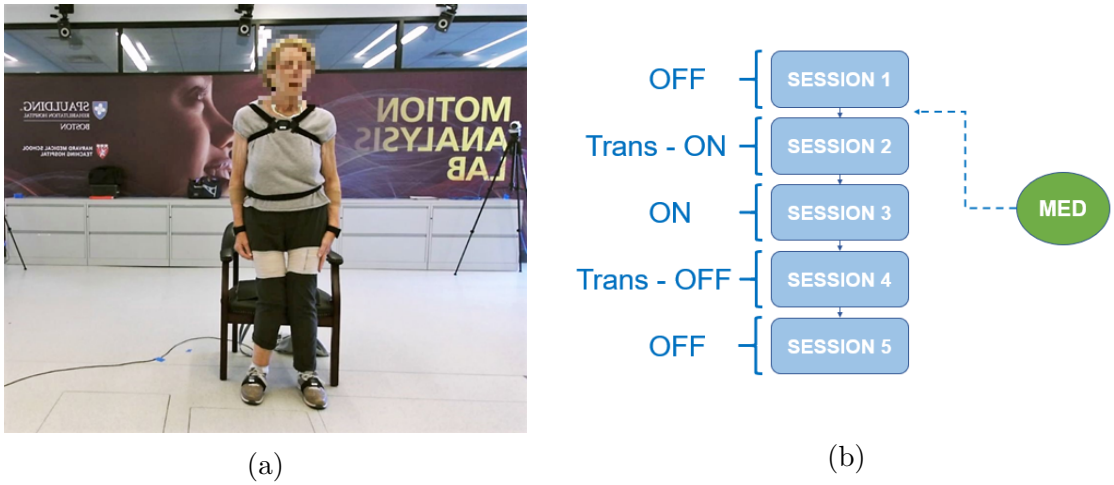

(a) (b)

Figure 4.2: Motion Analysis Lab (Spaulding Rehabilitation Hospital, Charlestown MA) data collection (a) and protocol (b).

4.1.2 Simulated apartment

Preliminary procedures

Visit 2 was performed in the simulated apartment inside the Spaulding Rehabilitation Hospital (Figure 4.3a). Twelve GoPro Cameras were positioned over the apartment to videotape the subjects during the entire visit. Only the restroom was not videotaped for privacy reasons.
The Opal sensors were placed on the left and right feet, left and right wrists, sternum and lower back to record the acceleration, the angular velocity, and the orientation data. The Biostamp RC sensors were positioned on the manubrium, right anterior thigh, left anterior thigh, left and right forearms (over the flexor muscles), left and right forearms (over the extensors muscles), and left and right shanks to record the acceleration, the angular velocity, the surface electromyographic data, and the electrocardiogram. The Shimmer sensors were positioned on the chest and clavicula to record the electrocardiogram and the galvanic skin response.
The visit started with a motor examination performed by the clinician through the MDS-UPDRS III inside the apartment. Then, subjects were left alone (or with the caregiver, when present) and free to autonomously perform activities of daily living. A short list of common tasks, including unloading grocery bags, brushing the teeth, and cooking a meal, has been assigned to subjects to reproduce normal activities of real-life.
The visit sustained approximately the duration of one cycle of the levodopa-carbidopa

administration. Contrarily to the laboratory, each session did not relate with a specific phase of the medication cycle and lasted about an hour (Figure 4.3b). Thus, the number of sessions was not fixed and varied according to the duration of the levodopa cycle.
Every hour subjects were examined via laptop agreeing to a short version of the MDS-UPDRS III and asked to access a tablet to fill a questionnaire providing the self-report state ("On"/ Transitioning to "On"/ "On" with dyskinesia/ Transitioning to "Off"/ "Off"), an explanation for the self-report state, and the level of fatigue, difficulty of movement and difficulty of concentration in a scale between 0 and 10 (where 0 identifies no fatigue and 10 high level of fatigue). The time of the last medication before the start of the visit was documented, whereas the times of intake inside the apartment are almost totally unknown.

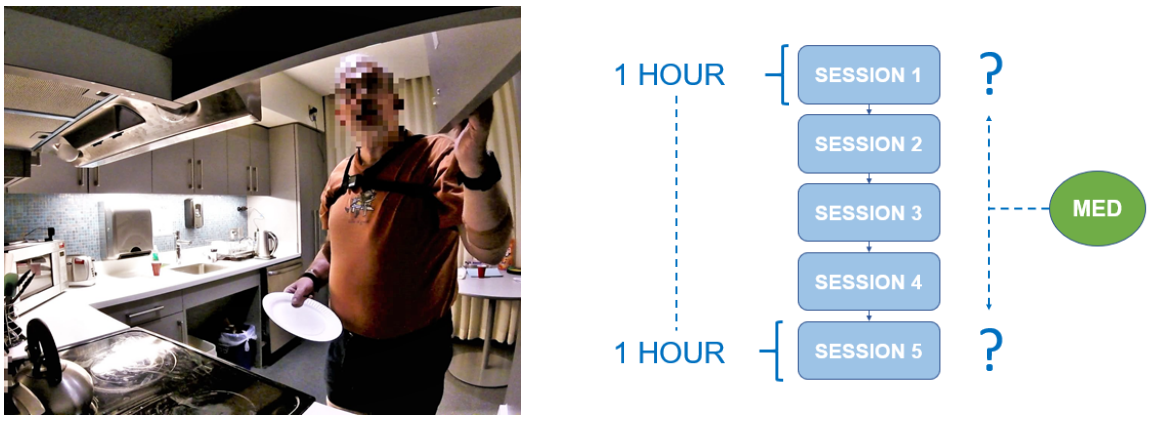

(a) (b)

Figure 4.3: Simulated apartment (Spaulding Rehabilitation Hospital, Charlestown MA) data collection (a) and protocol (b).

4.2 Participants

4.2.1 BlueSky participants

Twenty-six long-term levodopa-treated PD patients experiencing motor fluctuations were enrolled in Study 3 of the BlueSky Project (19 males, 7 females; age 66.1 ± 8.2 years; first symptom 53.3 ± 10.6 years; first diagnosis 54.8 ± 10.4 years; MoCA 27.2 ± 2.5; 85% with a Hoehn & Yahr of 2 and 15% of 3). Participants characteristics are summarized in Table 4.1.
All the participants met the Inclusion Criteria, which are briefly enumerated as following: 1) A clinical diagnosis of idiopathic Parkinson's disease consistent with the United Kingdom (UK) Parkinson's Disease Society Brain Bank Clinical Diagnostic Criteria by a qualified neurologist; 2) Incidence of motor fluctuations and dyskinesia; 3) The understanding of the "wearing off" condition and the confirm that there is usually an improvement after the next dose of antiparkinsonian medication; 4) A

Parkinson's disease Hoehn & Yahr Stage less than or equal to III (assessed during the "On" state); 5) The response to levodopa therapy; 6) A stable parkinsonian medication regimen including levodopa for at least 4 weeks, with strong preference for patients able to use only immediate release levodopa treatment during the study session; 7) Male of female aged between 30 and 80; 8) The capability to understand and cooperate with study procedures and give informed consent; 9) A Body Mass Index (BMI) of 17.5 to 35 kg/m^2 and a total body weight $\geq$ 45 kg; 10) A normal or corrected-to-normal vision.
Exclusion criteria were: 1) Any current history of neurological disease (except for Parkinson's disease), cognitive impairment, or psychiatric illness that in the investigator's judgment would interfere with subject participation (e.g. clinically significant stroke, brain tumor, hydrocephalus, epilepsy, other neurodegenerative disorders, encephalitis, repeated head trauma); 2) Any unstable medical condition; 3) Treatment with an investigational drug within 30 days, or 5 half-lives preceding the first study visit; 4) Subjects who are investigational site staff members directly involved in the conduct of the study and their family members, site staff members otherwise supervised by the investigator, or subjects who are study site employees directly involved in the conduct of the study; 5) History of head injury with clinically significant sequel (e.g. loss of consciousness); 6) The presence of any implanted medical devices, including deep brain stimulation devices; 7) A pregnancy; 8) An allergy to adhesives or silicone.

4.2.2 Controls

To compare the cardiovascular autonomic regulation in healthy controls and Parkinson's subjects, fourteen healthy controls enrolled in 2018 in the Respiratory Infection-like Symptom Study (age 40 $\pm$ 11.1 years) and eighteen Parkinson's subjects (age 62.5 $\pm$ 9.7 years, first diagnosis 55.3 $\pm$ 10.1 years, levodopa treatment 6.1 $\pm$ 3.6 years) have been analyzed.
For the healthy group, the sensors data recorded during the second visit of the study in the Motion Analysis Lab (Boston, MA) have been processed. Particularly, data were collected when applicants completely recovered from the flu. The ECG signals were recorded with the Biostamp sensors positioned on the chest and thigh during the entire session.

4.3 Signal segmentation

4.3.1 Laboratory

The raw ECG signals have been segmented in five distinct subdivisions, where every subdivision referred to a specific session. The segmentation has been done according to the labels with the time of beginning and end of each session. Each segment has been further processed separately.
As the RR intervals behavior is profoundly affected by several factors, such as stress-

Demographics	
Number of participants	26
Age (years)	66.1 ± 8.2 (42-80)
Height (cm)	175.4 ± 10.3 (152-196)
Weight (lbs)	182.7 ± 34.9 (16-260)
Gender (%)	
Male	19 (73.1)
Female	7 (26.9)
Handedness (%)	
Left	3 (11.5)
Right	23 (88.5)
Highest Education (%)	
High School	4 (15.5)
College	13(50.0)
Post Graduate	9 (34.6)
First Symptoms (years)	53.3 ± 10.6 (31-76)
First Diagnosis (years)	54.8 ± 10.4 (32-76)
MoCA	27.2 ± 2.5 (21-30)
Current Medications	
Ldopa (%)	26 (100)
Agonist (%)	13 (50)
MAO-B Inhibitor (%)	9 (35)
Anticholinergic (%)	1(4)
COMT Inhibitor (%)	7 (27)
Hoehn & Yahr (%)	
1	0
2	22 (85)
3	4 (15)

Table 4.1: BlueSky Participants

ful exercises, a baseline condition has to be considered to perform an accurate analysis. Particularly, the level of activity is crucial in the modulation of the HR. Thus, to assess consistently the RR intervals trend over the medication cycle, exclusively the signal segments concomitant to the 3 minutes of rest have been selected. During this time interval, the subjects were asked to be silent and seated in a comfortable position. This selection allowed us to avoid eventual distortions introduced by the tasks performed over the course of the visit or the speech. The 3 minutes of rest isolation has been adopted for the laboratory visits of both the Parkinson's subjects and the healthy controls.

4.3.2 Apartment

Accelerometer data

The signal segmentation for the apartment data has been performed differently, as the apartment visit does not provide specific labels for the tasks accomplished.
The first requirement that needs to be satisfied to be consistent with the laboratory-analysis is the sitting position. Segments of ECG signals during rest and in absence of movements have been isolated according to the processing of the accelerometer data recorded by the sensors located on the lower limbs.
The accelerometer time series have been first segmented into 5 seconds windows overlapped by the 50% and different parameters have been computed within every window. These parameters include the root mean square of the time series, the energy magnitude and the power, and different FFT-based parameters, such as the values of the dominant frequencies and the entropy of the power spectral density. A binary score has been assigned to each window: a score of 0 marked a higher level of movement, whereas a score of 1 featured a condition of rest.
Starting from these estimates, an additional algorithm has been implemented to isolate consecutive segments of accelerometer series identifying a very low level of activity. A code working with two different thresholds has been implemented to identify effective resting periods without considering potential artifacts or isolate movements not related to an effective stressful activity. The first threshold focused on the number of consecutive 5 s windows with a prediction of 0 (movement). Particularly, the algorithm identified and discarded segments with at least 3 5s-consecutive windows scored with a 0. In that way, if the prediction was 0 for less than 15 s, the algorithm marked it as an artifact and did not recognize an effective activity. The second threshold focused on the energy magnitude: if the mean of this parameter through at least three consecutive windows with a 0 score was higher than the maximum set as threshold (0.05 of the normalized energy magnitude), an activity was detected and those windows discarded, otherwise the movement was identified as an isolate episode, such as a tremor. To further avoid the erroneous detection of artifacts, both feet were considered: if the subject was moving according to a unique foot and resting according to the other one, the activity was not detected.
In this way, the signal segments where the subject was supposed to be at rest were identified. Figure 4.4 shows an example of the activity detection approach: the red line marks the resting condition (0 = movement, 1 = rest), whereas the energy magnitude is displayed by the blue line.
Finally, the accelerometer data recorded from the wrists and the trunk has been checked as well for those segments recognized as “resting times” to understand if the subject was performing strenuous activities with the upper part of the body.

Videos

Although the accelerometer analysis might allow a proper detection of periods of rest, it does not provide information about the speech, which is likely to affect the HRV signal as well. Even if the subjects were mostly alone inside the apartment,

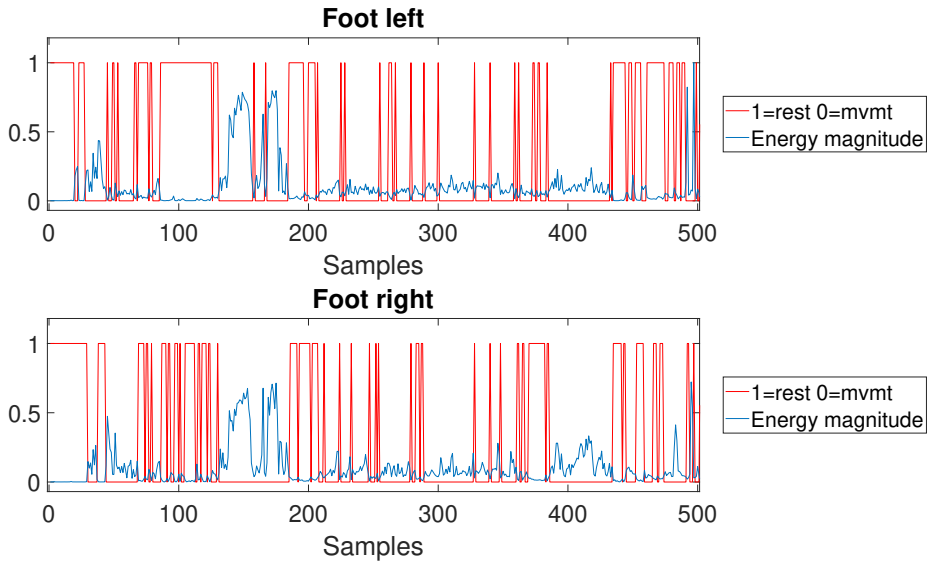

Figure 4.4: Energy magnitude of the accelerometer time series and resting prediction expressed in a binary code (0 or 1) for foot left and right.

a couple of them fulfilled the visit in the company of a caregiver and they were all free to talk at the phone. Moreover, the investigators of the study had to interfere at some point to substitute the sensors that were running out of battery.
To confirm a "silent condition", the video recordings collected with the twelve GoPro cameras located inside the simulated apartment have been checked and each segment involved with the speech has been discarded. This control also allowed to validate the output of the accelerometer analysis and to confirm the real posture of the subjects, discriminating between sitting or supine positions. Particularly, the supine posture has been discarded to remain consistent with the laboratory analysis. The resulting ECG segments have been isolated and the related RR intervals have been obtained.

4.4 Signal pre-processing

4.4.1 ECG filtering

The electrocardiographic (ECG) signals have been recorded with the Shimmer sensors with a sampling frequency of 256 Hz from twenty-six subjects with a diagnosis of PD and with the Biostamp sensors with a sampling frequency of 250 Hz from the healthy controls. Raw sensors data in .csv files have been loaded in Matlab and stored in a table containing two distinct variables, i.e. the ECG signal and the relative timestamps.
ECG signals have been filtered with a Chebyshev type II passband filter with the following specifics: a filter order set to 6, a frequency passband between 0.5 and 100 Hz, and ripples in the passband set to 80.

4.4.2 QRS-complexes detection

Two different approaches have been tested to identify the exact location in time of the R waves: a wavelet transform and the Pan-Tompkins Algorithm.

Wavelet transform

The wavelet transform is a signal-processing tool commonly implemented in non-stationary signals analysis. It decomposes the signal into distinct time-frequency levels, providing a representation of the signal that resemble the features of interest. Two principal categories of wavelet transform can be distinguished, the continuous wavelet transform (CWT) and the discrete wavelet transform (DWT), and they differ on how the wavelet is scaled and shifted. CWT is defined as the convolution of the signal of interest with a scaled and translated version of a wavelet function. DWT is defined as a discretized dilations and translations of the analyzing wavelet and is applied for discrete time-signals. DWT decomposition can be obtained by successive high-pass and low-pass digital filtering of the signal in time domain.
For the QRS complexes detection, the maximal overlap discrete wavelet transform (MODWT) has been implemented to enhance the R peaks in the ECG waveform. The ECG waveform has been decomposed down to level 5 using the "sym4" wavelet. Then, a frequency-localized version of the ECG waveform has been reconstructed using the wavelet coefficients at scale 4 and 5. Scale 4 encompasses frequencies between 11.25 and 22.5 Hz, whereas scale 5 frequencies between 5.625 and 11.25 Hz. These scales allow to cover the passband shown to maximize the energy associated with the QRS complex [55].

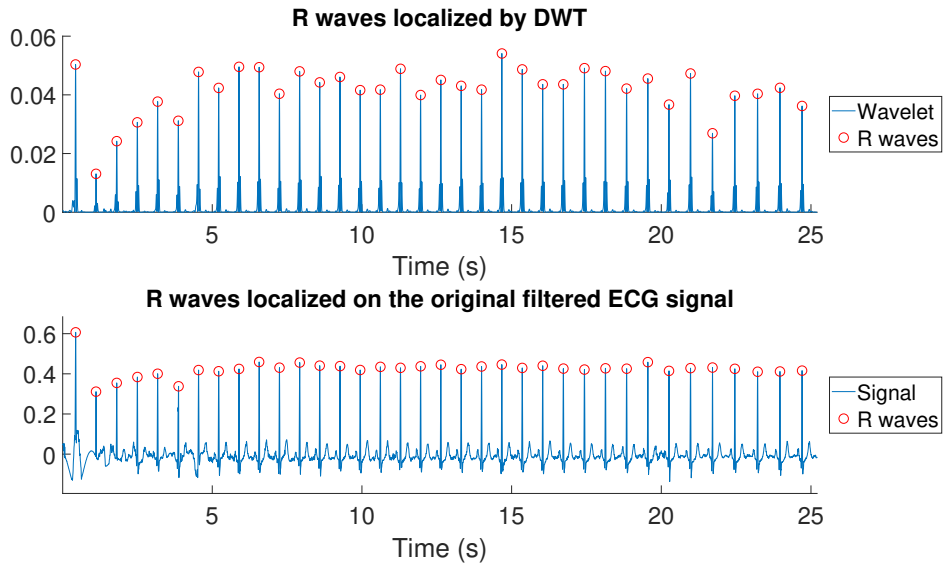

Figure 4.5: The first plot displays the peaks identified on the DWT, whereas the second reports the relative R waves on the filtered ECG signal.

Pan-Tompkins algorithm

This algorithm was developed in 1985 by Jiapu Pan and Willis J. Tompkins to recognize in real-time the QRS complexes from the electrocardiograms [56]. It is a reliable detector that combines adaptive thresholds to identify with high sensitivity the R waves in the ECG recordings.
First, the raw signal is bandpass filtered by subsequently applying low-pass and high-pass filters to remove the additional noise and maximize the QRS complexes energy in the bandpass between [5-15] Hz. After that, the filtered version of the signal is differentiated with a five-point derivative filter to obtain the slope of the QRS complexes. The following step involves a point-by-point squaring of the signal, to construct a positive version of it and to amplify the output of the differentiation. Finally, the signal is integrated with a properly shaped moving-window to further emphasize the QRS complexes.
The Pan-Tompkins approach implements two sets of thresholds for the peaks-detection: the first one thresholds the bandpass-filtered version of the ECG before the derivative, whereas the second set thresholds the signal obtained after the integration. To be identified as a R wave, a peak must be detected in both the filtered ECG and the integrated version. Each set entails two distinct levels, where the lower is the half of the upper one. Moreover, thresholds are not constant but adaptive: they are continuously regulated according to the local characteristics of the signal to overcome the noise.
Figure 4.6 shows an example of the implementation of the algorithm. The first plot displays the R waves detected on the filtered ECG signal, whereas the second presents the integrated version of it. Both of them report the adaptive threshold, the running signal level, and the running noise level. If the algorithm does not detect a R event in 1.66 times of the average of the previous RR intervals [57], the maximum value detected in that period is selected as R wave and the lower threshold is selected. Once a valid event is detected, a refractory period of 200 ms is started: during this period, other QRS-complexes cannot be recognized.

R waves localization

The wavelet method proved to be the most reliable. First, it displayed higher accuracy in identifying the exact peak locations. Second, it was not influenced by the presence of noisy data, as it does not implement adaptive thresholds that vary according to the quality of the signal. Thus, the wavelet approach has been implemented for all the ECG recordings.
The Matlab function “findpeaks” has been applied on the wavelet transform of the ECG signals with the following parameters: a minimum peak height set to three times the mean value of the wavelet and a minimum peak distance set to 400 milliseconds. The first specific has been selected trying different values and observing the results, as it proved to be the one with the highest sensitivity. The second specific has physiological reasons, since two R waves are unlikely to occur in

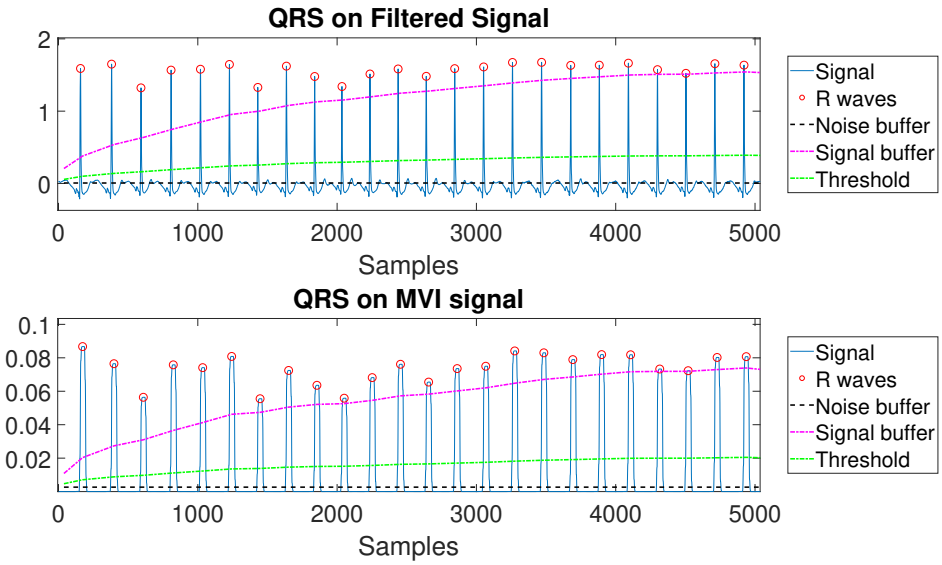

Figure 4.6: Peaks identified on the original filtered version of the ECG signal (first plot) and after the moving-window integration step (second plot).

a time interval shorter than 400 milliseconds.
The resulting peaks may be sometimes located a few milliseconds away from the exact position. For this reason, each peak has been shifted to the closest maximum value in the ECG signal, in order to match the exact location of the correspondent R wave. The output of the peak-detection algorithm implemented on the wavelet transformed signal is represented in Figure 4.5.
After the detection stage, each peak position has been carefully visually inspected and eventually corrected to add potential missed beats, to remove additional beats, or to shift erroneous beats.

4.4.3 Ectopic beats detection

Before computing the RR intervals, each series of R waves has been screened to remove occasional ectopic and arrhythmic events. These anomalous beats could negatively influence the characterization of the HRV signal and thus need to be adjusted.
This step has been performed by giving them as input to a software intended for the detection and correction of eventual erroneous beats. This software implements the real-time automated point-process method developed by Citi et al. in 2012 and it is available at the website page `http://neurostat-mit.appspot.com/` [58].
The algorithm evaluates the probability of the time occurrence of a R wave after observing the recent history of the heartbeats dynamics. Particularly, given a R event, the log probability density of observing it in that precise moment is compared with the probability of an alternative hypothesis that states that the event is invalid. If this probability exceeds the sum of the current probability and a pre-determined

threshold value, the event is labelled as erroneous. In this case, the algorithm attempts to adjust it by shifting it and computing an alternative series. Finally, this alternative series $\hat{u}_j$ is accepted only if the new probability of observing the event according to the past history exceeds the probability computed for the original series of events u_j.
The probability of observing Q events following the generic u_k for both series are:

$$P(\hat{U}_{k-P;k+Q}) = \sum_{j=k}^{k+Q-1} log[f(\hat{u}_{j+1} - \hat{u}_j|\hat{H}_j, \theta(u_k))], \tag{4.1}$$

$$P(U_{k-P;k+Q}) = \sum_{j=k}^{k+Q-1} log[f(u_{j+1} - u_j|H_j, \theta(u_k))] \tag{4.2}$$

where

- $\theta(u_k)$ is the vector of parameters
- H_j is the history of the previous events.

If $P(\hat{U}_{k-P;k+Q}) > P(U_{k-P;k+Q}) + \eta_a$, where η_a is a pre-defined threshold, then $\hat{u}_j$ replaces u_j and the algorithm continues with the successive event.
R events have been uploaded on the website page as a text file and screened according to this manner. The corrected series have been given as output in a new text file of two columns, the first containing the alternative series and the second with the action taken for each beat expressed in a number (0 if the beat was identified as correct and not modified, $\neq 0$ if the beat was identified as erroneous and a correction was attempted).
An example of an ectopic beat appropriately identified and corrected is presented in Figure 4.7. The resulting series of R waves have been loaded in Matlab and carefully inspected to withdraw eventual erroneous shift determined by the automated detector. Finally, the RR intervals have been obtained by computing the differences in time between consecutive R waves.

4.5 Point-process method

4.5.1 Heart rate probability model

The inhomogeneous point-process method of heartbeat dynamics developed by Barbieri et al. in 2005 [35] has been applied to model the R events by considering their stochastic nature together with the inputs of the sympathetic and parasympathetic nervous systems on the SA node activity. For this purpose, a HDIG probability distribution function has been implemented to model the RR intervals as following:

$$f(r|H_{u_k}, \theta) = \left[\frac{\theta_{p+1}}{\pi(t-u_k)^3}\right]^{\frac{1}{2}} \exp\left\{-\frac{1}{2}\frac{\theta_{p+1}\left[t-u_k-\mu(H_{u_k},\theta)\right]^2}{\mu(H_{u_k},\theta)^2(t-u_k)}\right\} \tag{4.3}$$

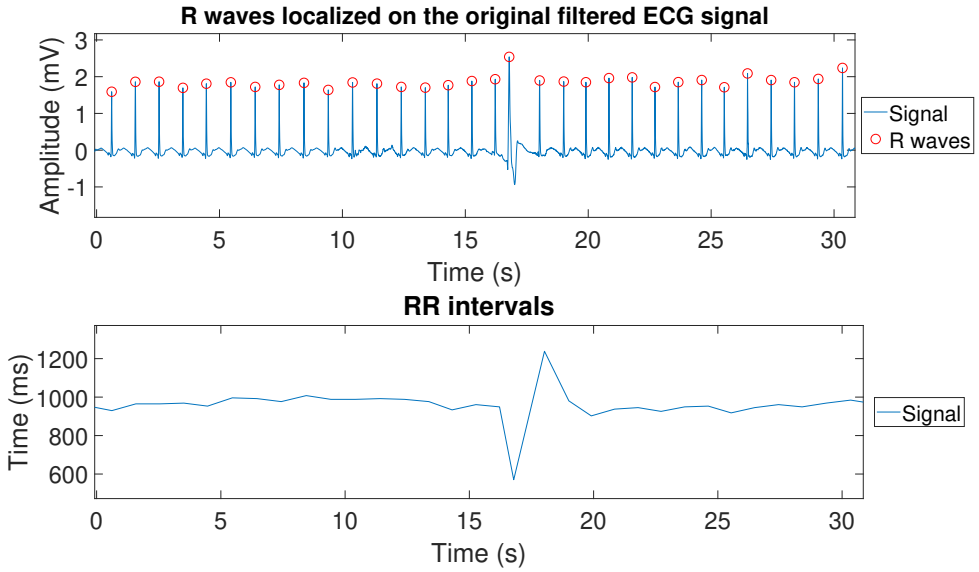

(a) Original RR series before being corrected by the ectopic beats detector.

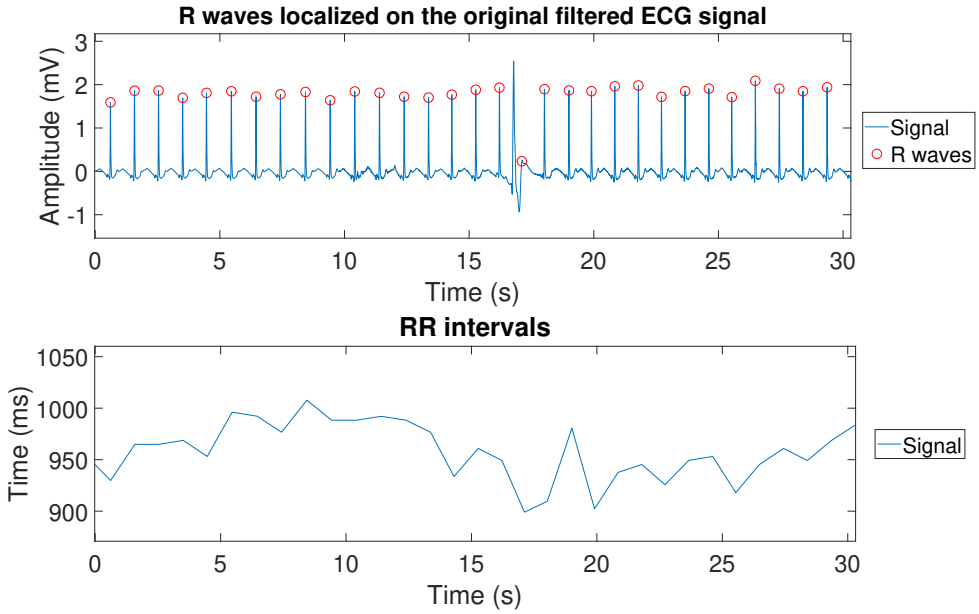

(b) Alternative RR series provided by the ectopic beats detector.

Figure 4.7: Ectopic beats correctly identified and corrected by the algorithm.

where:

- u_k is a generic R event
- H_{u_k} is the history of the RR intervals up to u_k
- θ is a time-varying vector of model parameters

- t is the time satisfying $t > u_k$.

According to this model, the mean and standard deviation of the RR intervals are

$$\mu_{RR}| = \mu(H_{u_k}, \theta) \tag{4.4}$$

$$\sigma_{RR}| = [\mu(H_{u_k}, \theta)^3(\theta_{p+1})^{-1}]^{\frac{1}{2}} \tag{4.5}$$

respectively, and the standard deviation is a function of the mean [36].
Since these two parameters are related to the parameters set θ, they are also time-varying. Moreover, the relation with H_{u_k} accords them the property of history-dependence.
According to this model, the most probable moment of next occurrence is given from 4.4 as a linear function of the last p events observed. Note that, under the assumption of independence for the RR intervals, $p = 0$ and 4.3 simplifies to an inverse Gaussian model unrelated to the effects of the autonomic branches.
Figure 4.8 plots together the observed RR intervals (red asterisks) and the result of the algorithm prediction, i.e. the first moment of the HDIG distribution (μ_{RR}).

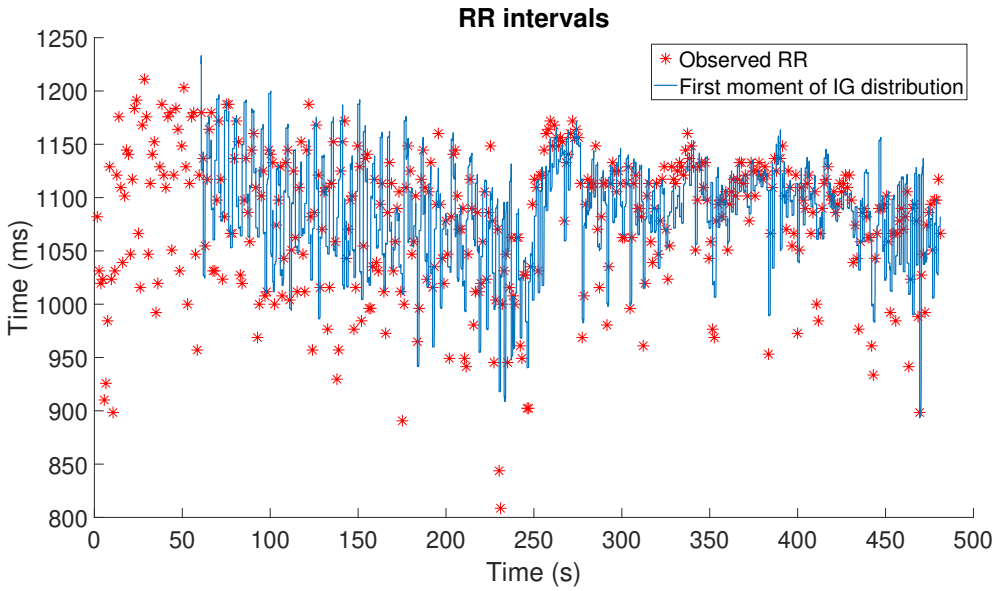

Figure 4.8: Real RR intervals (red asterisks) and predicted RR intervals (blue line).

Symmetrically, precise definitions of HR can be obtained. As the HR is computed as the reciprocal of the RR intervals, considering $t - u_k$ as the waiting time until the next R wave and $c = 6x10^4 ms/min$ as the constant to convert the milliseconds in seconds, the HR random variable is defined as $r = c(t - u_k)^{-1}$. Thus, with a standard change of variables the heart rate probability density can be defined as:

$$f(r|H_{u_k}, \theta) = \left|\frac{dt}{dr}\right| f(t|H_{u_k}, \theta) = \left(\frac{\theta^*_{p+1}}{2\pi r}\right)^{\frac{1}{2}} \exp\left\{-\frac{1}{2}\frac{\theta^*_{p+1}\left[1 - \mu^*(H_{u_k}, \theta)r\right]^2}{\mu^*(H_{u_k}, \theta)^2 r}\right\}. \tag{4.6}$$

The mean and standard deviation of the heart rate are

$$\mu_{HR} = \mu^*(H_{u_k}, \theta)^{-1} + (\theta^*_{p+1})^{-1} \tag{4.7}$$

$$\sigma_{HR} = \left[\frac{2\mu^*(H_{u_k}, \theta) + (\theta^*_{p+1})}{\mu^*(H_{u_k}, \theta)\theta^{*2}_{p+1}}\right]^{\frac{1}{2}} \tag{4.8}$$

,
respectively [35].
To account the continuous influence from the sympathetic and parasympathetic inputs on the SA node, the vector of model parameters θ is time-varying [35]. The time-varying parameters set θ is estimated by maximizing the local-likelihood through a Newton-Raphson procedure [35].
Considering T as the ECG recording period and J as the number of intervals with equal width Δ=T/J, the state model and the observation model can be defined. The adaptive parameter estimates are updated at $j\Delta$, where Δ is the time shift to compute the next parameters for j=1, ..., J. As the estimate for θ is provided in continuous time, given this parameters set, instantaneous time-domain estimates of mean RR intervals, RR intervals standard deviation, mean HR and HR standard deviation can be obtained any time and are

$$\mu_{RR}(j\Delta) = \mu(H_j, \theta_{j|j}) \tag{4.9}$$

$$\sigma_{RR}(j\Delta) = [\mu(H_j, \theta_{j|j})^3(\theta_{p+1,j|j})^{-1}]^{\frac{1}{2}} \tag{4.10}$$

$$\mu_{HR}(j\Delta) = \mu^*(H_j, \theta_{j|j})^{-1} + (\theta^*_{p+1,j|j})^{-1} \tag{4.11}$$

$$\sigma_{HR}(j\Delta) = \left[\frac{2\mu^*(H_j, \theta_{j|j}) + (\theta^*_{p+1})}{\mu^*(H_j, \theta_{j|j})(\theta^*_{p+1})^2}\right]^{\frac{1}{2}} \tag{4.12}$$

,
respectively [35].

In this particular application, a time resolution of 8 ms (Δ), a regressive order equal to 8 (p), and a window length of 60 seconds for local likelihood estimate have been selected.

4.5.2 Model goodness-of-fit

The agreement between the estimates provided by the model in terms of mean and standard deviation of the RR intervals and the human intervals dynamics has been investigated in terms of goodness-of-fit with a Kolmogorov-Smirnov (KS) test [35]. The KS test is a non-parametric test that compares a sample with a probability

distribution. Particularly, it can be framed by computing the KS plot or the KS distance [35].
The KS plot (Figure 4.9) is a graphical measure: the better the model describes the real data, the closer the KS plot lies along the 45° line and inside the 95% confidence bounds.
The major distance between a cumulative distribution function of the RR series and a cumulative distribution function of a uniform distribution provides the KS distance. The smallest the KS distance, the better the model describes the original data.

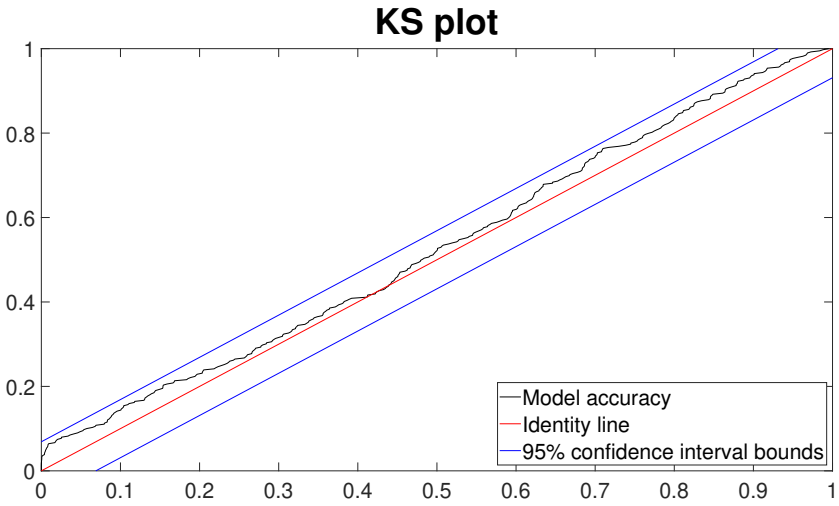

Figure 4.9: Kolmogorov-Smirnov graphic test.

4.5.3 Instantaneous frequency analysis

Instantaneous estimates in the frequency-domain have been computed from the point-process algorithm. Particularly, the time-varying parametric power spectrum $Q(f,t)$ can be easily obtained from the AR model [53]. The total power has been computed and so the content in each frequency range by integrating the total in the VLF (0.0033-0.04 Hz), LF (0.04-0.15 Hz), and HF (0.15-0.4 Hz) bands, as following

$$VLF(t) = \int_{0.0033}^{0.04} Q(f,t)df \tag{4.13}$$

$$LF(t) = \int_{0.04}^{0.15} Q(f,t)df \tag{4.14}$$

$$HF(t) = \int_{0.15}^{0.4} Q(f,t)df. \tag{4.15}$$

The balance between low-frequency and high-frequency has also been obtained as the ratio between LF and HF (LF/HF).

Figure 4.10 shows an example of LF and HF power trends over time, whereas Figure 4.11 reflects the balance between these two components.

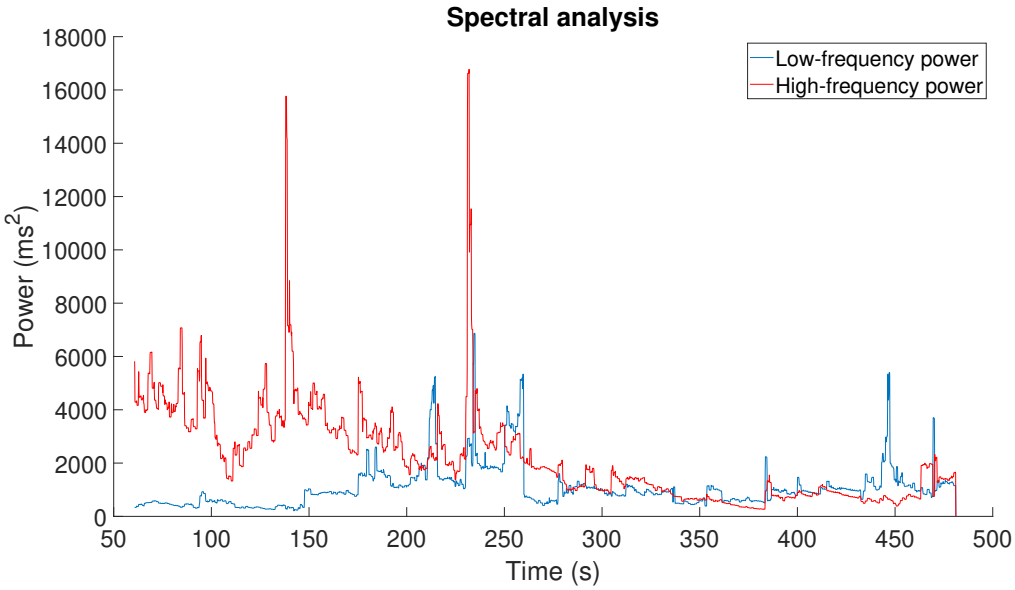

Figure 4.10: Low- and high-frequency power.

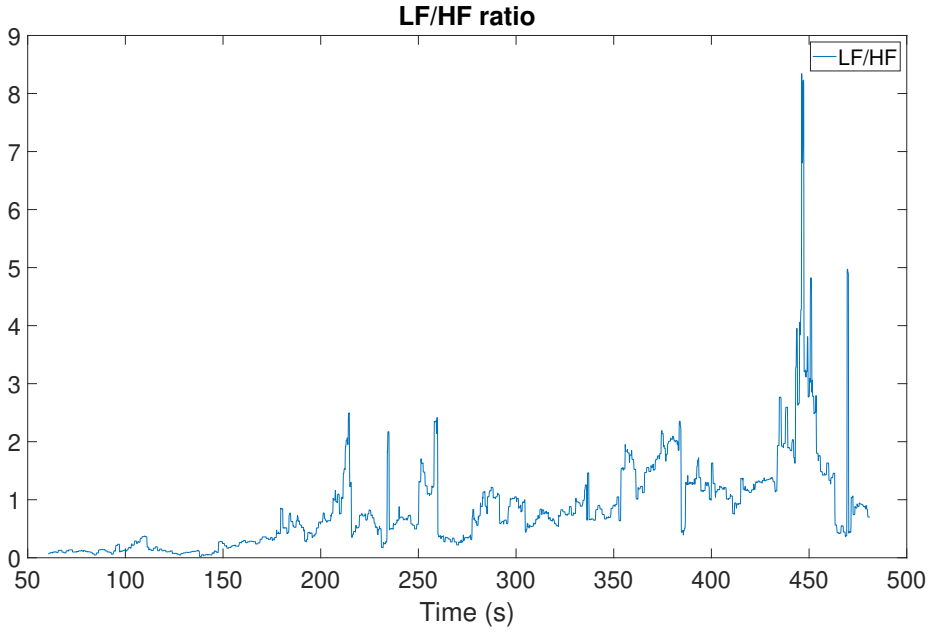

Figure 4.11: Ratio between low- and high-frequency power.

4.6 HRV features extraction

All features have been computed for each analyzed window. For the healthy controls and the laboratory data, single HRV time-domain and frequency-domain indices have been computed by averaging the parameters in time over each three minutes of rest-window. For the apartment data, the same indices have been computed by averaging the parameters over a time interval of three minutes selected according to the quality of the signal from the resting windows available.

4.6.1 Time-domain indices

Time-domain indices have been extracted both from the real observed RR intervals and the data estimated by the point-process framework. Since the two classes of values proved to be very similar, only the indices extracted from the real RR series have been considered for the analysis.
Time-domain indices include the mean of the RR intervals, the standard deviation of the RR intervals, the range of the RR intervals, the mean HR, the standard deviation of the HR, and the range of the HR. Table 4.2 reports the description of the index, the assigned name and the unity of measure.

Description	**Index**	**u.o.m.**
Mean of the RR intervals	Mean RR	(ms)
Standard deviation of the RR intervals	Std RR	(ms)
Range of the RR intervals	Range RR	(ms)
Mean of the heart rate	Mean HR	(bpm)
Standard deviation of the heart rate	Std HR	(bpm)
Range of the heart rate	Range HR	(bpm)

Table 4.2: Time-domain indices.

4.6.2 Frequency-domain indices

Frequency-domain indices have been calculated by averaging the spectral estimates provided by the point-process algorithm with a time resolution of $\Delta = 8ms$. These indices include the mean, standard deviation, and range of the HF and LF contents, the mean, standard deviation, and range of the LF/HF ratio, the HF component normalized by the sum of LF and HF contents and the HF component normalized by the total power. Table 4.3 reports the description of the index, the assigned name and the unity of measure.

Description	**Index**	**u.o.m.**
Mean of the HF content	Mean HF	(ms^2)
Standard deviation of the HF content	Std HF	(ms^2)
Range of the HF content	Range HF	(ms^2)
Mean of the LF content	Mean LF	(ms^2)
Standard deviation of the LF content	Std LF	(ms^2)
Range of the LF content	Range LF	(ms^2)
Mean of the LF/HF ratio	Mean LF/HF	-
Standard deviation of LF/HF ratio	Std LF/HF	-
Range of the LF/HF ratio	Range LF/HF	-
HF content normalized by the sum of LF and HF	HF/LF+HF	-
HF content normalized by the total power	HF/totPow	-

Table 4.3: Frequency-domain indices.

Chapter 5

Results

This chapter presents the results accomplished in the analysis of the HRV signal in patients suffering from PD.
The first section submits the statistical results achieved from the comparison between the Parkinsonian subjects and a population of healthy controls. Particularly, this analysis aimed to investigate and eventually corroborate the previous literature's assertion of diminished HF power in the affected patients.
The values of the time-domain and frequency-domain parameters extracted from the HRV signals are presented for each group and the differences are shown in terms of the p-values obtained from the Mann-Whitney U test. Moreover, the mean and standard deviation of the main indices (RR intervals, HF, and LF power) are graphically represented through box-plot plots to further highlight the differences between healthy and PD people.
The second section is addressed to analyze the HRV parameters over a full medication cycle during the laboratory data collection. This part aimed to investigate the effects of the levodopa's intake on the parasympathetic control of the heart. Since the parasympathetic system is deputed to decrease the HR at rest, a decrease in the HF power concurrent with an increased HR effectively marks a vagal failure. Thus, the trends of the HR and the HF have been assessed and presented in parallel to evaluate the vagal outflow over the entire data collection, starting from the "Off"-medication condition, encompassing the "On", and returning back "Off". The values of the mean HF and HR are presented for each subject to highlight the variations from a stage to the other. Differences between session 1, 3, and 5 are graphically represented through box-plot plots for the mean and standard deviations of the RR intervals, HF and LF power.
The last section presents the analysis accomplished on the apartment data. The HF power of the HRV has been assessed for a small subset of subjects over the entire data collection, aiming to investigate whether the HF behavior observed in the laboratory is consistent in the simulated apartment. The potential connection between the HF and the stage of the medication cycle has been evaluated considering the perceiving status and the motor performances of the participants and presenting them in parallel with the trend of the mean HF.

5.1 Healthy controls vs Parkinson's subjects

5.1.1 Statistical analysis

The following section reports the results obtained from the comparison between healthy controls and PD subjects.
For this purpose, the HRV parameters extracted from the ECG signal recorded during three minutes of rest have been analyzed. Particularly, for PD subjects, data collected during session 1 of the laboratory visit have been considered.
Between-groups differences have been investigated using the non-parametric Mann-Whitney U test under the null hypothesis that the two groups belong to the same population. The level of significance has been chosen to be 5%, hence statistical significance has been assumed for p-values lower than 0.05 ($p < 0.05$).

The results of group-wise statistics are shown in Table 5.1. Parameters are expressed as mean ± standard deviation and the p-values are indicated.

	Parameter	**Healthy**	**PD**	**P-value**
Time	Mean RR	893.8 ± 51.4	890.8 ± 128.0	0.635
	Std RR	51.4 ± 21.1	26.1 ± 11.3	**0.001**
Frequency	Mean HF	521.6 ± 700.5	204.4 ± 286.4	0.106
	Std HF	162.2 ± 223.8	76.1 ± 87.4	0.279
	Range HF	1119.5 ± 1473.3.4	510.3 ± 576.1	0.154
	Mean LF	921.3 ± 703.1	219.7 ± 347.8	**0.001**
	Std LF	698.0 ± 727.9	152.9 ± 231.3	**0.0008**
	Range LF	4010.5 ± 4140.4	1072.8 ± 1713.6	**0.002**
	Mean LF/HF	6.4 ± 13.2	4.4 ± 11.8	0.05
	Std LF/HF	6.4 ± 15.6	10.2 ± 36.9	0.024
	Range LF/HF	38.3 ± 97.6	109.9 ± 424.1	0.071

Table 5.1: Statistical analysis of group differences between healthy controls and Parkinson's subjects. Features are expressed as mean ± standard deviation. Significance has been marked in bold.

5.1.2 Time-domain parameters

No statistically significant differences have been observed between-groups in the mean value of the RR intervals ($p = 0.635$). Conversely, the standard deviation of the RR series is lower in Parkinson's subjects than healthy controls (26.1 ± 11.3 vs 51.4 ± 21.1), and the observed difference is significant ($p = 0.001$).

Figure 5.1a and 5.1b present the box-plot plots relative to mean and standard deviation, respectively.

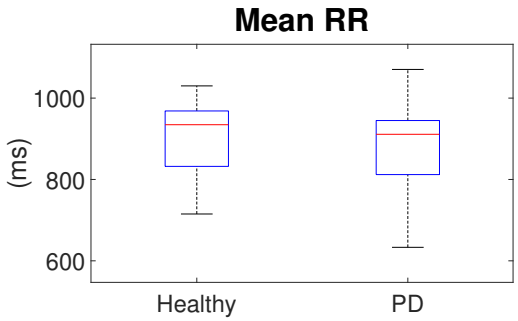

(a) Mean of RR intervals.

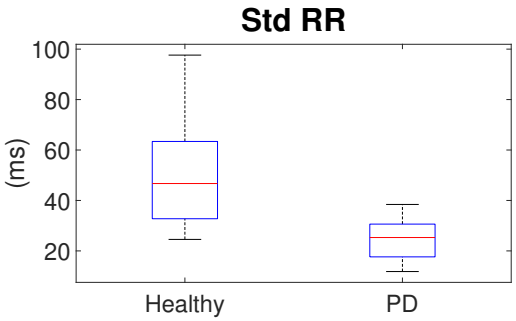

(b) Standard deviation of RR intervals.

Figure 5.1: Box-plot plots for the RR intervals in healthy and PD subjects.

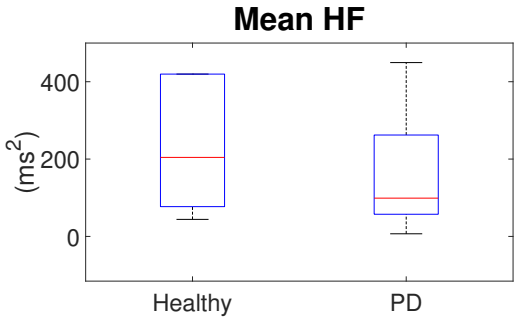

(a) Mean of the HF component.

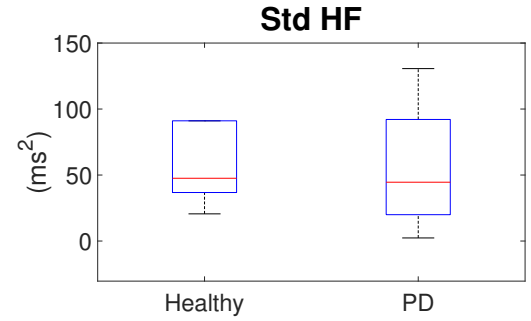

(b) Standard deviation of the HF component.

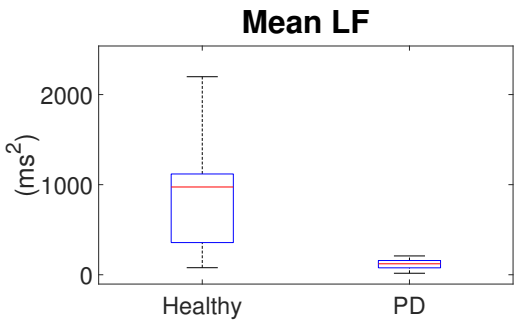

(c) Mean of the LF component.

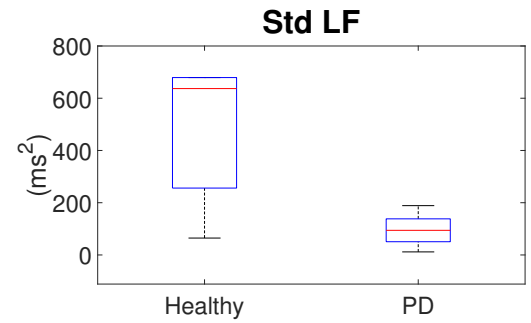

(d) Standard deviation of the LF component.

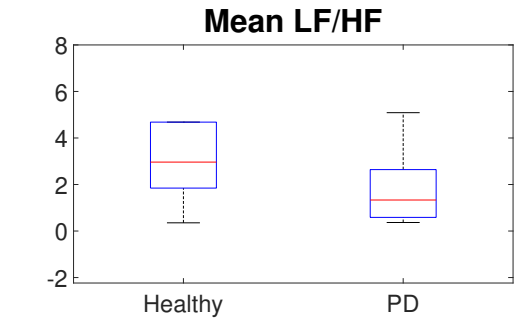

(e) Mean of the LF/HF ratio.

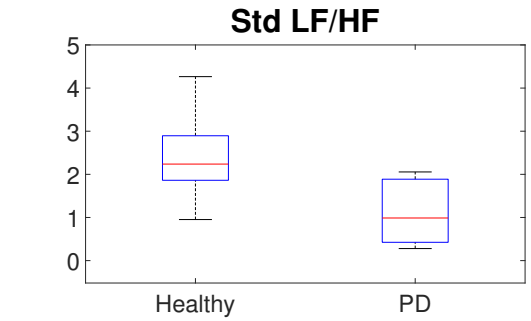

(f) Standard deviation of the LF/HF ratio.

Figure 5.2: Box-plot plots for the HF, LF, and LF/HF parameters in healthy and PD subjects.

5.1.3 Frequency-domain parameters

All the spectral measures are lower in Parkinson's subjects than in healthy controls, except for the standard deviation of the LF/HF ratio. Consistently with the results reported by the previous literature, the mean value of the HF component of the power spectrum is considerably higher in healthy subjects than Parkinson's patients (521.6 ± 700.5 vs 204.4 ± 286.4). However, no statistically significant differences are observed in the HF ($p = 0.106$). Oppositely, the LF component shows significant differences between-groups in all its indices (mean, standard deviation, and range).

Figure 5.2 shows the box-plot plots for the mean and standard deviation of the HF, LF, and LF/HF ratio.

5.2 Laboratory

The following section presents the results obtained from the laboratory analysis. Among the twenty-six participants enrolled in the BlueSky Project, only nineteen have been considered, whereas the others have been discarded due to noisy signals or the presence of arrhythmic events. The demographic characteristics of the subjects included in the laboratory analysis are reported in Table 5.2.
For the data analysis, only the three minutes of rest points featured by an admissible quality of the signal have been considered, whereas the others have been removed to avoid erroneous variations of the parameters that are not due to physiological basis. The laboratory analysis has been accomplished in two different stages. First, the HRV pattern has been qualitatively investigated over the full medication cycle. Then, the evaluation has been focused on the "Off" and "On" conditions, and the HRV parameters computed within these two phases have been statistically compared.

5.2.1 Full medication cycle

As an exploratory and preliminary analysis, the trend of the HRV features in both time- and frequency-domain has been visually evaluated over the entire medication cycle. For this purpose, every index extracted for each three minutes-window has been plotted against time on a graph encompassing the entire data collection. Particularly, a color code has been implemented and a legend indicated. Data points have been plotted in blue for session 1, granate red for session 2, green for session 3, yellow for session 4, and purple for session 5. The times of medication intake have been marked on each plot with a red dashed line and labeled with "MED". This step was accomplished to investigate whether the variations in the parameters were observed on an inter-session and intra-session basis and to visually estimate whether the levodopa had an influence on the indices fluctuations.
The trend of the principal time-domain and frequency-domain parameters are presented in the following plots. Note that, since not all the three minutes-windows have been included in the analysis due to a low quality of the data, successive data points are not evenly spaced by thirty minutes.

Demographics	
Number of subjects	19
Age (years)	62.4 ± 9.4 (42-80)
Gender (%)	
Male	16 (84.2)
Female	3 (15.8)
Handedness (%)	
Left	2 (10.5)
Right	17 (89.5)
First Symptoms (years)	53.6 ± 9.9 (31-70)
First Diagnosis (years)	55.2 ± 9.6 (32-76)
MoCA	27.2 ± 2.5 (21-30)
Current Medications	
Ldopa (%)	19 (100)
Hoehn & Yahr (%)	
1	0
2	19 (79)
3	4 (21)

Table 5.2: Laboratory subjects.

As the mean value of the HF content is the principal parameter of interest, it is explained more in detail. Particularly, the trend of this particular index is plotted in parallel with the mean value of the HR to properly establish whether the variations in the HF are imputable to a vagal response. Three representative subsets of subjects have been selected to exhibit the principal tendencies observed in the HF-HR. The first subset collects the only two subjects who are characterized by very low values of HF and no meaningful variations (Figure 5.3-5.4). The second subset groups part of the subjects that present a decrease in the HF from session 1 to 3 and then from session 3 to 5 (Figure 5.5-5.8). The third subset groups part of the subjects that present a decrease in the HF from session 1 to 3 succeeded by an increase from session 3 to 5 (Figure 5.9-5.12).
The mean value of the LF component and the LF/HF ratio are here reported only for a narrow subset of subjects (Figure 5.13 - Figure 5.16), since their behavior is not regular among the participants.
The plots representing the mean values of the RR intervals, the HF power, and the LF power for all the subjects are collected in the appendix A. All the other parameters are extracted from them. Thus, their behavior can be easily estimated and is not displayed here.

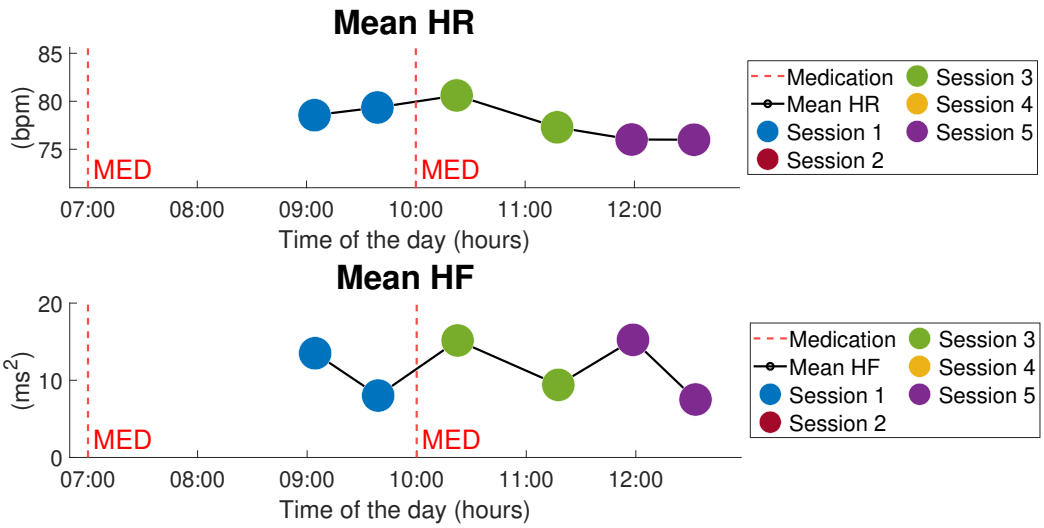

Figure 5.3: HR and HF trends in subject 10.

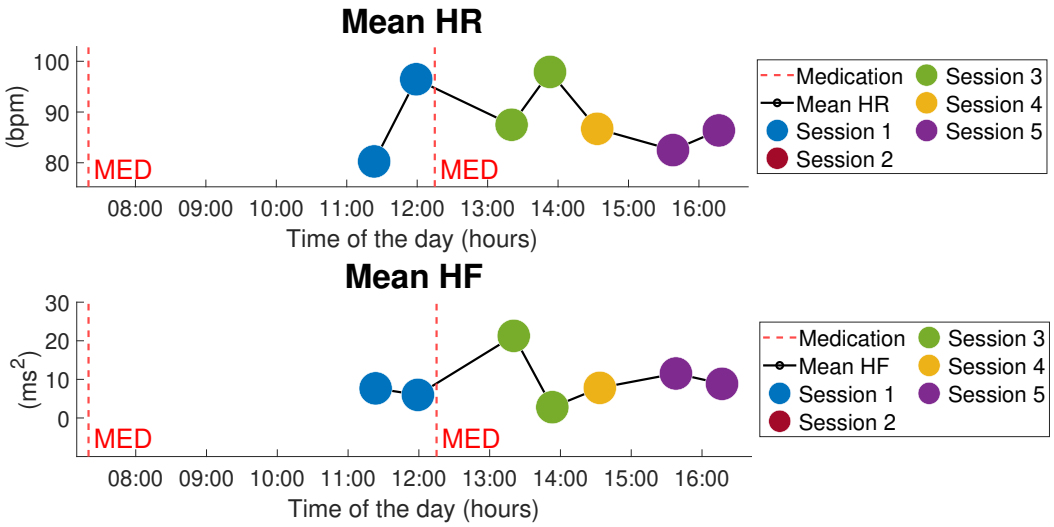

Figure 5.4: HR and HF trends in subject 21.

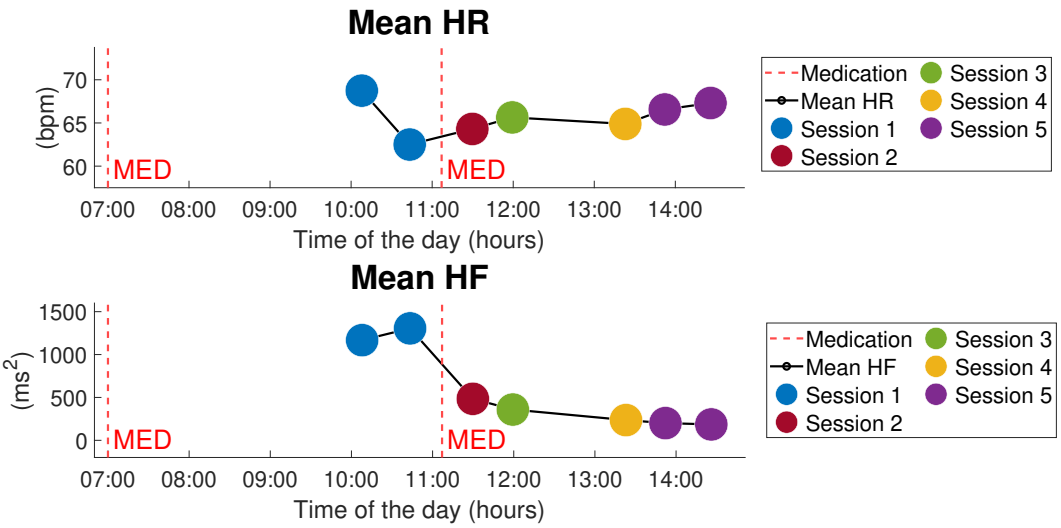

Figure 5.5: HR and HF trends in subject 13.

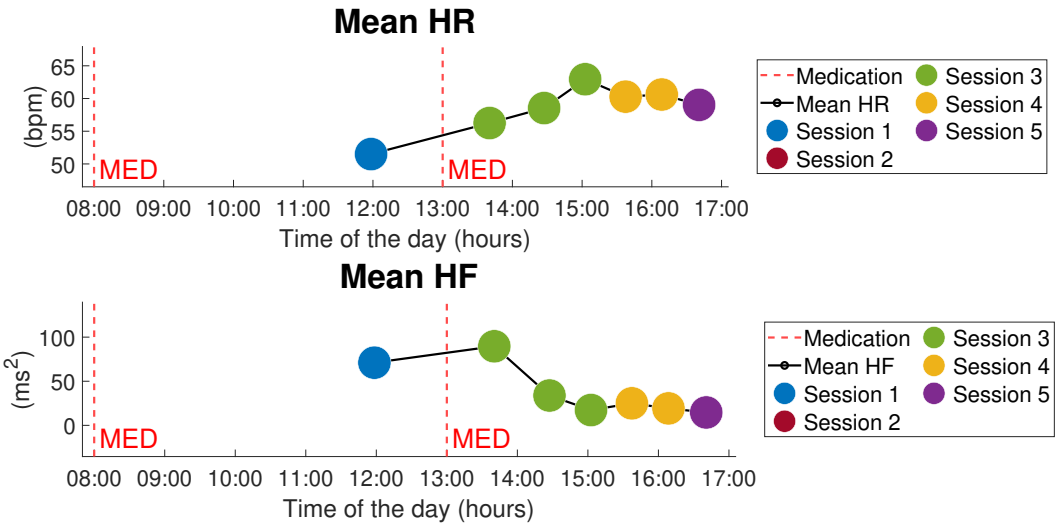

Figure 5.6: HR and HF trends in subject 15.

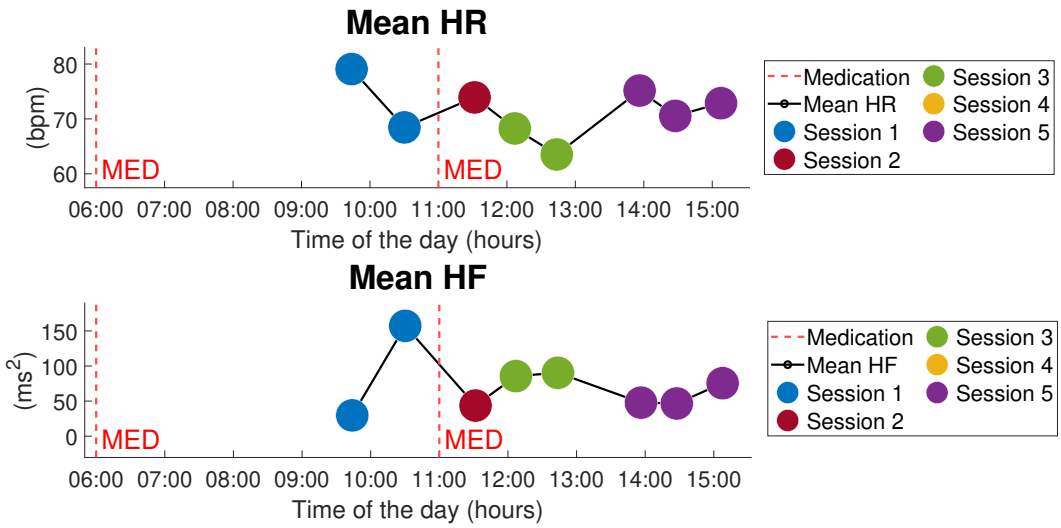

Figure 5.7: HR and HF trends in subject 16.

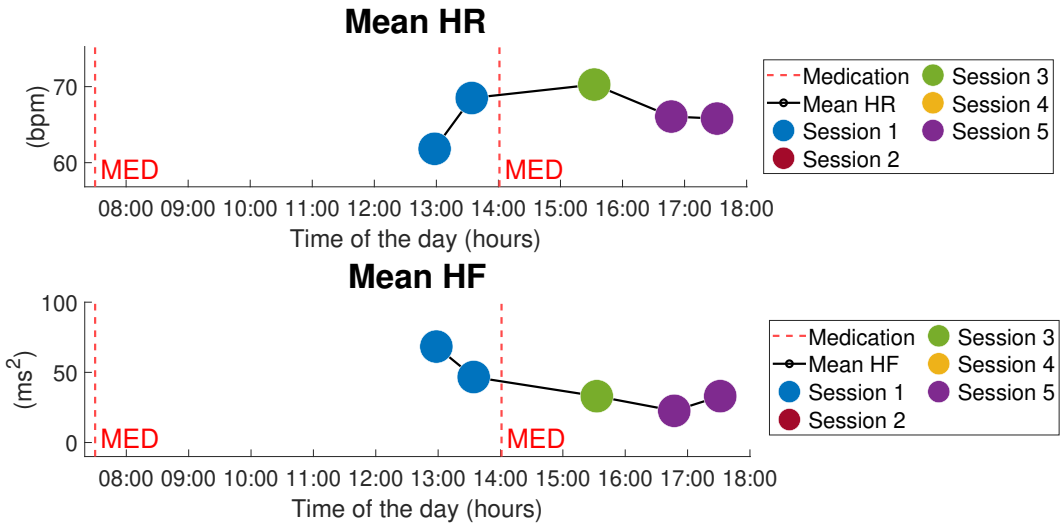

Figure 5.8: HR and HF trends in subject 22.

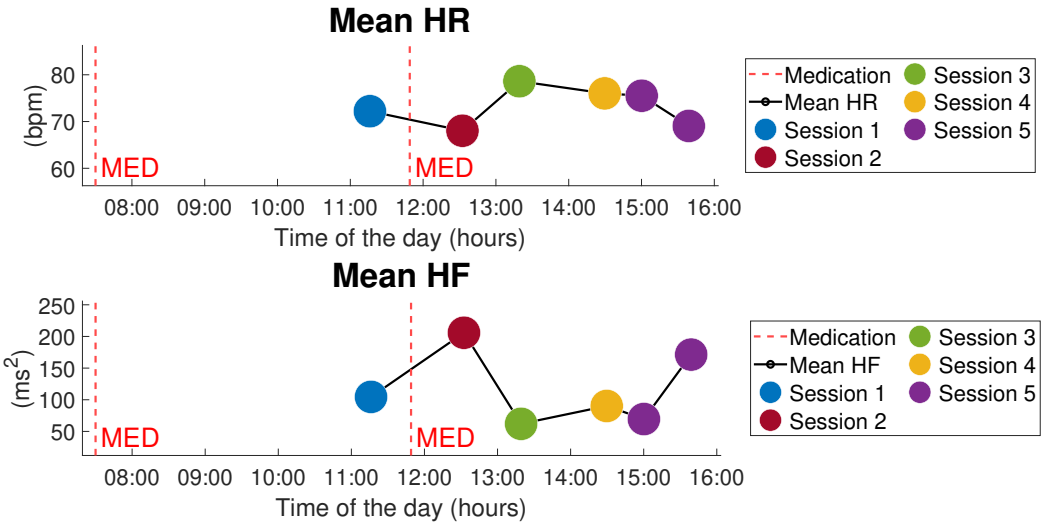

Figure 5.9: HR and HF trends in subject 7.

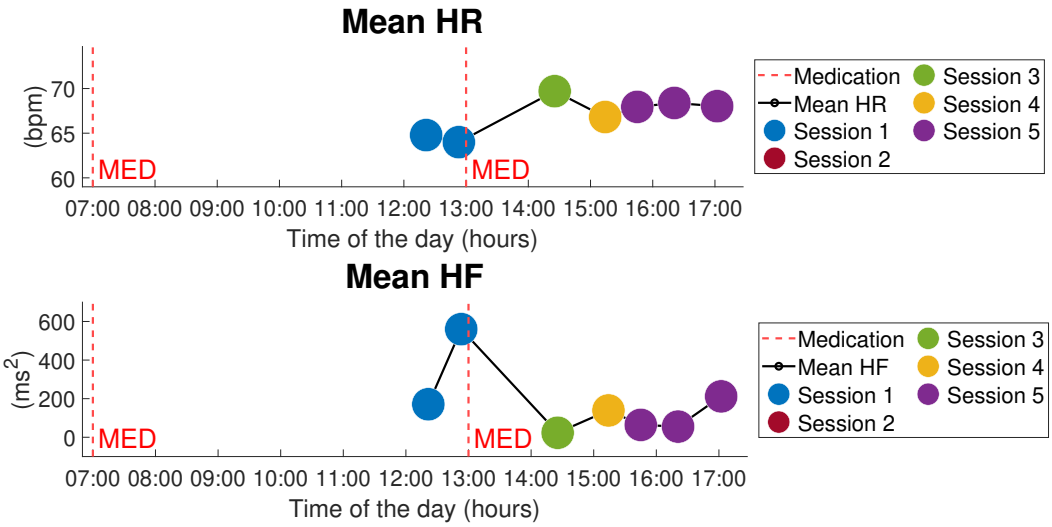

Figure 5.10: HR and HF trends in subject 9.

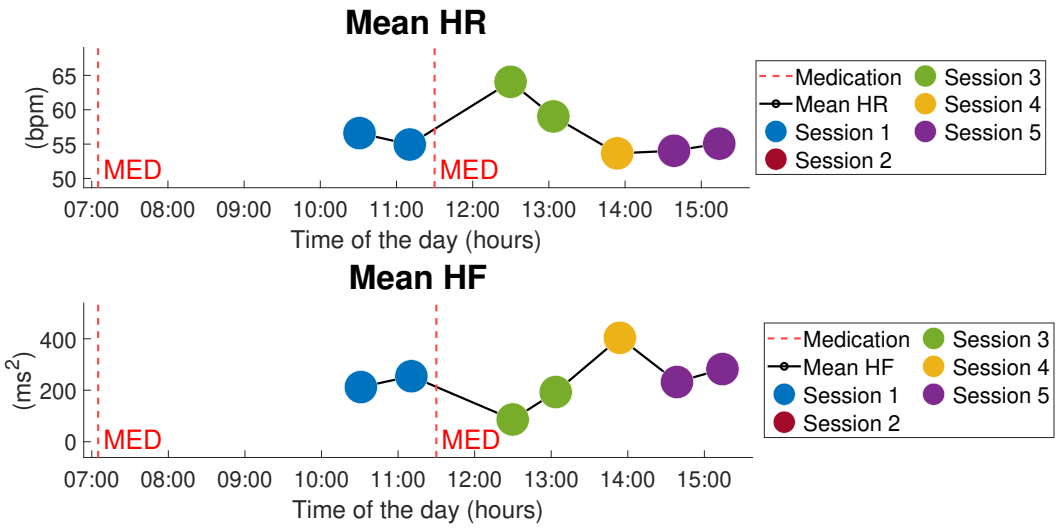

Figure 5.11: HR and HF trends in subject 12.

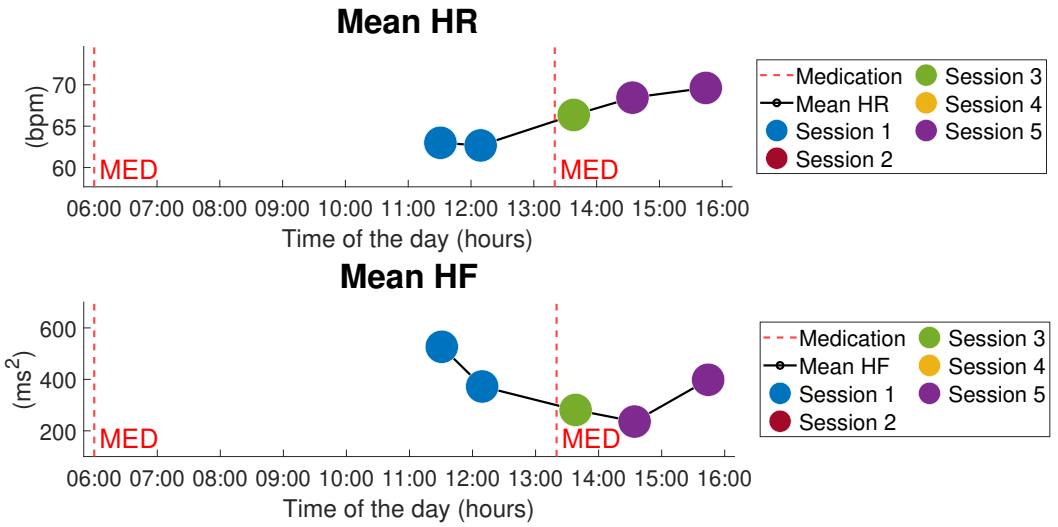

Figure 5.12: HR and HF trends in subject 20.

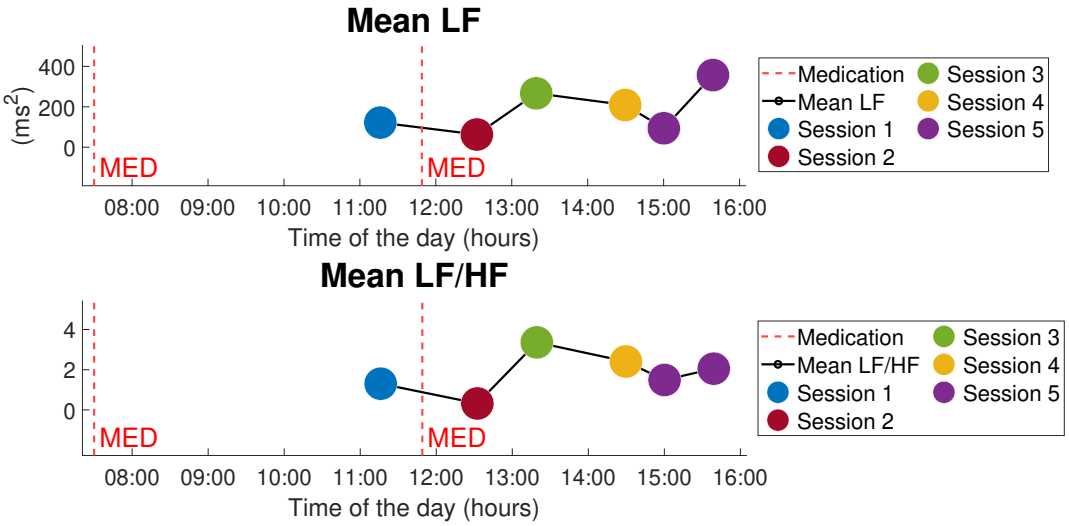

Figure 5.13: LF and LF/HF trends in subject 7.

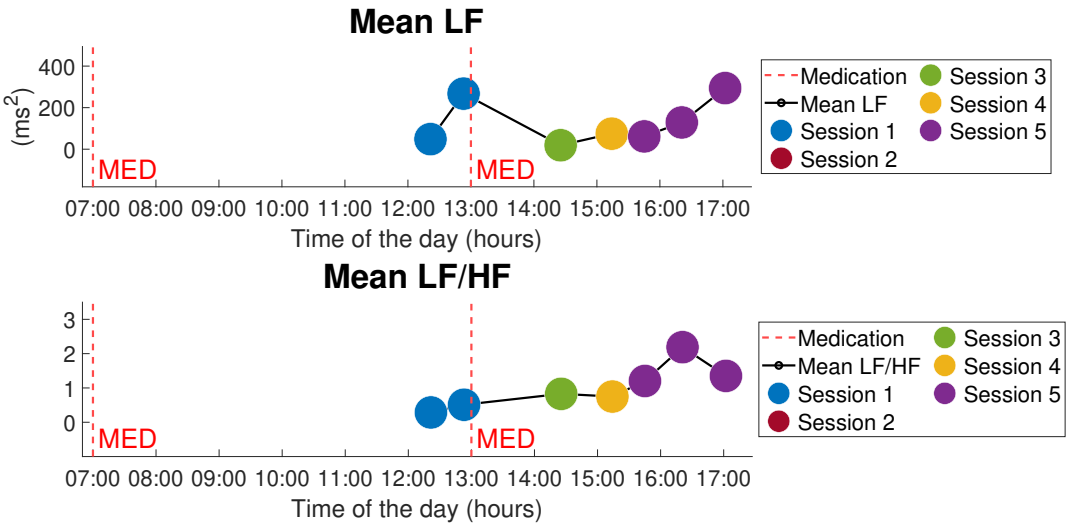

Figure 5.14: LF and LF/HF trends in subject 9.

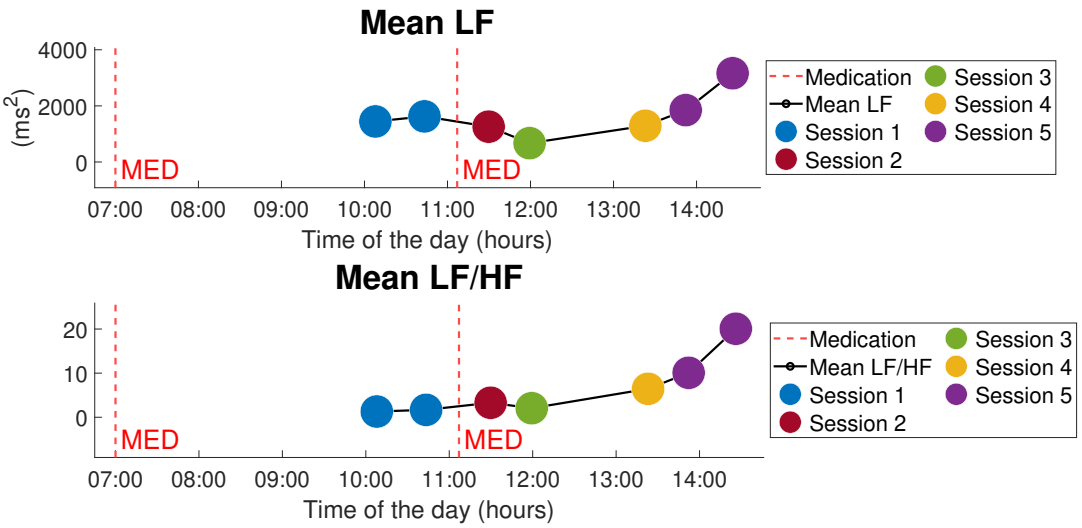

Figure 5.15: LF and LF/HF trends in subject 13.

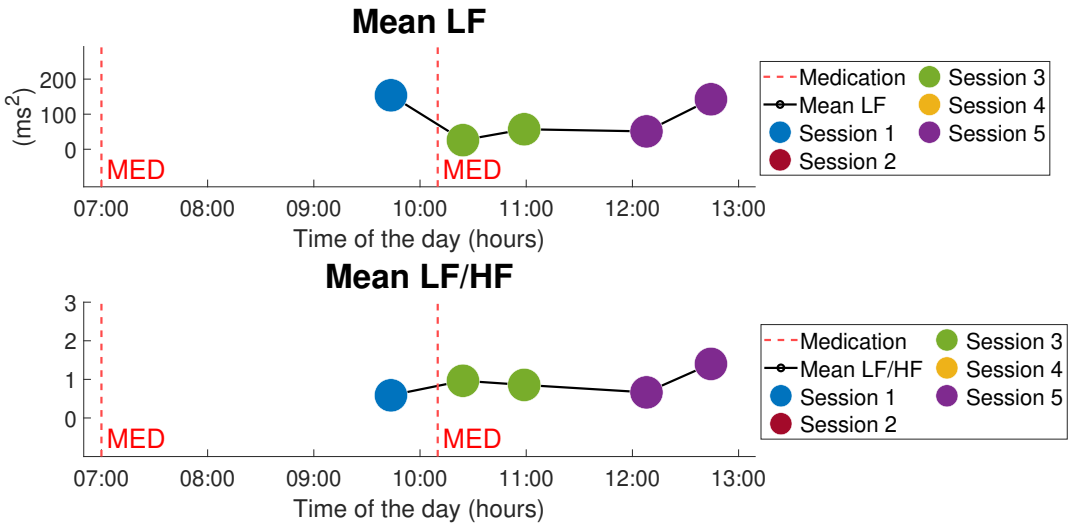

Figure 5.16: LF and LF/HF trends in subject 17.

The monitoring of the HRV over the entire medication cycle shows that both time-domain and frequency-domain indices do not have a constant behavior and are fluctuating with a trend that, at least in first instance, does not appear to be related only with the medication intake. Furthermore, these variations are appreciable in all the analyzed subjects, both on a inter-session and intra-session basis.
To further investigate the inter-session variability of the HF component, data points values belonging to the same session have been merged together in a distinct averaged value for each single subject.
Averaged values of the mean HF are presented in Table 5.3, whereas averaged values of the mean HR are presented in Table 5.4. A color code has been employed to show whether the HF and HR are increasing or decreasing from session 1 to 3. Particularly, gold denotes a diminished value, whereas green indicates an increase in the parameter.Note that empty cells are appreciable within session 2 and 4, since these two transitional stages have not been accomplished by the totality of the subjects. Moreover, subject 3 lacks session 1 due to the presence of considerable gaps in the raw signal.

Mean HF					
Subject	**Session 1**	**Session 2**	**Session 3**	**Session 4**	**Session 5**
3		92.8	18.5	39.2	106.3
4	157.7	37.7	18.3	17.8	
7	104.5	205.9	62.0	90.2	120.5
9	365.6		23.3	139.0	110.4
10	10.8		12.2		11.4
12	233.4		139.7	403.8	257.1
13	1236.5	484.0	358.9	235.8	193.0
14	42.0		26.91	36.8	30.0
15	71.1		46.9	22.1	14.6
16	93.4	43.6	88.0		56.6
17	262.2		43.7		115.2
19	277.6		231.5		239.9
20	449.5		281.2		317.2
21	6.8		12.0	7.8	10.2
22	57.5		33.0		27.8
23	114.4	44.9	29.2		16.1
24	93.4		17.0		
26	45.2		18.5	27.5	31.2
27	57.3	57.8	46.5		110.3

Table 5.3: Averaged values of the mean HF component computed within every distinct session. A color code is implemented for presentation purpose: gold reflects a diminished HF, whereas green represents an increase.

Mean HR					
Subject	**Session 1**	**Session 2**	**Session 3**	**Session 4**	**Session 5**
3		66,7	64,4	65,7	69,1
4	63,8	83,8	82,2	85,8	
7	71,5	67,9	79	76,4	72,3
9	64,4		69,7	67,3	68,1
10	79,1		79,2		76,2
12	56,1		61,6	53,6	54,8
13	65,8	64,9	65,8	65,4	67,3
14	68,3		64,8	67,3	69,2
15	51,5		59,3	60,6	59,5
16	74,2	74,3	66,1		72,5
17	66		71,9		68
19	63,5		65,7		70,3
20	63,1		66,4		69
21	88,2		92,3	86,9	85
22	65,5		70,3		66,1
23	94,8	93,6	97,5		101
24	76,1		80,9		
26	68,1		68	63	68,2
27	59,5	58,9	60,2		60,8

Table 5.4: Averaged values of the mean HR computed within every distinct session. A color code is implemented for presentation purpose: gold reflects a diminished HR, whereas green represents an increase.

5.2.2 Between-sessions analysis

Session 1, 3, and 5 have been further analyzed as the stages of the medication cycle characterized by a definite status ("Off" for session 1 and 5, "On" for session 3). Differences between session 1 and 3, 1 and 5, and 3 and 5 have been evaluated through the non-parametric and paired Wilcoxon signed rank test, whereas session 1, 3, and 5 have been investigated together with the Friedman test. In both cases, the statistical analysis has been accomplished under the null hypothesis that the tested variables belong to the same population and statistical significance has been assumed for $p < 0.05$.

Session 1 vs 3

Table 5.5 reports the p-values resulting from the signed parametric Wilcoxon's test between session 1 and 3. Significance between features computed within session 1 and 3 has been observed in the mean of the RR intervals and in all the HF indices (mean, standard deviation, range, HF normalized by the total power, and HF normalized by the sum of LF and HF).
Table 5.3 clearly shows that the HF power is mostly decreasing from session 1 to 3. Notably, this occurs for all the subject except subject 10 and 21, who rather show an increase in the parameter when shifting from "Off" to "On". However, these are also the only two subjects that display a very low HF among all the sessions, even at the baseline (10.8 and 6.8, respectively). Furthermore, the variations over time are very modest, suggesting that these small changes can be purely addressed to noise instead of proper autonomic fluctuations. Except them, all the other subjects show decreased HF in the "On" status, and the magnitude of the decrease is different on a subject-by-subject basis. Part of them displays high variations, with an averaged mean HF in session 3 that approximately halves the averaged mean HF in session 1. This occurs in subjects 7, 12, 14, 20, 22, and 26. Others show even higher magnitudes of variation, as subject 4, 13, o 17.

Test variable	**P-value**
Mean RR	**0.011**
Std RR	0.231
Mean HR	**0.016**
Mean HF	**0.0003**
Std HF	**0.002**
Range HF	**0.007**
HF/totPow	**0.008**
HF/LF+HF	0.085
Mean LF	0.231
Std LF	0.528
Range LF	0.528
Mean LF/HF	0.058
Std LF/HF	0.102
Range LF/HF	0.170

Table 5.5: Statistical analysis between session 1 and 3. Significance has been marked in bold.

Session 3 vs 5

As session 5 marks the end of the medication cycle and occurs in parallel with the return in the "Off" state, we would expect the HF power content recovering to the baseline values of session 1. However, observing the averaged values of the mean HF in session 3 and 5 shown in Table 5.3, we can affirm that the trend is not consistent among all the subjects. A subset of them, including subject 7, 12, 19, 20, and 27, displays an increased mean HF content when shifting from session 3 to 5, whereas others, as subject 13, 15, 16, and 22, show an ulterior decrease in the parameter.

Table 5.6 reports the results of the statistical analysis performed to evaluate the significance of the differences between session 3 and 5. Curiously, no significant differences have been observed, neither in the HF indices. This may appear perplexing and may query the finding that states a decreased HF following the levodopa's administration. However, other factors need to be considered. First among all of them are the circadian rhythms. Since the transitioning to session 5 occurs in parallel with the entry in the afternoon, circadian fluctuations of the HF power are expected. Particularly, it is likely to diminish during the afternoon, and this may explain the lessened HF values observed in session 5.

Test variable	**P-value**
Mean RR	0.868
Std RR	0.619
Mean HR	0.906
Mean HF	0.177
Std HF	0.554
Range HF	0.381
HF/totPow	0.407
HF/LF+HF	0.758
Mean LF	0.093
Std LF	0.332
Range LF	0.266
Mean LF/HF	0.523
Std LF/HF	0.523
Range LF/HF	0.619

Table 5.6: Statistical analysis between session 3 and 5.

Session 1 vs 5

To further investigate whether the circadian rhythms have an effect on the HF fluctuations without the bias of the effects of the medication, the differences between session 1 and 5 have been evaluated.

Table 5.7 displays the results of Wilcoxon's test for session 1 and 5: significant differences have been found in the mean, standard deviation, and range of the HF contents, as well as in the HF normalized by the total power. Hence, these findings may suggest the influence of other inputs external to the medication intake that need to be considered, and that they may be related with the time of day.

Test variable	**P-value**
Mean RR	0.056
Std RR	0.717
Mean HR	0.079
Mean HF	**0.023**
Std HF	**0.034**
Range HF	**0.049**
HF/totPow	**0.034**
HF/LF+HF	0.535
Mean LF	0.215
Std LF	0.134
Range LF	0.469
Mean LF/HF	0.109
Std LF/HF	0.196
Range LF/HF	0.179

Table 5.7: Statistical analysis between session 1 and 5. Significance has been marked in bold.

Session 1 vs 3 vs 5

Table 5.8 reports the p-values gathered from the non-parametric Friedman's test. Significant differences have been found in the mean of the RR intervals, the mean HR, the mean and standard deviation of the HF, the HF normalized by the total power, and the mean LF/HF ratio.
According to these results, the HF content significantly differs over the three sessions, suggesting that its behavior is modulated by a combination of influences that can not be addressed only to the absorption of the medication. The box-plot plots relative to session 1, 3, and 5 for the mean and standard deviation of the RR intervals, mean and standard deviation of the HF, mean and standard deviation of the LF, and mean and standard deviation of the LF/HF are shown in Figure 5.17a, Figure 5.17b, Figure 5.18a, Figure 5.18b, Figure 5.19a, Figure 5.19b, Figure 5.20a, and Figure 5.20b, respectively.

Test variable	P-value
Mean RR	**0.022**
Std RR	0.939
Mean HR	**0.047**
Mean HF	**0.015**
Std HF	**0.039**
Range HF	0.305
HF/totPow	**0.050**
HF/LF+HF	0.829
Mean LF	0.174
Std LF	0.530
Range LF	0.646
Mean LF/HF	**0.022**
Std LF/HF	0.185
Range LF/HF	0.305

Table 5.8: Statistical analysis between session 1, 3, and 5. Significance has been marked in bold.

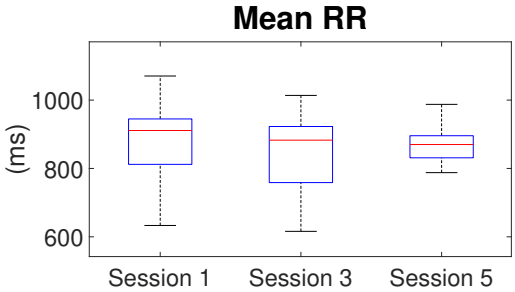

(a) Mean of RR intervals.

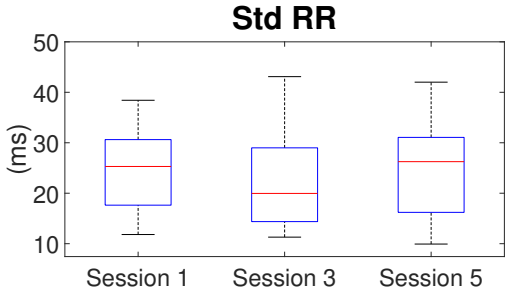

(b) Standard deviation of RR intervals.

Figure 5.17: Box-plot plots for mean and std of the RR intervals.

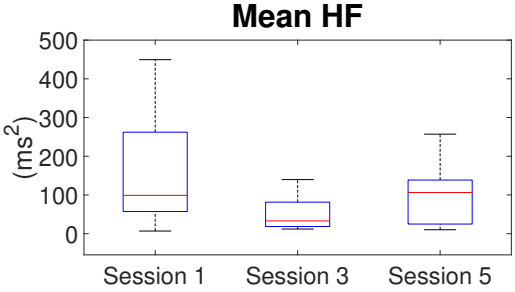

(a) Mean of HF component.

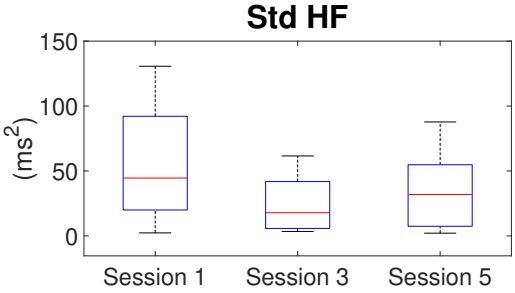

(b) Standard deviation of HF component.

Figure 5.18: Box-plot plots for mean and std of the HF.

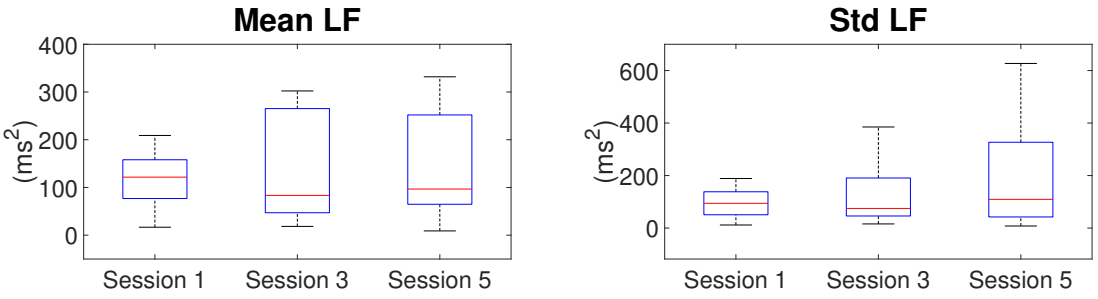

(a) Mean of LF component. (b) Standard deviation of LF component.

Figure 5.19: Box-plot plots for mean and std of the LF.

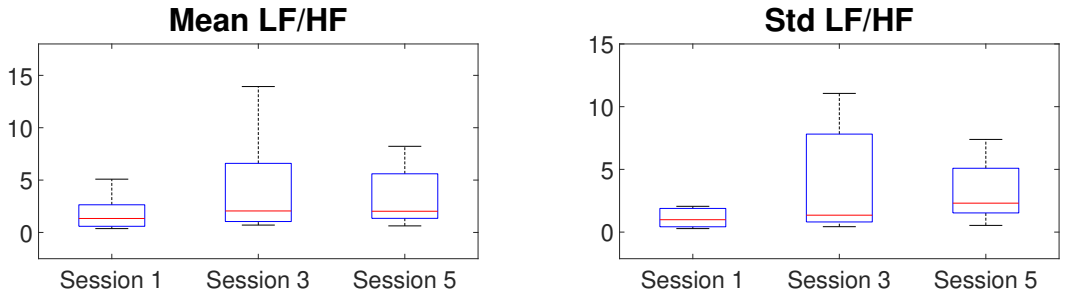

(a) Mean of LF/HF ratio. (b) Standard deviation of LF/HF ratio.

Figure 5.20: Box-plot plots for mean and std of the LF/HF ratio.

5.3 Apartment

The apartment analysis has been performed on three subjects (7, 12, and 17) to investigate whether the behavior of the HF in visit 2 is consistent with the results observed in the laboratory. These participants are characterized by a favorable amount of data points well distributed over the entire data collection. Thus, they have been selected to continuously monitor the trend of the HF.
Furthermore, the aim was to examine whether a shift in the HF toward lower values in concurrence with lessened motor symptoms (especially tremor), presumably indicating an "On" status, is appreciable during the afternoon, when the HF values are reported to be sensibly lower than during the morning. If it is, the diminished HF content can be primarily addressed to autonomic levodopa's effects rather than to the circadian rhythms, justifying the decreases observed in session 3 in the laboratory visit.

The following section presents the results of the apartment analysis, highlighting the parallel trend between the level of tremor, the perceived status of the subject, and the HF of the HRV in connection with the time of the day and the stage of the medication cycle.

5.3.1 Circadian rhythms

To understand whether the circadian rhythms have an impact on the magnitude of the HF, the mean value of the HF over the totality of the available data points has been computed for the laboratory and the apartment visits and differences have been investigated in parallel with the time of the day. Results are shown in Table 5.9. Start and end of the visit are presented as the time of the first and last data points available, respectively.
The mean value of the HF component over the apartment data collection proved to be significantly lower than in the laboratory in subject 7 and 17 (72 ± 24.6 vs 116.6 ± 54.3 and 72.6 ± 37.1 vs 140.4 ± 111.4, respectively). However, this has not been observed in subject 12, who showed a higher mean value of the HF in the apartment than in the laboratory (478.7 ± 153.7 vs 285.5 ± 109.3).

		Subject 7	**Subject 12**	**Subject 17**
Laboratory	**Start**	11:16	10:30	09:43
	End	15:38	15:14	12:44
	Mean HF	116 ± 54.3	285.5 ± 109.3	140.4 ± 111.4
Apartment	**Start**	14:12	15:11	11:11
	End	17:04	18:24	15:31
	Mean HF	72 ± 24.6	478.7 ± 153.7	72.6 ± 37.1

Table 5.9: Time of start and end of the laboratory and apartment assessment and relative mean values of HF.

5.3.2 Medication cycle

The apartment data collection does not provide specific labels for the times of medication intake, which have been estimated as following.

- Considering the regular cycle of medication of the subjects: the time of the dose can be estimated by looking at the last intake before the start of the visit (known) and at the daily dosage-schedule (e.g. five times a day, every two hours, etc.).

- Considering the motor assessment performed every hour via laptop by a clinician through a short version of the MDS-UPDRS III: the phase of the medication cycle can be estimated by evaluating the motor performances of the subject. Particularly, the scores relative to the postural and kinetic tremor for right and left sides have been taken into account in order to remove the eventual and improper contribution of the dyskinesia, which is more likely to be associated to the "On" status and thus needs to be discarded.
  Total score for the short MDS-UPDRS III, total, minimum, and maximum score for the postural and kinetic tremor are shown in Table 5.11.

- Considering the self-reports fulfilled by the subjects during the visit. Every hour they were asked to complete a questionnaire consisting of the self-reported status expressed in a numeric code between 0 and 4 (Figure 5.10), the level of fatigue, and the difficulty to move and concentrate in a severity scale between 0 and 10 (where 0 indicates no fatigue and 10 high fatigue).
  The self-reports are presented in Table 5.12.

Code	**Status**
0	ON
1	ON with dyskinesia
2	OFF
3	trans-to-ON
4	trans-to-OFF

Table 5.10: Numeric code implemented to define the status of the subject.

Subject	**Time**	**Short UPDRS**	**Tot P-K**	**Min P-K**	**Max P-K**
7	13:37	15	6	1	2
	14:37	17	6	1	2
	15:36	18	4	1	1
	16:35	14	4	1	1
	17:37	21	5	1	2
12	14:34	7	1	0	1
	15:41	9	2	0	1
	16:40	12	4	1	1
	17:41	14	2	0	1
	18:45	8	2	0	1
	19:34	10	2	0	1
17	10:54	13	4	1	1
	11:49	11	2	0	1
	12:51	10	2	0	1
	13:50	11	3	0	1
	14:52	12	2	0	1
	15:51	14	3	0	1

Table 5.11: Total short MDS-UPDRS III score, total, minimum, and maximum scores for postural and kinetic tremor.

Subject	Time	Status	Fatigue	Movement	Concentration
7	13:37	4	3	2	1
	14:37	3	3	4	2
	15:36	1	3	2	1
	16:35	0	4	3	2
	17:37	2	7	7	5
12	14:34	0	7	2	5
	15:41	0	3	0	0
	16:40	0	4	1	4
	17:41	4	7	2	4
	18:45	4	2	4	2
	19:34	2	6	6	6
17	10:54	3	3	3	1
	11:49	0	1	1	1
	12:51	0	2	2	1
	13:50	0	1	1	1
	14:52	0	2	1	1
	15:51	3	4	3	1

Table 5.12: Self-reports fulfilled by the subjects.

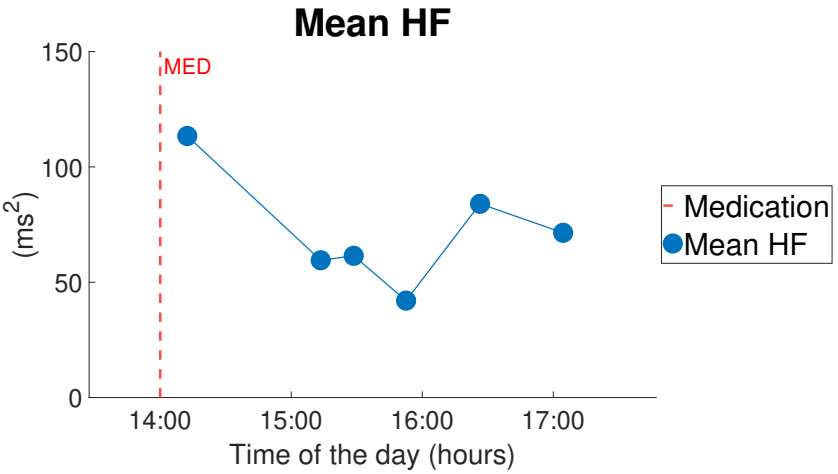

(a)

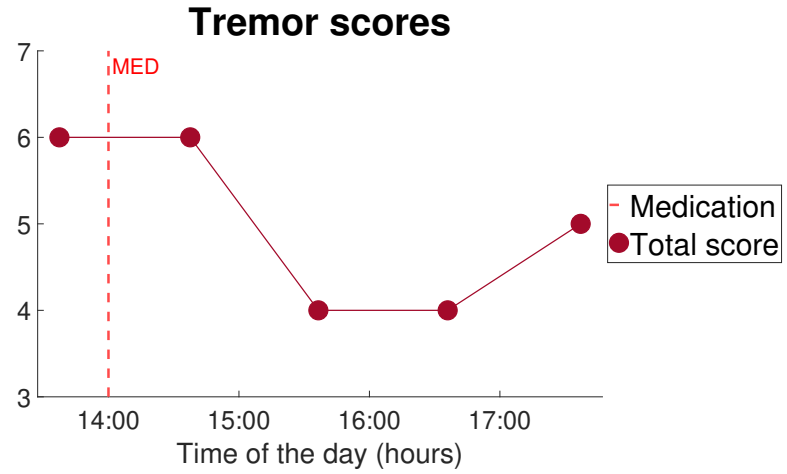

(b)

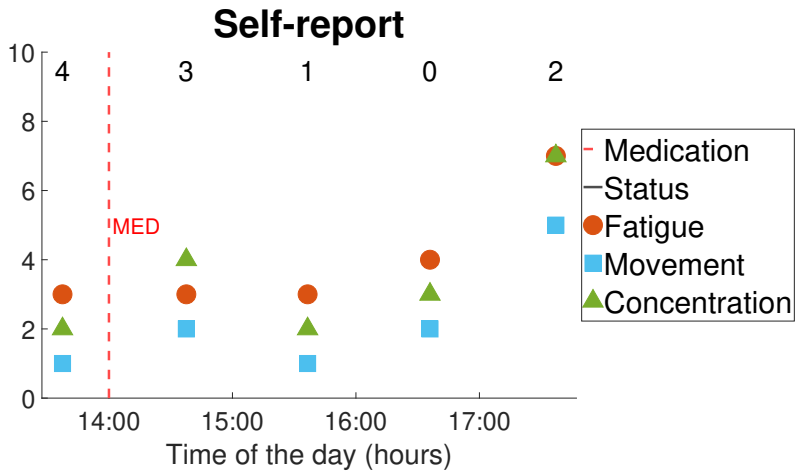

(c)

Figure 5.21: Mean HF (a), tremor scores (b), and self-reports (c) in subject 7.

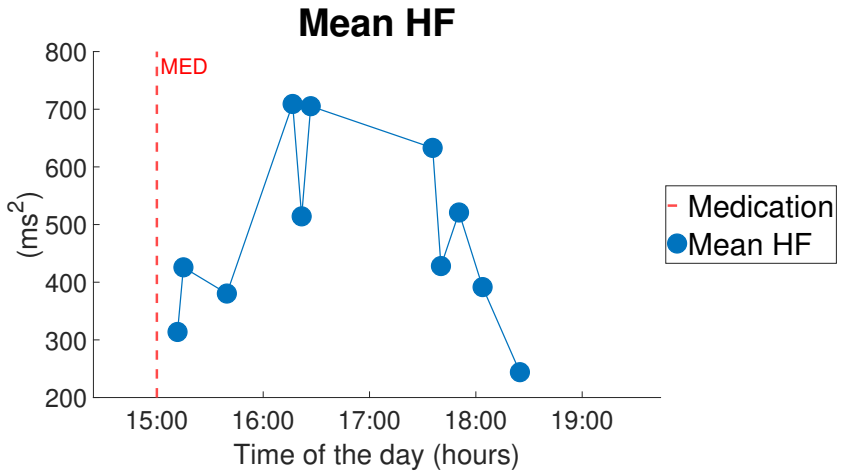

(a)

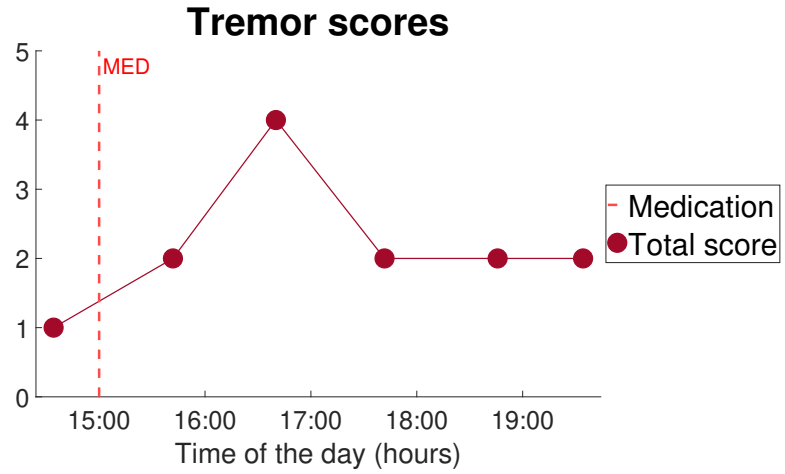

(b)

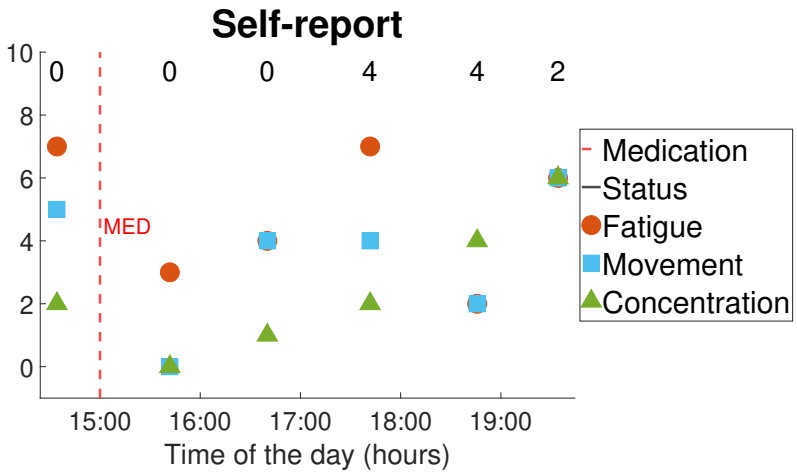

(c)

Figure 5.22: Mean HF (a), tremor scores (b), and self-reports (c) in subject 12.

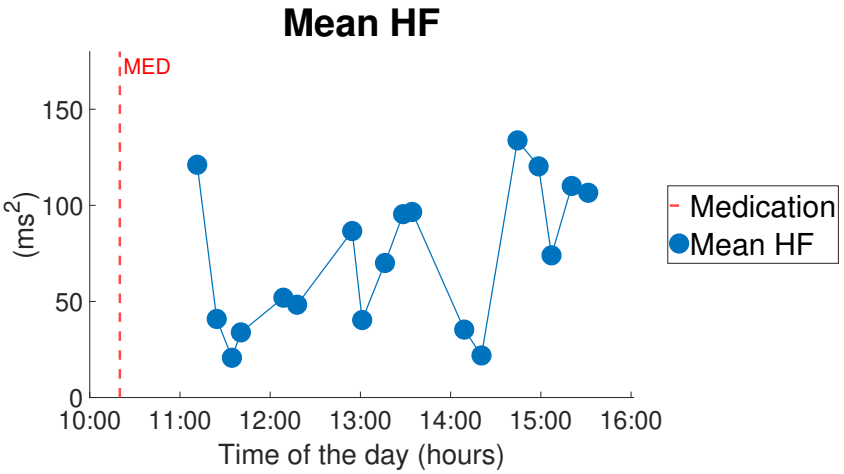

(a)

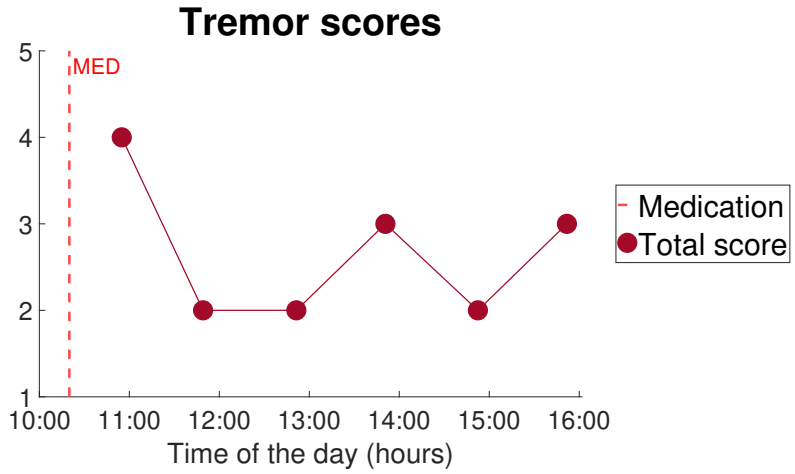

(b)

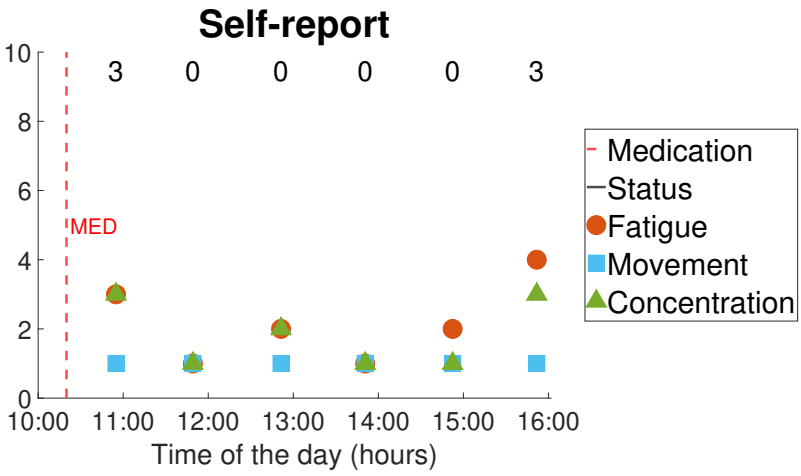

(c)

Figure 5.23: Mean HF (a), tremor scores (b), and self-reports (c) in subject 17.

The parallel trend of the mean HF power, the total tremor score, and the self-reported condition is shown in Figure 5.21 for subject 7, Figure 5.22 for subject 12, and Figure 5.23 for subject 17.
The HF positively correlates with the tremor pattern, as larger values of the HF are appreciable in parallel with higher motor scores.
All the analyzed subjects manifest a consistent behavior with the laboratory results. Subject 7 and 17 exhibit a diminished HF in concurrence with an expected "On" status, confirmed by tremor scores and self-reports. Subject 12 displays a different tendency. Particularly, although the HF magnitude first diminishes after the levodopa's intake, it also appears higher during the vanishing of the medication's effects and decreases again concurrently with the entry in the "Off" stage. This might appear in contrast with the other two participants and the final decrease in the HF can not be addressed to circadian variations. However, this particular subject presented a similar behavior in the laboratory assessment, as the HF power increased during the transition between session 3 and 4 (Figure 5.11). Moreover, the tremor scores are higher during the transition to the "Off" condition as well, validating the coordinate behavior between HF and motor performances.

Chapter 6

Discussion

This thesis has been focused on the assessment of the heart rate variability in subjects with Parkinson's disease to investigate whether the disorder is associated with impaired autonomic control of the heart and the levodopa absorption has an additional effect.
The evaluation has been centered on the high-frequency component of the power spectrum, since this parameter has been reported as the most reliable and interpretable marker of vagal outflow. The spectral analysis has been extracted by employing a novel point-process framework to model the RR intervals, as this approach allows us to obtain instantaneous measures without interpolating between consecutive R waves.

The first part of the study investigated the potential differences in the HRV pattern between healthy controls and PD subjects. In both cases, data have been collected within three minutes of rest, during which participants have been asked to be sitting and silent. The analysis has been accomplished by comparing the HRV parameters of healthy controls and affected patients measured at baseline before the intake of the levodopa, in order to remove the potential bias introduced by the medication.
Consistently with the previous literature, the HF content of the power spectrum has been found diminished in subjects with a diagnosis of PD, denoting a suppressed vagal modulation of the cardiac response. However, the differences are not statistically significant according to the Mann-Whitney U test. Significance has been observed in all the indices extracted from the LF component, which has been reported to be influenced by both sympathetic and parasympathetic activities. Hence, this results suggests that signs of impairment of the autonomic modulation of the heart rate are present over the progression of the disorder and, at least in first instance, are not directly related to the intake of the antiparkinsonian medication.

The second part of the thesis focused on the assessment of the potential effects of the medication intake on the autonomic nervous system. Particularly, the analysis has been accomplished by evaluating the heart rate variability parameters over a full medication cycle in subjects with a diagnosis of PD treated with levodopa-carbidopa.
The results prove that features extracted from both time-domain and frequency-

domain do not show a constant trend but are fluctuating on an inter-session and intra-session basis. These variations can not be addressed purely to the action of the medication and additional factors must be considered. Among them, the circadian rhythms are well established to play a fundamental role in the modulation of the cardiac response, inflecting the HF content differently between morning and afternoon. Thus, a consistent analysis has to take in account both the potential effects deriving from the intake of the levodopa and the genuine variations occurring during the day. To accurately investigate the contribution of the antiparkinsonian medication on the autonomic modulation of the heart, every distinct session has been analyzed separately.

Results prove that considerable differences are appreciable among the distinct stages of the medication cycle, denoting an influence that might not be addressed only to the circadian variations. Particularly, statistically significant differences have been found in the mean value of the RR intervals and in all the HF parameters between session 1, which denotes a clear "Off" condition, and session 3, which follows the levodopa's intake and marks a clear "On" status. Both the RR intervals and the HF indices have been found to be decreased after the drug dose, disclosing an additional vagal suppression that can be addressed to the action of the medication. Moreover, the trend of the HF is generally contrary to the one of the HR, proving that the diminished HF is effectively due to a parasympathetic deficiency. No other spectral indices show significant differences between the "Off" and "On" status, once again supporting the superiority of the HF power in the investigation of the autonomic outflow.

Although the above-mentioned behavior has been observed in almost all the analyzed participants, subject 10 and 21 disclose a different trend. Particularly, they manifest an averaged value of the HF that is higher within session 3 than session 1, appearing to be strongly in contrast with the other cases. However, subject 10 and 21 are also the only two situations that encompasses a considerably low HF extent, even at the baseline condition. Thus, the small variations observed for these two outliers that approximate a ten of squared milliseconds might be purely addressed to noise rather than to the medication intake. Nevertheless, the reason behind this behavior is not clear, as these two participants do not markedly differ from the other subjects in terms of age, disease progression, levodopa's therapy duration, and symptoms appearance. Further analysis might be necessary to investigate wherefore they are featured by very low values of HF.

A vagal suppression after the medication dose is consistent with what has been observed by Ruonala et al. [25], who investigated the HRV parameters before, 30 minutes, and 60 minutes after the levodopa's intake and reported a decreased HF content after 30 and 60 minutes. This current work differs from that previous one, principally for two aspects. First, the eleven subjects investigated by Ruonala et al. were assessed in a practically defined "Off" condition, as their last intake dated back to the day before. Contrarily, this thesis aimed to evaluate a real-life behavior and participants were investigated during a normal medication cycle. Second, here the time-dependence has been abandoned and the attention has been posed on the perceived condition of the subjects, proving that the vagal inhibition caused by

levodopa's absorption is likely to occur simultaneously with an improvement of the motor performances.

Contrarily to what expected, the trend of the HF over session 4 and 5 do not show a consistent behavior but varies on an individual basis. Particularly, a subset of about half the participants manifests an increased HF after shifting from session 3 to 5, coherently with the hypothesis of reversible levodopa's effects on the vagal outflow. The others show a diminished HF in session 5, leading to the assumption that the variations in the HF are modulated by multiple factors.
As session 5 was in most of the cases concomitant with the transition from the morning to the afternoon, this stage of the medication cycle might be influenced by the circadian rhythms, which are established to play a key role in the control of the HRV parameters, especially for the HF pattern. Past works reported a diminished HF in the afternoon compared with the morning, suggesting that genuine variations occur over the course of the day. Thus, even if the vanishing of the levodopa's effects is triggering an increase in the HF during the transition from session 3 to 5, the overall HF power content in session 5 might be lower due to the circadian changes.

To further investigate the separate contributions of the antiparkinsonian medication and the circadian rhythms, data collected in the simulated apartment environment have been analyzed for a subset of subjects that accomplished the apartment visit during the afternoon. This aimed to investigate whether the behavior observed in the laboratory was consistent also in a different time of the day.
The real stage of the medication cycle in the apartment has been estimated by evaluating the motor scores assigned by the clinician and the self-reports fulfilled by the subjects during the data collection. When possible, the estimated time of medication intake has been verified by checking the videos.
The results accomplished in the apartment analysis proved that lower values of HF can be observed during the afternoon hours and confirms the parallel behavior between HF and medication stage observed in the laboratory. Although considerable fluctuations of the HRV parameters are appreciable, the HF power content has been found overall lower during the "On" intervals, again suggesting a depressive effect of the levodopa on parasympathetic system. Apparently, the HF trend seems to correlate with the motor behavior, especially the tremor, as higher values of HF are appreciable together with higher motor scores that denote an increased level of tremor and a likely "Off" condition. This is particularly evident for subject 12, who presents a different behavior from the other subjects. Particularly, both the HF and the tremor scores manifest an increase in concurrence with the transition from the "On" to the "Off" status and decrease again at the end of the medication cycle. Curiously, the same trend is appreciable in the laboratory data. Although subject 12 shows a decrease in the HF from session 1 to 3, this subject also manifests an increased HF within session 4, concurrently with heightened tremor. Moreover, the HF magnitude seems not to be diminished during the afternoon. Thus, this participant might be considered as an outlier both in the laboratory and simulated apartment data collection, exhibiting a consistent different behavior.
The apartment findings allow to claim that the medication intake definitely plays

a role in the autonomic modulation of the cardiac response, weakening the vagal activation that dominates during rest. Moreover, this also confirms that the circadian rhythms have an impact on the parasympathetic activity and that consistent differences can be observed in the HF between morning and afternoon.

Chapter 7

Conclusion

This thesis aimed to assess the HRV pattern, with particular attention to the high-frequency component of its power spectrum, in patients affected by Parkinson's disease. Although it is a preliminary analysis with several limitations, three main discoveries have been accomplished.
The first result shows that the HF power content is reduced in PD subjects compared with healthy controls, suggesting an impaired parasympathetic modulation of the heart featuring the disorder. This finding is consistent with the previous literature and the concept of cardiac autonomic denervation supported by neuroimaging evidences.
The second result sustains the hypothesis of vagal suppression induced by the intake of levodopa, disclosing diminished RR intervals and HF content during the "On" status of the medication cycle. In this particular case, statistical significance has been reached in the comparison of the two samples ("Off" and "On").
Finally, the third finding denotes the influence of the circadian rhythms on the HRV pattern. Afternoon HF is overall lower than morning HF due to the genuine fluctuations that occur over the course of the day. This provides an explanation for the diminished HF observed from session 3 to 5 for a subset of subjects, highlighting the contribution of the circadian changes during the transition from the first to the second part of the day.

The main limitations of the study are a small sample size and a considerable amount of sources of noise. The larger BlueSky Project was not primarily addressed to collect and analyze the ECG signals and more attention has been offered to the motor assessment. Thus, fundamental conditions for a proper HRV monitoring, such as resting periods and silence, have been neglected, lessening the amount of data valid for the analysis. Moreover, the scarcity of clean raw signals forced us to exclude a non-indifferent subset of subjects, limiting the statistical power of the analysis.

As future steps, it would be necessary to plan a data collection optimized for the HRV assessment. First, more attention needs to be addressed to the quality of the recording of the signals and the environmental conditions. Particularly, it is of fundamental importance to assess the subjects when they are at rest and in silence. Second, more subjects need to be included in the study to heighten the statistical

power of the analysis.
Moreover, it would be interesting to collect additional patients information, such as a detailed list of impairing symptoms and their occurrence during the medication cycle. Particularly, it would be meaningful to evaluate the potential connection between the appearance of the typical observed non-motor symptoms, as gastrointestinal disturbances, urinary dysfunctions, and sweating anomalies, and the character of the cardiac response through the HRV analysis. This would allow to investigate whether there is a co-occurrence of the separate non-motor manifestations and the eventual contribution of the levodopa on their incidence.

Appendix A

Full medication cycle

This appendix collects the plots computed to display the parallel trend of the three principal HRV parameters over the full medication cycle experienced in the laboratory data collection. All the other indices are extracted from these three. Hence, their tendency can be easily estimated.
Note that, instead of plotting the mean RR, is here reported the mean HR, as the parallel trend of the mean HR and mean HF is meaningful to provide a physiologic intepretation and to assess the vagal contribution.

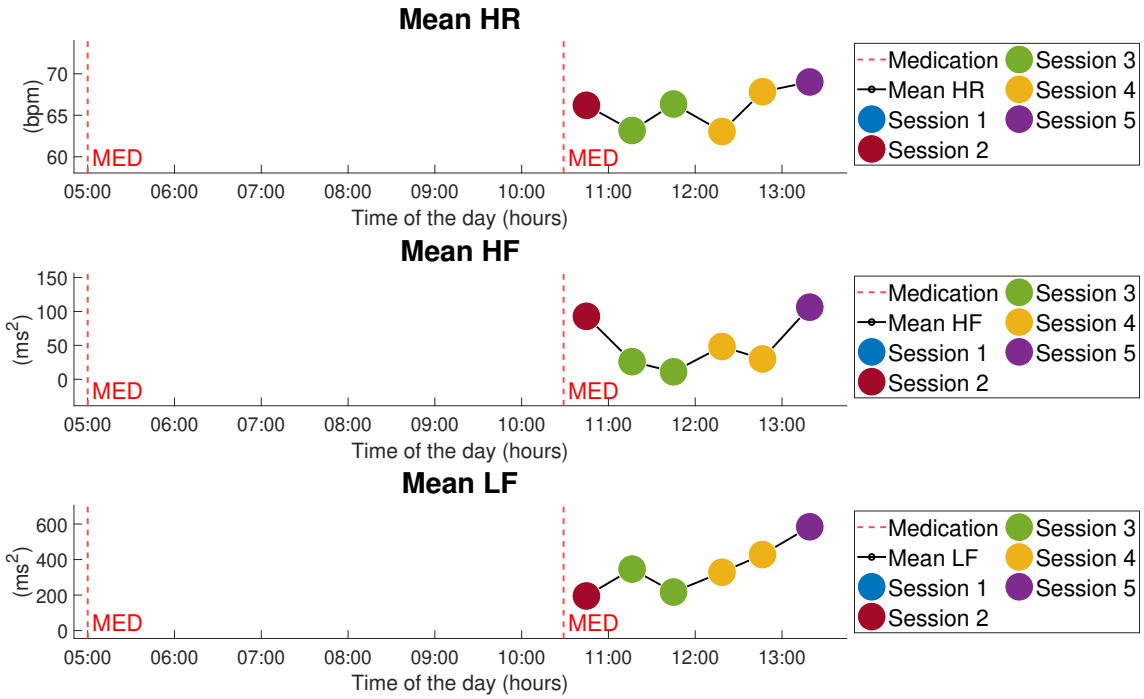

Figure A.1: Subject 3.

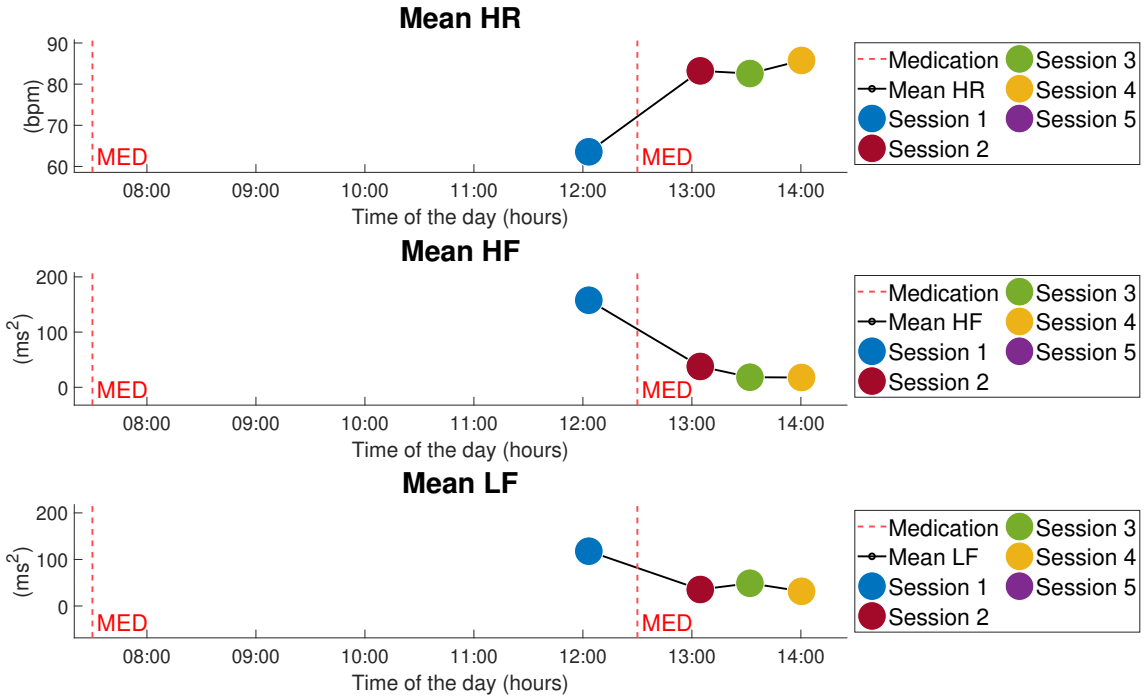

Figure A.2: Subject 4.

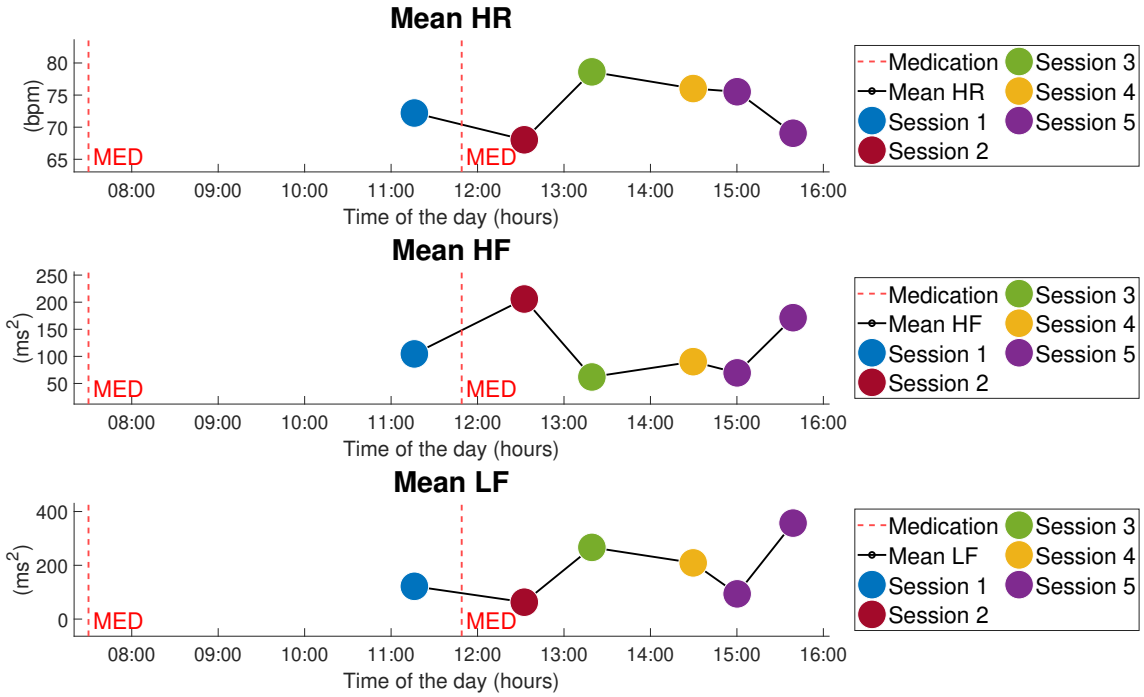

Figure A.3: Subject 7.

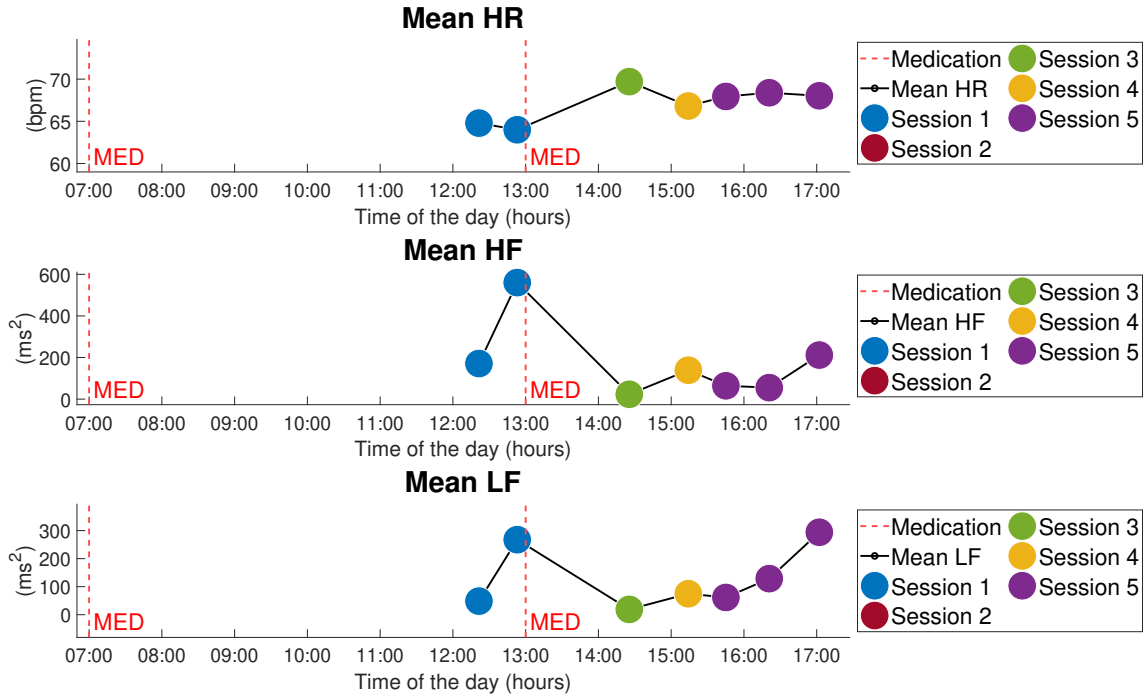

Figure A.4: Subject 9.

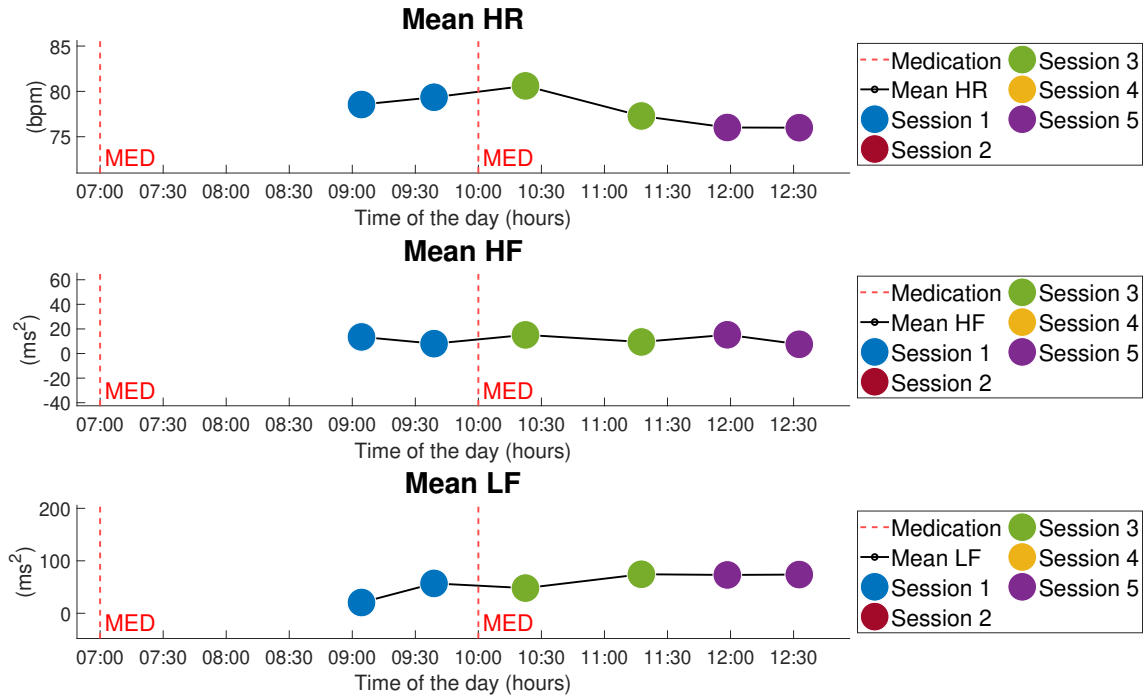

Figure A.5: Subject 10.

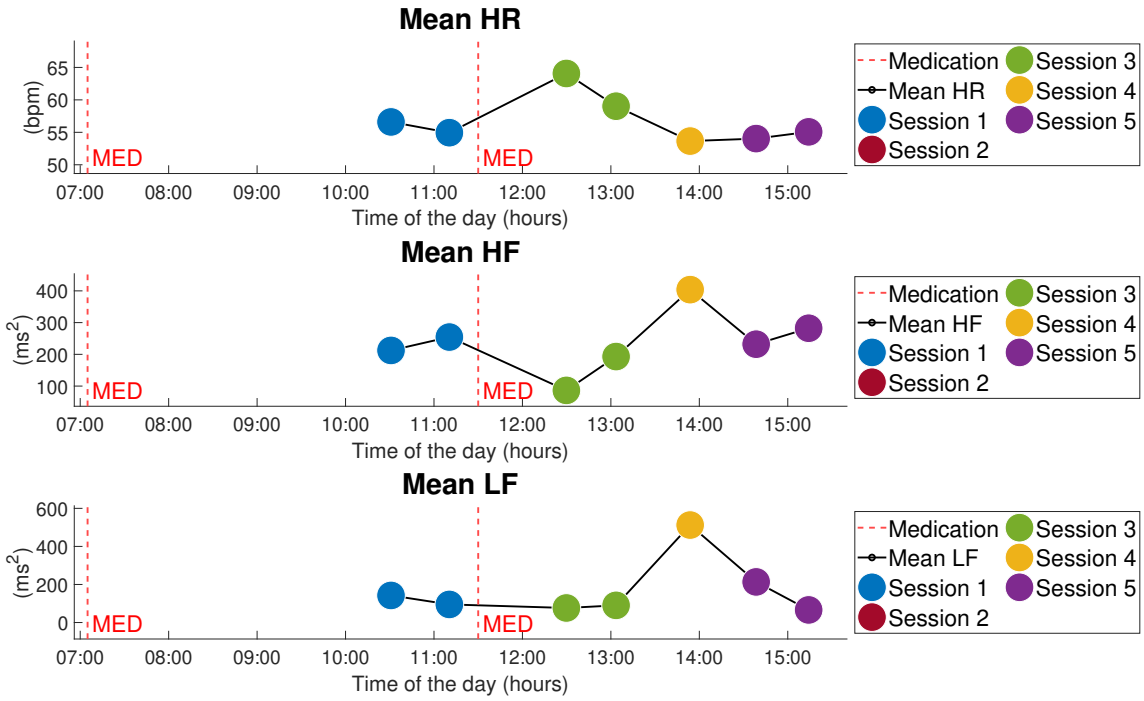

Figure A.6: Subject 12.

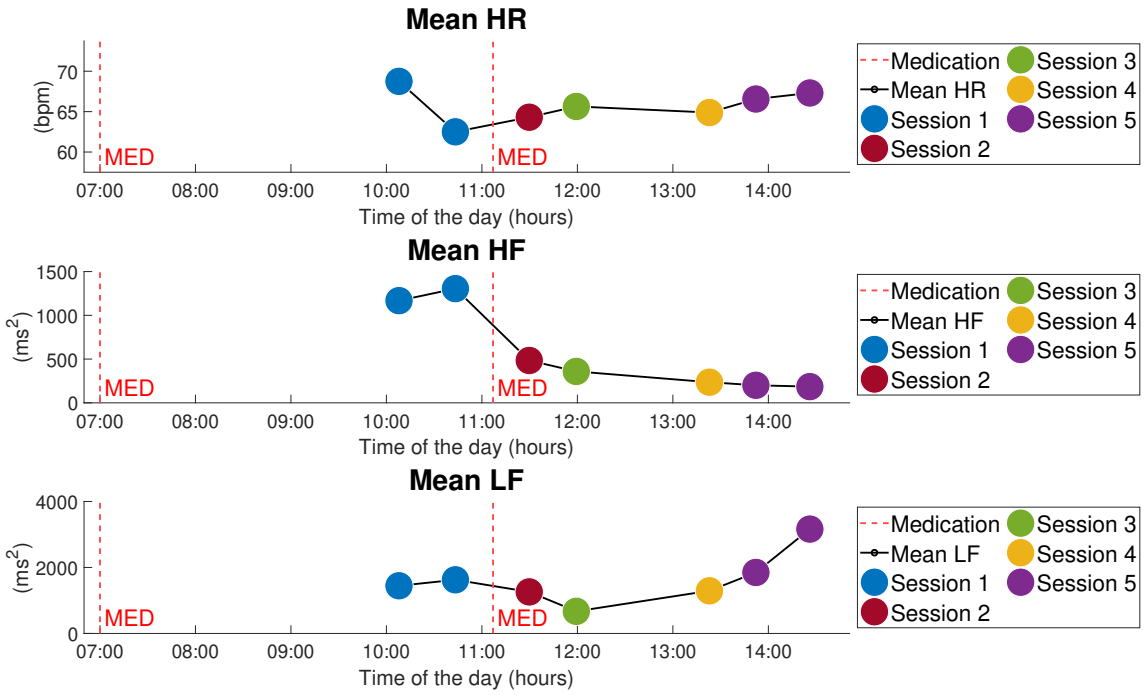

Figure A.7: Subject 13.

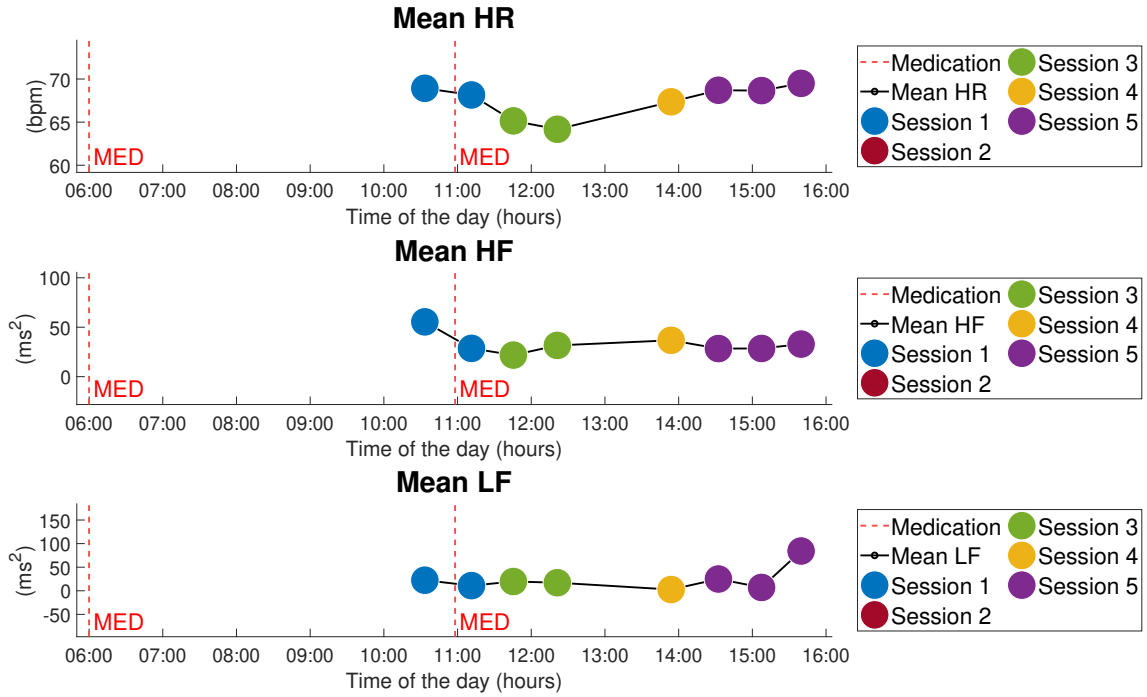

Figure A.8: Subject 14.

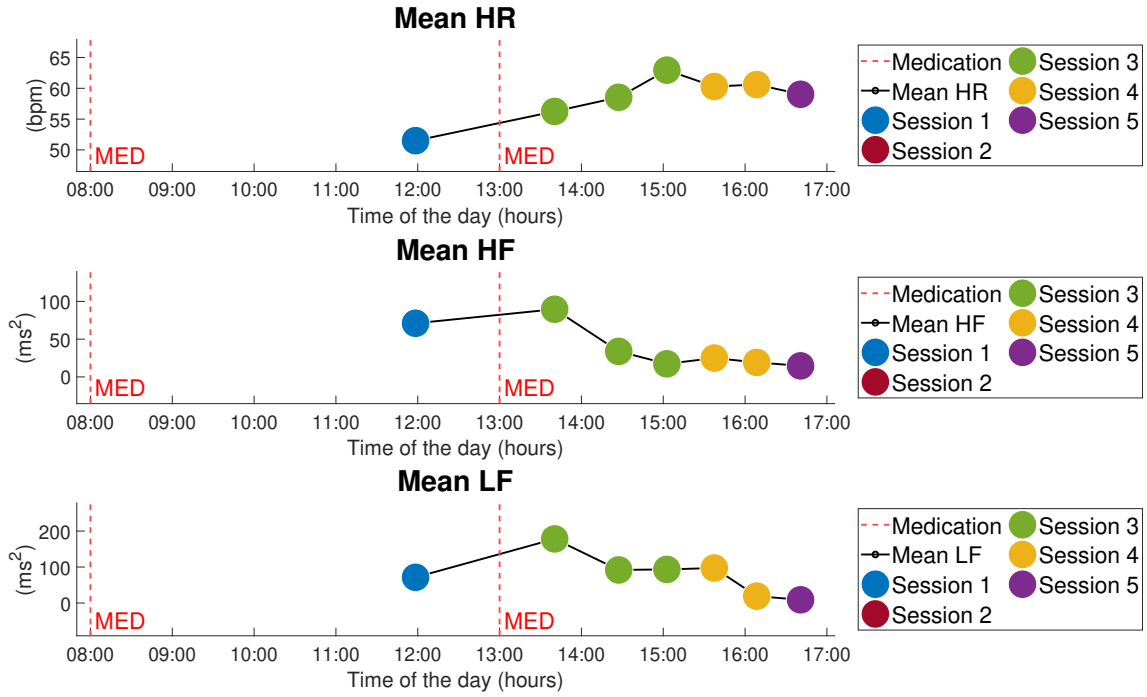

Figure A.9: Subject 15.

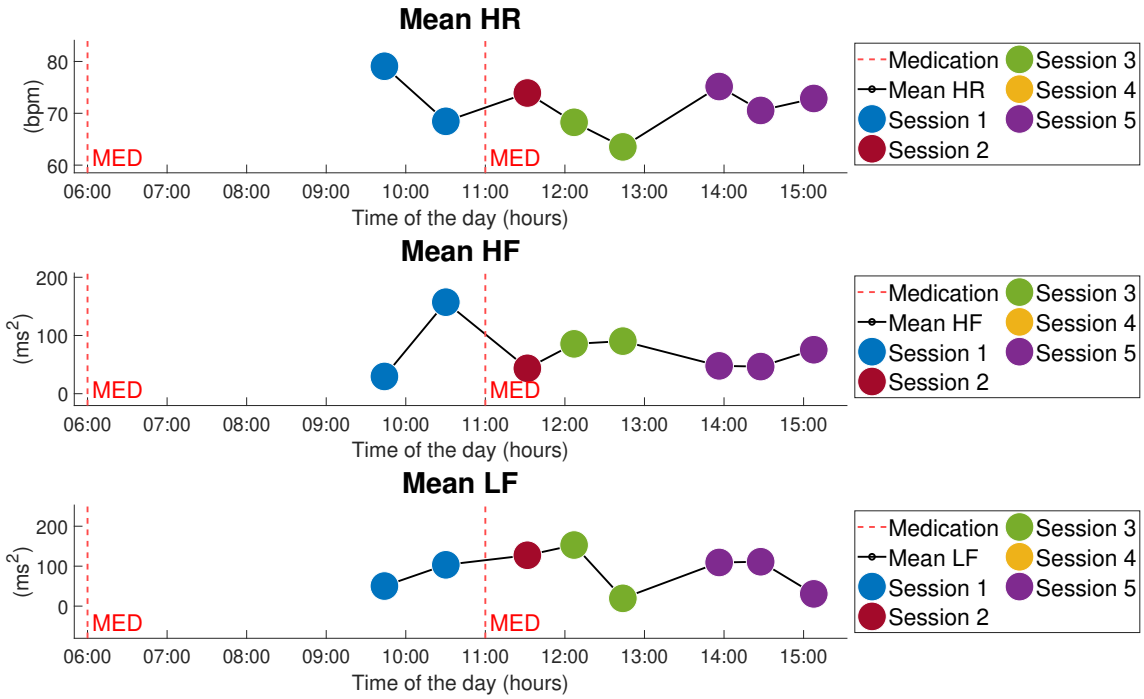

Figure A.10: Subject 16.

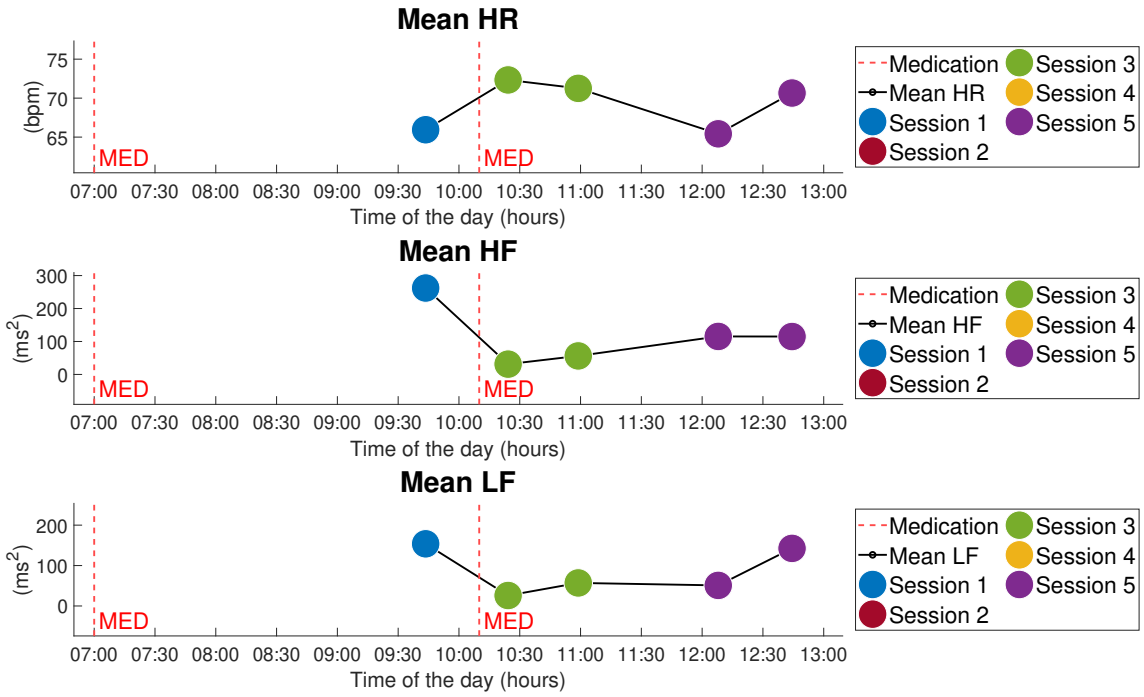

Figure A.11: Subject 17.

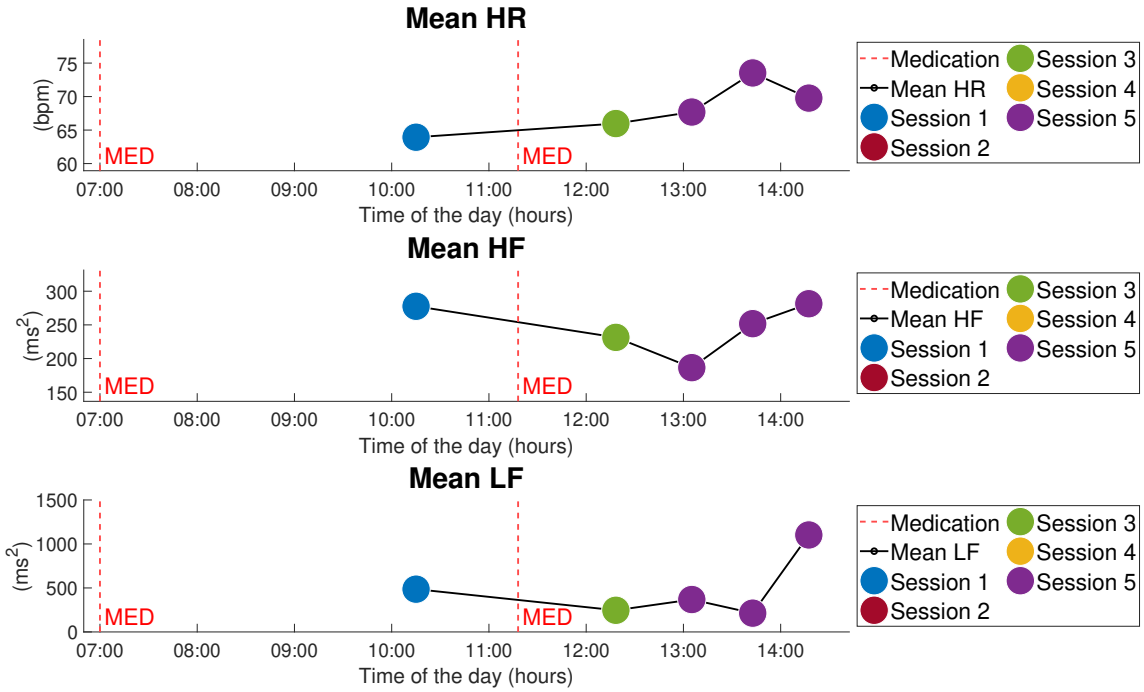

Figure A.12: Subject 19.

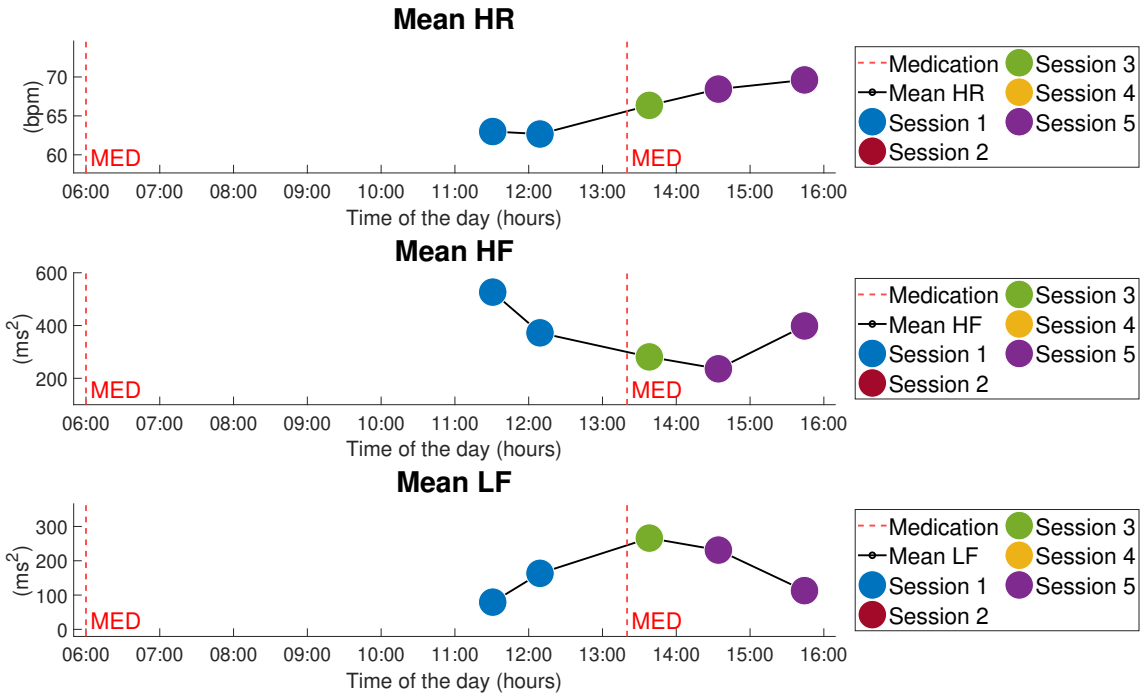

Figure A.13: Subject 20.

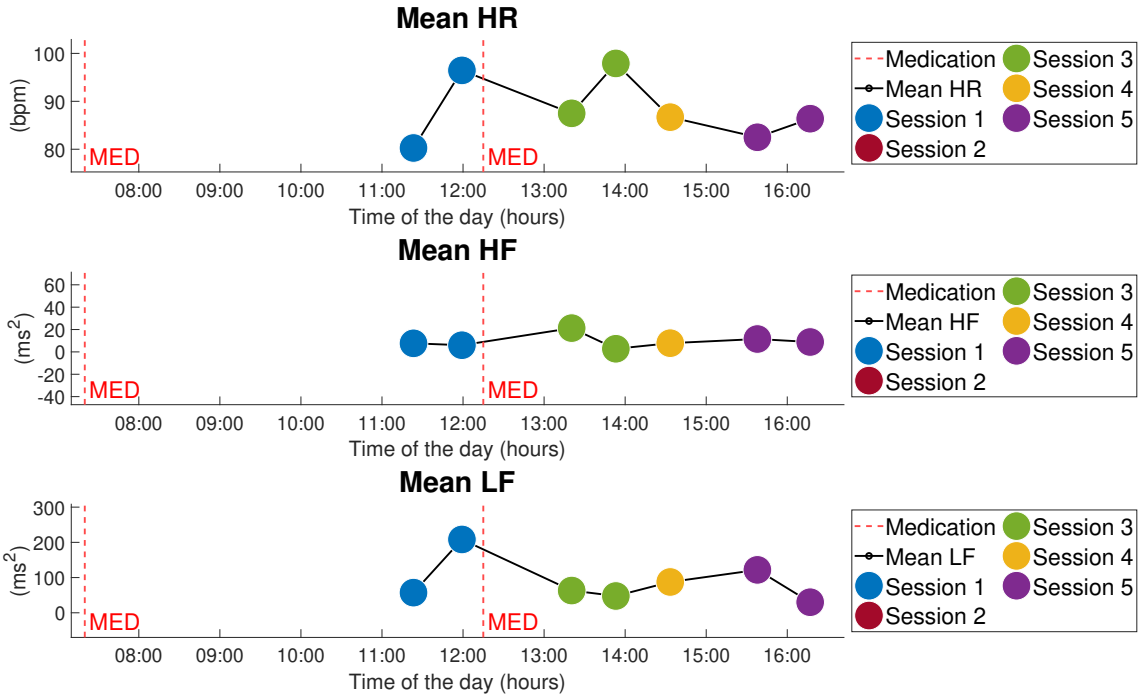

Figure A.14: Subject 21.

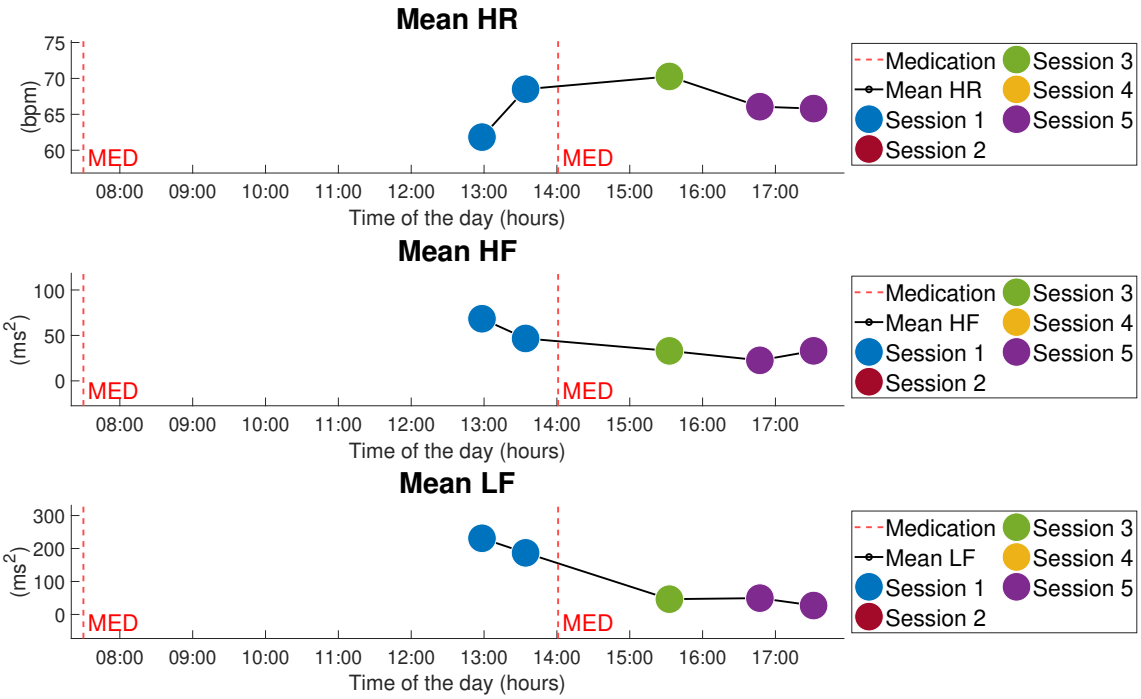

Figure A.15: Subject 22.

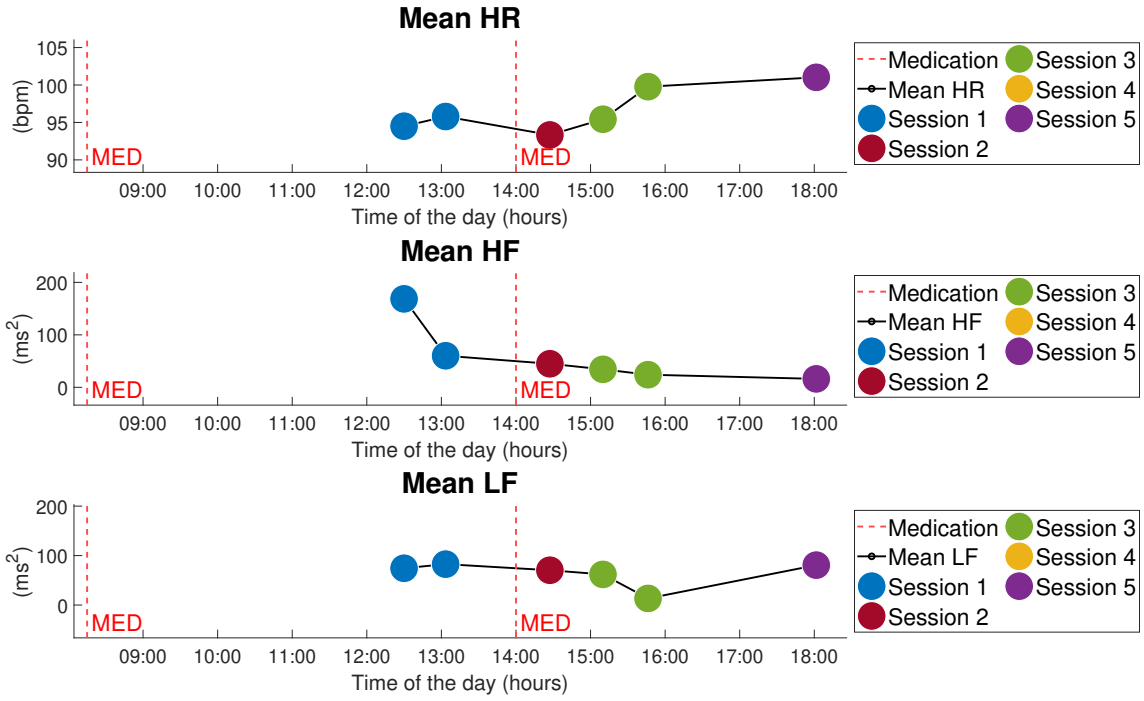

Figure A.16: Subject 23.

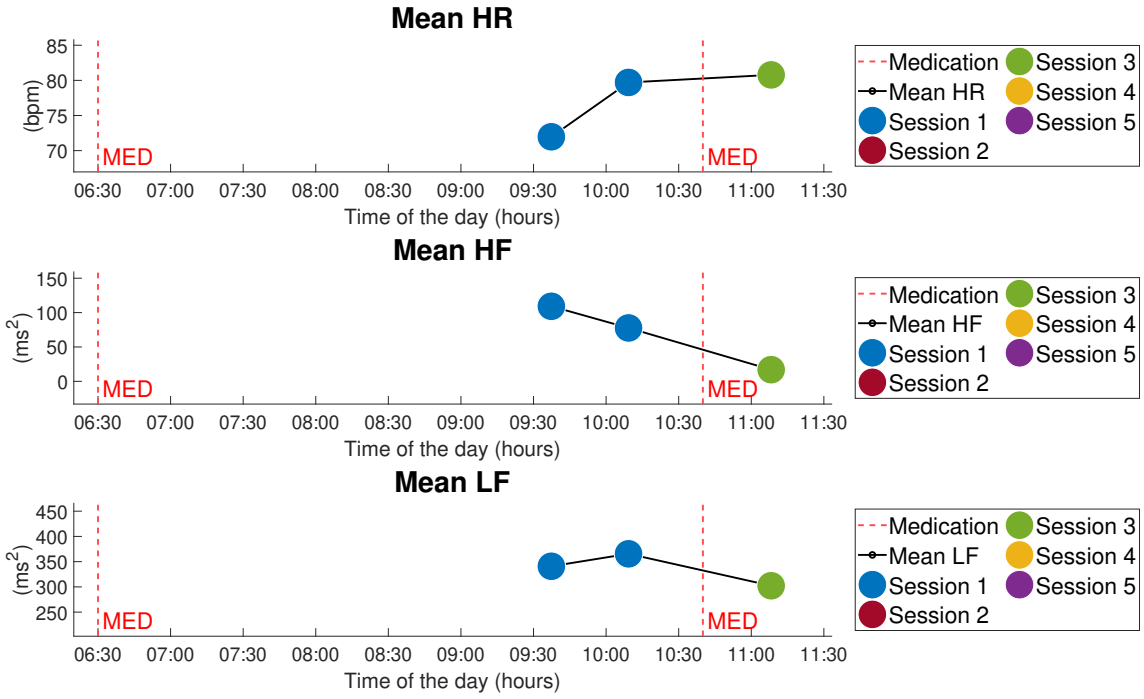

Figure A.17: Subject 24.

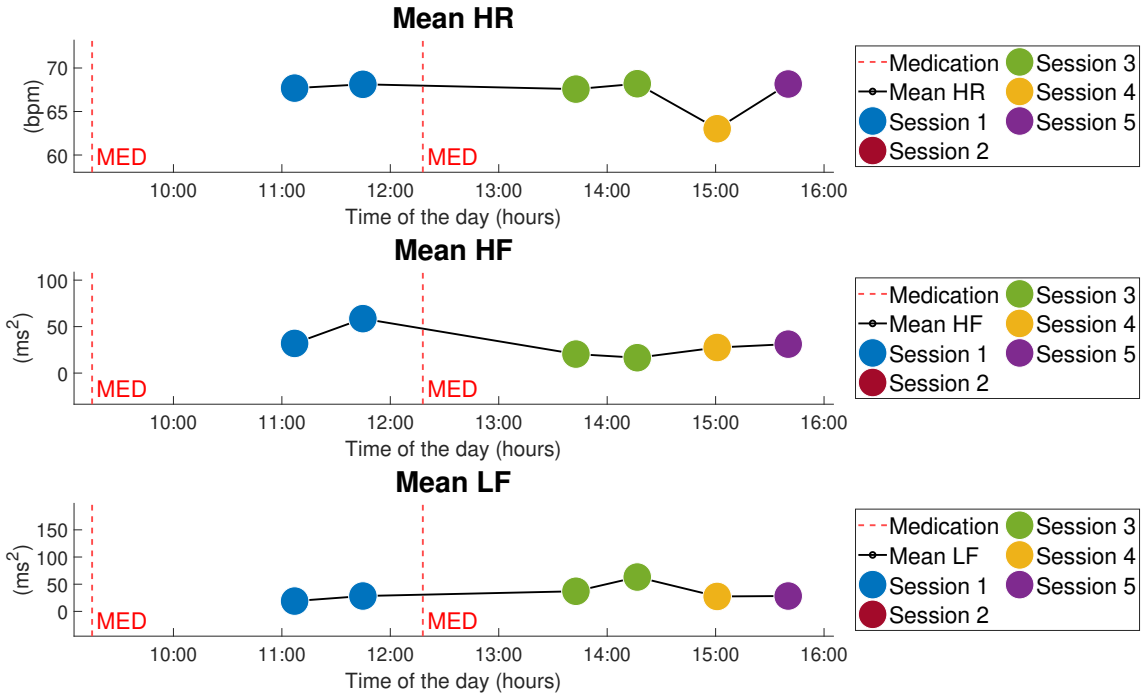

Figure A.18: Subject 26.

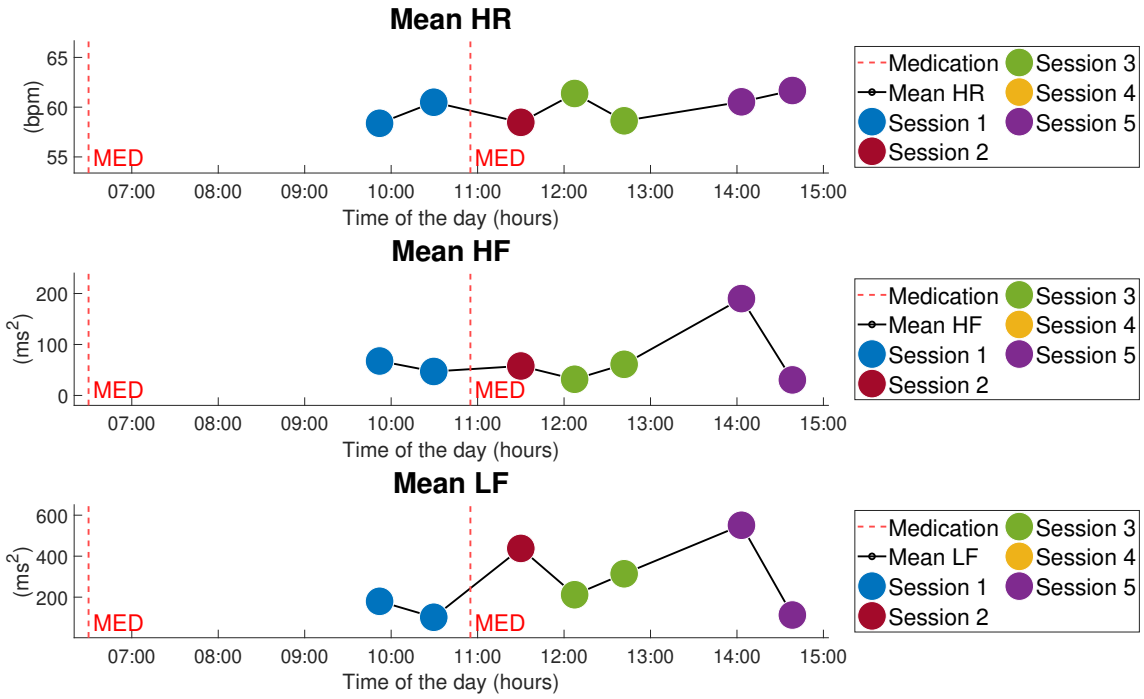

Figure A.19: Subject 27.

Bibliography

[1] D. P. Zipes and M. J. Shen, "Role of the autonomic nervous system in modulating cardiac arrhythmias," *Circulation Research*, vol. 114, no. 6, pp. 1004–1021, Mar. 14, 2014.

[2] H. K. Jamali, F. Waqar, and M. C. Gerson, "Cardiac autonomic innervation," *Journal of Nuclear Cardiology*, vol. 24, no. 5, pp. 1558–1570, Oct. 2017.

[3] D. S. Goldstein, "Dysautonomia in parkinson disease," *Comprehensive Physiology*, vol. 4, p. 22, 2014.

[4] J. S. Mulcahy, D. E. Larsson, S. N. Garfinkel, and H. D. Critchley, "Heart rate variability as a biomarker in health and affective disorders: A perspective on neuroimaging studies," *NeuroImage*, vol. 202, p. 116 072, Nov. 2019.

[5] O.-B. Tysnes and A. Storstein, "Epidemiology of parkinson's disease," *Journal of Neural Transmission*, vol. 124, no. 8, pp. 901–905, Aug. 2017.

[6] J. Parkinson, "An essay on the shaking palsy," 1817.

[7] R. Martínez-Fernández, E. Schmitt, P. Martinez-Martin, and P. Krack, "The hidden sister of motor fluctuations in parkinson's disease: A review on non-motor fluctuations," *Movement Disorders*, vol. 31, no. 8, pp. 1080–1094, Aug. 2016.

[8] L. V. Kalia and A. E. Lang, "Parkinson's disease," *The Lancet*, vol. 386, no. 9996, pp. 896–912, Aug. 2015.

[9] E. A. Coon, J. K. Cutsforth-Gregory, and E. E. Benarroch, "Neuropathology of autonomic dysfunction in synucleinopathies: Autonomic neuropathology in synucleinopathies," *Movement Disorders*, vol. 33, no. 3, pp. 349–358, Mar. 2018.

[10] J. G. Betts, P. Desaix, and E. Johnson, *Anatomy & Physiology*. 2013.

[11] D. Brisinda, A. R. Sorbo, R. Di Giacopo, A. Venuti, A. R. Bentivoglio, and R. Fenici, "Cardiovascular autonomic nervous system evaluation in parkinson disease and multiple system atrophy," *Journal of the Neurological Sciences*, vol. 336, no. 1, pp. 197–202, Jan. 2014.

[12] H. Braak, E. Ghebremedhin, U. Rüb, H. Bratzke, and K. Del Tredici, "Stages in the development of parkinson's disease-related pathology," *Cell and Tissue Research*, vol. 318, no. 1, pp. 121–134, Oct. 2004.

[13] H. Braak, U. Rüb, W. Gai, and K. Del Tredici, "Idiopathic parkinson's disease: Possible routes by which vulnerable neuronal types may be subject to neuroinvasion by an unknown pathogen," *Journal of neural transmission*, vol. 110, no. 5, pp. 517–536, 2003.

[14] A. Fanciulli, S. Strano, C. Colosimo, C. Caltagirone, G. Spalletta, and F. E. Pontieri, "The potential prognostic role of cardiovascular autonomic failure in α-synucleinopathies," *European Journal of Neurology*, vol. 20, no. 2, pp. 231–235, Feb. 2013.

[15] N. Pyatigorskaya, M. Mongin, R. Valabregue, L. Yahia-Cherif, C. Ewenczyk, C. Poupon, E. Debellemaniere, M. Vidailhet, I. Arnulf, and S. Lehéricy, "Medulla oblongata damage and cardiac autonomic dysfunction in parkinson disease," *Neurology*, vol. 87, no. 24, pp. 2540–2545, Dec. 13, 2016.

[16] D. M. Raffel, R. A. Koeppe, R. Little, C.-N. Wang, S. Liu, L. Junck, M. Heumann, and S. Gilman, "PET measurement of cardiac and nigrostriatal denervation in parkinsonian syndromes," p. 10,

[17] D. S. Goldstein, Y. Sharabi, B. I. Karp, O. Bentho, A. Saleem, K. Pacak, and G. Eisenhofer, "Cardiac sympathetic denervation preceding motor signs in parkinson disease*," *Cleveland Clinic Journal of Medicine*, vol. 76, S47–S50, Suppl_2 Apr. 1, 2009.

[18] S. Orimo, A. Takahashi, T. Uchihara, F. Mori, A. Kakita, K. Wakabayashi, and H. Takahashi, "Degeneration of cardiac sympathetic nerve begins in the early disease process of parkinson?s disease," *Brain Pathology*, vol. 17, no. 1, pp. 24–30, Jan. 2007.

[19] H. Fujishiro, R. Frigerio, M. Burnett, K. J. Klos, K. A. Josephs, A. Delle-Donne, J. E. Parisi, J. E. Ahlskog, and D. W. Dickson, "Cardiac sympathetic denervation correlates with clinical and pathologic stages of parkinson's disease," *Movement Disorders*, vol. 23, no. 8, pp. 1085–1092, Jun. 15, 2008.

[20] D. S. Goldstein, L. Sewell, and Y. Sharabi, "Autonomic dysfunction in PD: A window to early detection?" *Journal of the Neurological Sciences*, vol. 310, no. 1, pp. 118–122, Nov. 2011.

[21] D. S. Goldstein, C. Holmes, L. Sewell, M. Y. Park, and Y. Sharabi, "Sympathetic noradrenergic before striatal dopaminergic denervation: Relevance to braak staging of synucleinopathy," *Clinical Autonomic Research*, vol. 22, no. 1, pp. 57–61, Feb. 2012.

[22] J.-A. Palma and H. Kaufmann, "Treatment of autonomic dysfunction in parkinson disease and other synucleinopathies: TREATMENT OF AUTONOMIC DYSFUNCTION IN PD," *Movement Disorders*, vol. 33, no. 3, pp. 372–390, Mar. 2018.

[23] C. Noack, C. Schroeder, K. Heusser, and A. Lipp, "Cardiovascular effects of levodopa in parkinson's disease," *Parkinsonism & Related Disorders*, vol. 20, no. 8, pp. 815–818, Aug. 2014.

[24] J. H. Burn, "Hypotension caused by l-dopa.," *BMJ*, vol. 1, no. 5696, pp. 629–629, Mar. 7, 1970.

[25] V. Ruonala, M. P. Tarvainen, P. A. Karjalainen, E. Pekkonen, and S. M. Rissanen, "Autonomic nervous system response to l-dopa in patients with advanced parkinson's disease," in *2015 37th Annual International Conference of the IEEE Engineering in Medicine and Biology Society (EMBC)*, Milan: IEEE, Aug. 2015, pp. 6162–6165.

[26] J. Classen, J. Koschel, C. Oehlwein, K. Seppi, P. Urban, C. Winkler, U. Wüllner, and A. Storch, "Nonmotor fluctuations: Phenotypes, pathophysiology, management, and open issues," *Journal of Neural Transmission*, vol. 124, no. 8, pp. 1029–1036, Aug. 2017.

[27] T. Witjas, E. Kaphan, J. P. Azulay, O. Blin, M. Ceccaldi, J. Pouget, M. Poncet, and A. A. Cherif, "Nonmotor fluctuations in parkinson's disease: Frequent and disabling," *Neurology*, vol. 59, no. 3, pp. 408–413, Aug. 13, 2002.

[28] C. Ossig, D. Sippel, M. Fauser, F. Gandor, W. H. Jost, G. Ebersbach, and A. Storch, "Timing and kinetics of nonmotor fluctuations in advanced parkinson's disease," *Journal of Parkinson's Disease*, vol. 7, no. 2, pp. 325–330, May 16, 2017.

[29] NoMoFlu-PD study group, M. Fauser, M. Löhle, G. Ebersbach, P. Odin, G. Fuchs, W. H. Jost, K. R. Chaudhuri, R. Koch, and A. Storch, "Intraindividual variability of nonmotor fluctuations in advanced parkinson's disease," *Journal of Parkinson's Disease*, vol. 5, no. 4, pp. 737–741, Nov. 26, 2015.

[30] G. D. Clifford, *Signal processing methods for heart rate variability analysis*. University of Oxford, 2002.

[31] C. Tessa, N. Toschi, S. Orsolini, G. Valenza, C. Lucetti, R. Barbieri, and S. Diciotti, "Central modulation of parasympathetic outflow is impaired in de novo parkinson's disease patients," *PLOS ONE*, vol. 14, no. 1, J. Koenig, Ed., e0210324, Jan. 17, 2019.

[32] A. L. Goldberger, Z. D. Goldberger, and A. Shvilkin, "Chapter 3 - how to make basic ecg measurements," in *Goldberger's Clinical Electrocardiography (Ninth Edition)*, A. L. Goldberger, Z. D. Goldberger, and A. Shvilkin, Eds., Ninth Edition, Elsevier, 2018, pp. 11–20.

[33] F. Shaffer and J. P. Ginsberg, "An overview of heart rate variability metrics and norms," *Frontiers in Public Health*, vol. 5, p. 258, 2017.

[34] "Heart rate variability," *Eur Heart J*, vol. 17, p. 28, 1996.

[35] R. Barbieri, E. C. Matten, A. A. Alabi, and E. N. Brown, "A point-process model of human heartbeat intervals: New definitions of heart rate and heart rate variability," *American Journal of Physiology-Heart and Circulatory Physiology*, vol. 288, no. 1, H424–H435, Jan. 2005.

[36] R. Barbieri and E. Brown, "Analysis of heartbeat dynamics by point process adaptive filtering," *IEEE Transactions on Biomedical Engineering*, vol. 53, no. 1, pp. 4–12, Jan. 2006.

[37] M. Kallio, T. Haapaniemi, J. Turkka, K. Suominen, U. Tolonen, K. Sotaniemi, V.-P. Heikkilä, and V. Myllylä, "Heart rate variability in patients with untreated parkinson's disease," *European Journal of Neurology*, vol. 7, no. 6, pp. 667–672, Dec. 2000.

[38] T. H. Haapaniemi, "Ambulatory ECG and analysis of heart rate variability in parkinson's disease," *Journal of Neurology, Neurosurgery & Psychiatry*, vol. 70, no. 3, pp. 305–310, Mar. 1, 2001.

[39] M. Kallio, K. Suominen, A. M. Bianchi, T. Mäkikallio, T. Haapaniemi, S. Astafiev, K. A. Sotaniemi, V. V. Myllylä, and U. Tolonen, "Comparison of heart rate variability analysis methods in patients with parkinson's disease," *Medical & Biological Engineering & Computing*, vol. 40, no. 4, pp. 408–414, Jul. 2002.

[40] V. Pursiainen, T. H. Haapaniemi, J. T. Korpelainen, H. V. Huikuri, K. A. Sotaniemi, and V. V. Myllylä, "Circadian heart rate variability in parkinson's disease," *Journal of Neurology*, vol. 249, no. 11, pp. 1535–1540, Nov. 1, 2002.

[41] J. D. Guieu, C. Libersa, A. Destee, D. Devos, M. Kroumova, R. Bordet, and H. Vodougnon, "Heart rate variability and parkinson's disease severity," *Journal of Neural Transmission*, vol. 110, no. 9, pp. 997–1011, Sep. 1, 2003.

[42] G. A. Reyes del Paso, W. Langewitz, L. J. M. Mulder, A. van Roon, and S. Duschek, "The utility of low frequency heart rate variability as an index of sympathetic cardiac tone: A review with emphasis on a reanalysis of previous studies: LF HRV and sympathetic cardiac tone," *Psychophysiology*, vol. 50, no. 5, pp. 477–487, May 2013.

[43] L. Mourot, M. Bouhaddi, S. Perrey, S. Cappelle, M.-T. Henriet, J.-P. Wolf, J.-D. Rouillon, and J. Regnard, "Decrease in heart rate variability with overtraining: Assessment by the poincare plot analysis," *Clinical Physiology and Functional Imaging*, vol. 24, no. 1, pp. 10–18, Jan. 2004.

[44] I. Antelmi, R. S. De Paula, A. R. Shinzato, C. A. Peres, A. J. Mansur, and C. J. Grupi, "Influence of age, gender, body mass index, and functional capacity on heart rate variability in a cohort of subjects without heart disease," *The American journal of cardiology*, vol. 93, no. 3, pp. 381–385, 2004.

[45] M. M. Massin, K. Maeyns, N. Withofs, F. Ravet, and P. Gérard, "Circadian rhythm of heart rate and heart rate variability," *Archives of disease in childhood*, vol. 83, no. 2, pp. 179–182, 2000.

[46] A. Bilan, A. Witczak, R. Palusiński, W. Myśliński, and J. Hanzlik, "Circadian rhythm of spectral indices of heart rate variability in healthy subjects," *Journal of Electrocardiology*, vol. 38, no. 3, pp. 239–243, 2005.

[47] F. Portaluppi, R. Tiseo, M. H. Smolensky, R. C. Hermida, D. E. Ayala, and F. Fabbian, "Circadian rhythms and cardiovascular health," *Sleep medicine reviews*, vol. 16, no. 2, pp. 151–166, 2012.

[48] S. Li, Y. Wang, F. Wang, L.-F. Hu, and C.-F. Liu, "A new perspective for parkinson's disease: Circadian rhythm," *Neuroscience bulletin*, vol. 33, no. 1, pp. 62–72, 2017.

[49] P. Pospıšil, L. Konečny, P. Vank, M. Pohanka, H. Srovnalová, I. Rektorova, and J. Siegelova, "Autonomic dysfunction and progression of parkinson's disease," *Scr Med (Brno)*, vol. 81, pp. 239–48, 2008.

[50] R. Barbieri and E. N. Brown, "Application of dynamic point process models to cardiovascular control," *Biosystems*, vol. 93, no. 1, pp. 120–125, Jul. 2008.

[51] R. Barbieri, L. Citi, M. Guerrisi, S. Orsolini, C. Tessa, S. Diciotti, and N. Toschi, "Increased instability of heartbeat dynamics in parkinson's disease," p. 4,

[52] R. Barbieri, L. Citi, M. Guerrisi, S. Orsolini, C. Tessa, S. Diciotti, and N. Toschi, "Lower instantaneous entropy of heartbeat dynamics characterizes cognitive impairment in parkinson's disease," p. 4,

[53] G. Valenza, S. Orsolini, S. Diciotti, L. Citi, E. P. Scilingo, M. Guerrisi, S. Danti, C. Lucetti, C. Tessa, R. Barbieri, and N. Toschi, "Assessment of spontaneous cardiovascular oscillations in parkinson's disease," *Biomedical Signal Processing and Control*, vol. 26, pp. 80–89, Apr. 2016.

[54] C.-A. Haensch, H. Lerch, J. Jörg, and S. Isenmann, "Cardiac denervation occurs independent of orthostatic hypotension and impaired heart rate variability in parkinson's disease," *Parkinsonism & Related Disorders*, vol. 15, no. 2, pp. 134–137, Feb. 2009.

[55] M. Misiti, Y. Misiti, G. Oppenheim, J.-M. Poggi, *et al.*, "Wavelet toolbox user's guide," *The Math Works Ins*, 1996.

[56] J. Pan and W. J. Tompkins, "A real-time QRS detection algorithm," *IEEE Transactions on Biomedical Engineering*, vol. BME-32, no. 3, pp. 230–236, Mar. 1985.

[57] H. Sedghamiz, "Matlab implementation of pan tompkins ecg qrs detector.," Mar. 2014.

[58] L. Citi, E. N. Brown, and R. Barbieri, "A real-time automated point-process method for the detection and correction of erroneous and ectopic heartbeats," *IEEE Transactions on Biomedical Engineering*, vol. 59, no. 10, pp. 2828–2837, Oct. 2012.